



**Nélia Lopes  
Ferreira**

**Evaluation of the structural capacity of historical  
constructions**

**Avaliação da capacidade estrutural de construções  
históricas**



**Nélia Lopes  
Ferreira**

## **Evaluation of the structural capacity of historical constructions**

### **Avaliação da capacidade estrutural de construções históricas**

Dissertação apresentada à Universidade de Aveiro para cumprimento dos requisitos necessários à obtenção do grau de Mestre em Engenharia Civil, realizada sob a orientação científica do Professor Doutor Romeu da Silva Vicente, Professor Associado do Departamento de Engenharia Civil da Universidade de Aveiro e co-orientação científica do Professor Doutor Pere Roca Fabregat, Professor Catedrático do Departamento de Engenharia da Construção da Universidade Politécnica da Catalunha e do Professor Doutor Hugo Filipe Pinheiro Rodrigues, Professor Adjunto do Departamento de Engenharia Civil do Instituto Politécnico de Leiria.

Aos meus pais e irmão.

**o júri / the jury**

presidente / president

Professora Doutor Joaquim Miguel Gonçalves Macedo  
Professor Auxiliar do Departamento de Engenharia Civil da Universidade de Aveiro

vogais / committee

Professora Doutora Graça de Fátima Moreira de Vasconcelos  
Professora Auxiliar da Universidade do Minho

Professor Doutor Romeu da Silva Vicente  
Professor Associado do Departamento de Engenharia Civil da Universidade de Aveiro.



## **agradecimentos / acknowledges**

A realização do presente trabalho contou com importantes apoios e incentivos aos quais estarei eternamente grata, aproveito este momento para manifestar a minha gratidão a todos aqueles que sem eles este trabalho não se teria tornado uma realidade e aos que contribuíram de qualquer forma para a minha formação académica ao longo dos últimos anos, que sem dúvida nunca irei esquecer.

Agradeço à Universidade de Aveiro, ao Departamento de Engenharia Civil e a todo o corpo docente que não falharam em me fazer sentir em casa e por me terem proporcionado todas as condições necessárias para que eu alcançasse os meus objetivos.

O meu profundo agradecimento ao Professor Romeu Vicente, que como orientador, demonstrou sempre dedicação, apoio, incentivo e acompanhamento contínuo bem como partilha de conhecimentos fundamentais para a elaboração do presente trabalho.

Ao Professor e co-orientador Hugo Rodrigues, por todo o apoio incansável e disponibilidade total, por toda a simpatia, paciência, incentivo, partilha do saber e pelas valiosas contribuições neste trabalho, o meu muito obrigado.

My appreciation to my co-supervisor, Professor Pere Roca Fabregat for his guidance and sharing of knowledge and tools to initiate this work, particularly, during the period of studies in Barcelona.

I would like to express my sincere grateful to Savvas Saloustos for his help and for his always availability to answer my questions.

To Midas FEA support, specially to Rubén Fernández, for his availability, help and disposition to provide a quick and written answer to my questions.

Agradeço a todos os meus amigos por toda a amizade, especialmente à Sofia e à Inês, por todo o incentivo e apoio, por todos os momentos partilhados, sorrisos e gargalhadas que nunca irei esquecer.

Ao João, pela compreensão, paciência, apoio, incondicional confiança, muito muito obrigado, por tudo que é para mim.

Por fim, um agradecimento muito especial aos meus pais Herondina e Manuel e irmão Pierre pela incessante amizade, amor e confiança, por todos os valores transmitidos e por terem tornado este sonho realidade.

A todos, um muito obrigado, do coração.

## **palavras-chave**

construções históricas, análise estrutural, método dos elementos finitos, mecanismos de dano, abóbadas, análise pushover, estratégias de reabilitação

## **resumo**

As construções históricas são uma parte importante do património mundial construído, símbolos arquitetónicos das cidades, países e culturas. Os museus, monumentos, castelos, igrejas, catedrais, entre outros, são edifícios e locais que oferecem experiências únicas tornando-se difusores de conhecimento. Estes edifícios históricos são alvo da comunidade turística que representa recursos económicos importantes. Por estas razões, a sociedade realiza grandes esforços técnicos e económicos para a conservação e valorização do seu património histórico.

Ao longo do tempo, desde a sua construção até aos dias de hoje, um edifício histórico é exposto a diversos fatores que afetam o seu estado de conservação tais como, a degradação e envelhecimento do material, alterações arquitetónicas, desastres naturais com grandes períodos de retorno, destruição causada por algum tipo de conflito, ações de reabilitação e reforço, entre outros. Assim, a avaliação de construções históricas é um tópico que detém alguma preocupação, não só do ponto de vista da preservação do património, mas também pela segurança estrutural e durabilidade dos edifícios ao longo do tempo.

A análise estrutural é bastante importante para a identificação do motivo pela qual os edifícios exibem danos e deformações e também para compreender o seu efeito no equilíbrio estrutural do edifício. Através de uma abordagem correta e apropriada é possível avaliar a capacidade estrutural de um edifício histórico e definir e validar uma futura estratégia de reabilitação, tentando assim recuperar e manter o comportamento da estrutura original.

O principal objetivo desta dissertação é avaliar a capacidade estrutural de duas construções históricas, a Catedral de Palma de Mallorca (Mallorca, Espanha) e um edifício de alvenaria que faz parte do complexo do Castelo de São Jorge (Lisboa, Portugal).

Para os casos de estudo apresentados realizou-se modelação numérica recorrendo a diversos softwares de elementos finitos, desenvolvendo um estudo paramétrico para compreender a influência das propriedades dos materiais no comportamento global de uma estrutura e ainda se definiram e analisaram diferentes estratégias de reabilitação.

**keywords**

historical constructions, structural analysis, finite element method, damage mechanisms, masonry vaults, pushover analysis, retrofitting strategies

**abstract**

The historical constructions are an important part of the world built heritage, architectural valued symbols of their cities, countries and cultures. Museums, monuments, castles, churches, cathedrals, among others, are buildings and sites that offer unique experiences as centres of knowledge. These historical buildings are the target of the tourist community which represent important economic resources. For these reasons, the society holds great technical and economical effort for the conservation and value of their historical heritage.

Overtime, since their construction until the present day, a historical building is exposed to several factors that could affect their state of conservation such as, the material degradation and aging, architectural alterations, natural disasters with high return periods, destruction in occasion of conflicts, retrofitting actions, amongst others. Therefore, the assessment of historical constructions is a concerning subject, not only from the heritage safeguarding point of view, but also from the structural safety and durability over time.

The structural analysis is of full importance to identify the origin of existing damage and deformations and their effect on the durability of the structure. With the correct and appropriate approach, it is possible evaluate the structural capacity of the historical construction in analysis and define/validate future rehabilitation strategies, strengthening and maintaining an improved behaviour of the original structure.

The main focus of this dissertation is to evaluate the structural capacity of two historical constructions, the Palma Mallorca Cathedral (Spain) and one-story masonry arched building of the Castelo of São Jorge complex (Lisbon, Portugal).

For these case studies were performed numerical modelling resourcing to different finite element software's, developing a parametric study to understand the influence of the material properties on the overall behaviour of the structures, as well as proposing and analysing retrofitting strategies.



# TABLE OF CONTENTS

<b>Table of contents</b>	<b>i</b>
<b>List of figures</b>	<b>vii</b>
<b>List of tables</b>	<b>xix</b>
<b>Chapter 1 Introduction</b>	<b>1</b>
1.1 Motivation	1
1.2 Objectives	2
1.3 Dissertation outline	3
<b>Chapter 2 Damage mechanisms of historical constructions</b>	<b>5</b>
2.1 Façade damage mechanisms	7
2.2 Nave damage mechanisms	9
2.3 Transept damage mechanisms	11
2.4 Triumphal arch damage mechanisms	12
2.5 Dome damage mechanisms	12
2.6 Apse damage mechanisms	13
2.7 Roof damage mechanisms	14
2.8 Chapel or adjacent constructions damage mechanisms	15
2.9 Secondary elements damage mechanisms	16
2.10 Bell tower damage mechanisms	16

2.11	Belfry damage mechanisms	17
2.12	Final synthesis	18
<b>3</b>	<b>Structural analysis of historical constructions</b>	<b>19</b>
3.1	Limit analysis	21
3.2	Finite Element Method (FEM)	22
3.2.1	FEM based approaches: Macro-modelling	23
3.2.2	FEM based approaches: Micro-modelling	24
3.3	Discrete Element method (DEM)	25
3.4	Main difficulties and assumptions in historical constructions modelling	27
3.5	Numerical modelling software	29
3.5.1	GiD Software	30
3.5.2	COMET Software	31
3.5.3	MIDAS FEA Software	31
3.6	Final synthesis	33
<b>4</b>	<b>Mallorca Cathedral</b>	<b>35</b>
4.1	History of construction	36
4.2	Description of the building	39
4.3	Existing damage and deformation	42
4.4	Numerical model	44
4.4.1	Geometrical configuration	48
4.4.2	Material properties	49

4.4.3	Loading and boundary conditions	51
4.4.4	Finite element meshing	51
4.5	Sensitivity analysis	52
4.5.1	Compressive strength	54
4.5.2	Elastic modulus	58
4.5.3	Fracture energy	61
4.5.4	Tensile strength	64
4.6	Final synthesis	67
<b>5</b>	<b>São Jorge Castle – Paço Real II building</b>	<b>69</b>
5.1	History of construction	70
5.2	Description of the building	72
5.3	Existing damage and deformation	76
5.3.1	Generalized Cracking	77
5.3.2	Terrace roof and masonry vaults deformation	79
5.3.3	Exterior walls deformation	80
5.3.4	Floors deformation	81
5.3.5	Partial rotation of the exterior wall	82
5.3.6	Non-structural damage	82
5.4	Dynamic identification in situ	83
5.4.1	Ambient vibration testing (AVT)	85
5.4.2	Acquisition and signal processing	86

5.4.2.1	Sampling frequency and acquisition time	87
5.4.2.2	Errors	88
5.4.3	Modal identification	92
5.4.3.1	Analysis in the frequency domain	93
5.4.3.2	Analysis in the time domain	96
5.4.4	Data acquisition system	97
5.4.5	Test setup	98
5.4.6	Results	100
5.5	Numerical model	102
5.5.1	Geometrical configuration	102
5.5.2	Material properties	104
5.5.2.1	Core sampling	105
5.5.3	Loading and boundary conditions	108
5.5.4	Finite element meshing	110
5.6	Results	110
5.6.1	Linear analysis with a continuous undamaged model	112
5.6.2	Linear analysis with a damaged model	116
5.6.3	Non-linear analysis with a continuous undamaged model	120
5.6.4	Non-linear analysis with a damaged model	125
5.7	Retrofitting strategy proposals	131
5.7.1	Remove excess load	132



5.7.2	Steel tie-rods	138
5.7.2.1	Intrados steel tie-rods	139
5.7.2.2	Extrados steel tie-rods	145
5.7.3	Fibre Reinforced Polymer strips (FRP)	152
5.8	Final synthesis	154
<b>6</b>	<b>Final considerations</b>	<b>157</b>
6.1	Conclusions	158
6.1.1	Mallorca Cathedral	159
6.1.2	São Jorge Castle – Paço Real II building	159
6.1.2.1	Retrofitting strategy proposals	160
6.2	Future developments	160
6.2.1	Mallorca Cathedral	161
6.2.2	São Jorge Castle – Paço Real II building	161
	<b>References</b>	<b>163</b>
	<b>Appendix A</b>	<b>173</b>
A.1	Remove excess load with accessible roof	174
A.2	Steel tie-rods with accessible roof	177
A.2.1	Intrados steel tie-rods	177
A.2.2	Extrados steel tie-rods	181



# LIST OF FIGURES

## Chapter 2 Damage mechanisms of historical constructions

Figure 2.1 – Principal macro-elements that define the church/cathedral structure.	7
Figure 2.2 – Façade damage mechanisms (LineeGuida 2006).	8
Figure 2.3 – Nave damage mechanisms (LineeGuida 2006).	10
Figure 2.4 – Transept damage mechanisms (LineeGuida 2006).	11
Figure 2.5 – Triumphal arch damage (LineeGuida 2006).	12
Figure 2.6 – Dome damage mechanisms (LineeGuida 2006).	13
Figure 2.7 – Apse damage mechanisms (LineeGuida 2006).	14
Figure 2.8 – Roof damage mechanisms (LineeGuida 2006).	14
Figure 2.9 – Chapel or adjacent constructions damage mechanisms (LineeGuida 2006).	15
Figure 2.10 – Projections of secondary elements such as gable belfry, spires and statues (LineeGuida 2006).	16
Figure 2.11 – Damage in Santa Maria della Concezione Church near L'Aquila region (NYT 2009).	16
Figure 2.12 – Bell tower cracking (LineeGuida 2006).	17
Figure 2.13 – Damaged bell tower of San Bernardino Church (WSJ 2009).	17
Figure 2.14 – Belfry damage (LineeGuida 2006).	17

## **Chapter 3 Structural analysis of historical constructions**

Figure 3.1 – Numerical modelling strategies for masonry structures based on FEM: a) detailed micro-modelling, b) simplified micro-modelling and c) macro-modelling (Furtado, Rodrigues et al. 2015). 23

Figure 3.2 – Dynamic on-site test of the S. Marcello Pistoiese Bridge, mode 1 (Pelà, Aprile et al. 2009). 24

Figure 3.3 – Distribution of tensile damage for the dead load in the analysis of Küçük Ayasofya Mosque in Istanbul (Roca, Massanas et al. 2004). 24

Figure 3.4 – Tensile damage results of a seismic analysis of Mallorca Cathedral in GiD. 30

Figure 3.5 – Mode 3 of structural eigenvalue analysis of Paço Real II by Midas FEA. 32

## **Chapter 4 Mallorca Cathedral**

Figure 4.1 – Progress of Mallorca cathedral construction from 1306 to 1601 (Mohamed 2015). 37

Figure 4.2 – Comparison between the original west façade a) with the new design b) of Mallorca cathedral. 38

Figure 4.3 – Plan at roof level of Mallorca cathedral (Roca, Cervera et al. 2013). 40

Figure 4.4 – Longitudinal section of Mallorca cathedral (Roca, Cervera et al. 2013). 40

Figure 4.5 – Mallorca cathedral interior arrangement (Das 2008). 41

Figure 4.6 – Double battery of flying arches of Mallorca cathedral (Das 2008). 41

---

Figure 4.7 – Additional overloads of Mallorca cathedral: a) over the transversal arches key and b) over the vaults keys.	42
Figure 4.8 – Existing damage and deformation of Mallorca cathedral: a) at the top pf the pier, b) cracks at the base of the pier, c) cracks in a buttress following the perimeters of a false window and c) deformed flying arches d).	43
Figure 4.9 – Composite damage surface adopted for masonry (Roca, Cervera et al. 2013).	46
Figure 4.10 – Static graphical analysis of Mallorca cathedral (Rubió 1912).	47
Figure 4.11 – Photo elastic analysis with the distribution of internal forces (Mark 1982).	47
Figure 4.12 – Analyses by line pressures of Mallorca cathedral (Maynou 2001)	48
Figure 4.13 – Collapse mechanism of Mallorca cathedral (Salas 2002).	48
Figure 4.14 – Different structural elements in the two-dimensional FE model.	49
Figure 4.15 – Equivalence between the 2D and the 3D models.	50
Figure 4.16 – Finite element mesh adopted for the analysis.	52
Figure 4.17 – Location of the analysed nodes for the vertical load analysis and seismic assessment.	53
Figure 4.18 – Damage mechanism with half of the tensile strength value for the vertical load analysis.	54
Figure 4.19 - Damage mechanism with double of the elastic modulus value for the seismic analysis.	54
Figure 4.20 – Vertical displacement vs load factor regarding the compressive strength variation – vertical load analysis.	55

---

Figure 4.21 – Relationship between the compressive strength variation with the collapse load factor– vertical load analysis.	56
Figure 4.22 – Horizontal displacement vs load factor regarding the compressive strength variation – seismic assessment.	57
Figure 4.23 – Relationship between the compressive strength variation with the collapse load factor – seismic assessment.	57
Figure 4.24 – Vertical displacement vs load factor regarding the Elastic modulus variation – vertical load analysis.	59
Figure 4.25 – Relationship between the elastic modulus variation with the collapse load factor– vertical load analysis.	59
Figure 4.26 – Horizontal displacement vs load factor regarding the elastic modulus variation – seismic assessment.	60
Figure 4.27 – Relationship between the elastic modulus variation with the collapse load factor – seismic assessment.	61
Figure 4.28 – Vertical displacement vs load factor regarding the fracture energy variation – vertical load analysis.	62
Figure 4.29 – Horizontal displacement vs load factor regarding the fracture energy variation – seismic assessment.	63
Figure 4.30 – Vertical displacement vs load factor regarding the tensile strength variation – vertical load analysis.	65
Figure 4.31 – Relation between the tensile strength variation with the collapse load factor – vertical load analysis.	65

Figure 4.32 – Horizontal displacement vs load factor regarding the tensile strength variation – seismic assessment. 66

Figure 4.33 – Relationship between the tensile strength variation with the collapse load factor – seismic assessment. 67

## **Chapter 5 São Jorge Castle - Paço Reall II building**

Figure 5.1 – Location of the building, Paço II, through an aerial view of the city (Google earth, 2016). 70

Figure 5.2 – Distribution of the ancient fortress of Lisbon areas (Cruz 2013). 72

Figure 5.3 – Ground floor plan of the Paço Real II, Casa do Leão restaurant. 73

Figure 5.4 – South elevation of the Paço Real II. 73

Figure 5.5 – Detail of the south façade of Paço Real II. 74

Figure 5.6 – Roof top view of Paço Real II: a) surrounding wallet of the terrace b) detail of the translucent tempered glass guard on the south façade. 74

Figure 5.7 – Interior of the building Paço Real II, Casa do Leão restaurant. 75

Figure 5.8 – Interior details of the building Paço Real II: a) fireplace (only as a decorative element) b) tile wainscot that cover a part of the wall. 75

Figure 5.9 – Longitudinal cracking on the roof: a) longitudinal alignment of the crack b) cracking detail of the terrace. 77

Figure 5.10 – Longitudinal cracking inside the building: a) longitudinal alignment b) cracking detail in the arch. 78

Figure 5.11 – Cracking in the connection between the vault and the wall. 79

Figure 5.12 – Cracking in the tiles in the lower part of the wall bellow the window.	79
Figure 5.13 – Cracking in the exterior northeast wall.	79
Figure 5.14 – Cracking between the staircase and the northeast wall.	79
Figure 5.15 – Longitudinal cracking inside the building: a) continuous longitudinal alignment b) cracking detail of the masonry vault.	80
Figure 5.16 – Linearity break along the spans in the west façade.	81
Figure 5.17 – Plumb of some elements around the span in the west façade.	81
Figure 5.18 – Floor tile cracking inside the building.	81
Figure 5.19 – Irregular stone pavement outside the building.	81
Figure 5.20 – Cracking in the east façade.	82
Figure 5.21 – North façade out-of-plumb, visible on the north and east direction.	82
Figure 5.22 – Inefficient rainwater drainage and the waterproofing system.	83
Figure 5.23 – Efflorescence and paint blistering on the south wall.	83
Figure 5.24 – Ambient vibration testing scheme (Cantieni 2005).	85
Figure 5.25 – Original signal vs a signal with noise (WaveletToolbox 2016).	89
Figure 5.26 – Effect of the signal saturation.	90
Figure 5.27 – Impact of observation interval on FFT (GaussianWaves 2016).	91
Figure 5.28 – Adequate and inadequate signal sampling through aliasing effect (Corportation 2016).	92
Figure 5.29 – System and piezoelectric unidirectional accelerometers.	98
Figure 5.30 – Representative scheme of the setup 1 relative to the dynamic test.	99



---

Figure 5.31 – Representative scheme of the setup 2 relative to the dynamic test.	99
Figure 5.32 – Spectrum peaks identification through the PP technique.	101
Figure 5.33 – Vibration modes representation of the a) 1 <sup>st</sup> mode – 6.29 Hz; b) 2 <sup>nd</sup> mode – 12.26 Hz; c) 3 <sup>rd</sup> mode – 18.55 Hz and d) 4 <sup>th</sup> mode – 20.65 Hz.	101
Figure 5.34 – Single groined vault by Rhinoceros 3D.	103
Figure 5.35 – Group of groined vaults by Rhinoceros 3D.	103
Figure 5.36 – Final geometry of the building Paço Real II by Rhinoceros 3D.	103
Figure 5.37 – Core sampling on the terrace of the building Paço Real II: a) equipment used before starting the extraction with a 55mm crown, b) bore hole execution resourcing to metal extenders of 500mm.	106
Figure 5.38 – The two cores samples extracted, representing the layers.	107
Figure 5.39 – Filling layer of sand leached during the extraction process.	107
Figure 5.40 – Applied load on the vaults induced by the terrace roof layers over the brick vaults: a) central strip area; b) lateral strip area.	109
Figure 5.41 – Finite element meshing of the numerical model.	110
Figure 5.42 – Location of the changed elements simulating the existent vault cracks.	111
Figure 5.43 – Non-linear behaviour functions: a) Hordijk function in tension; b) Parabolic function in compression (ManualMidasUser 2016).	112
Figure 5.44 – Maximum principal stresses for a) tension and b) tension higher than 0.1 MPa.	114
Figure 5.45 – Maximum principal stresses for compression.	114

---

Figure 5.46 – Displacements in the direction a) XX; b) YY and c) ZZ.	116
Figure 5.47 – Maximum principal stresses for a) tension and b) tension higher than 0.1 MPa.	117
Figure 5.48 - Maximum principal stresses for compression.	118
Figure 5.49 – Displacements in the direction a) XX; b) YY and c) ZZ.	119
Figure 5.50 – Position of the analysed points in the: a) transversal direction and b) longitudinal direction.	121
Figure 5.51 – Transversal displacement vs load factor regarding the vertical load analysis with a continuous undamaged model.	122
Figure 5.52 – Longitudinal displacement vs load factor regarding the vertical load analysis with a continuous undamaged model.	122
Figure 5.53 – Transversal displacement vs load factor regarding the pushover analysis in the XX direction with a continuous undamaged model.	123
Figure 5.54 –Longitudinal displacement vs load factor regarding the pushover analysis in the XX direction with a continuous undamaged model.	123
Figure 5.55 – Transversal displacement vs load factor regarding the pushover analysis in the YY direction with a continuous undamaged model.	124
Figure 5.56 – Longitudinal displacement vs load factor regarding the pushover analysis in the YY direction with a continuous undamaged model.	125
Figure 5.57 – Transversal displacement vs load factor regarding the vertical load analysis with a damaged model.	126
Figure 5.58 – Longitudinal displacement vs load factor regarding the vertical load analysis with a damaged model.	126

Figure 5.59 – Transversal displacement vs load factor regarding the pushover analysis in the XX direction with a damaged model.	127
Figure 5.60 – Longitudinal displacement vs load factor regarding the pushover analysis in the XX direction with a damaged model.	128
Figure 5.61 – Transversal displacement vs load factor regarding the pushover analysis in the YY direction with a damaged model.	128
Figure 5.62 – Longitudinal displacement vs load factor regarding the pushover analysis in the YY direction with a damaged model.	129
Figure 5.63 – Transversal displacement vs load factor regarding the pushover analysis in the XX direction with an undamaged and a damaged model.	130
Figure 5.64 – Longitudinal displacement vs load factor regarding the pushover analysis in the YY direction with an undamaged and a damaged model.	131
Figure 5.65 – Transversal displacement vs load factor regarding the vertical load analysis.	133
Figure 5.66 – Longitudinal displacement vs load factor regarding the vertical load analysis.	134
Figure 5.67 – Transversal displacement vs load factor regarding the pushover analysis in the XX direction.	135
Figure 5.68 – Longitudinal displacement vs load factor regarding the pushover analysis in the XX direction.	135
Figure 5.69 – Transversal displacement vs load factor regarding the pushover analysis in the YY direction.	136

Figure 5.70 – Longitudinal displacement vs load factor regarding the pushover analysis in the YY direction. 136

Figure 5.71 – Tension stress distribution for the pushover analysis in XX direction: a) before and b) after the retrofitting strategy. 137

Figure 5.72 – Tension stress distribution for the pushover analysis in YY direction: a) before and b) after the retrofitting strategy. 138

Figure 5.73 – Steel tie-rods positioning: a) vaults intrados and b) vaults extrados. 139

Figure 5.74 – Transversal displacement vs load factor regarding the vertical load analysis. 140

Figure 5.75 – Longitudinal displacement vs load factor regarding the vertical load analysis. 140

Figure 5.76 – Transversal displacement vs load factor regarding the pushover analysis in the XX direction. 141

Figure 5.77 – Longitudinal displacement vs load factor regarding the pushover analysis in the XX direction. 141

Figure 5.78 – Transversal displacement vs load factor regarding the pushover analysis in the YY direction. 142

Figure 5.79 – Longitudinal displacement vs load factor regarding the pushover analysis in the YY direction. 143

Figure 5.80 – Tension stress distribution for the pushover analysis in XX direction: a) before and b) after the retrofitting strategy. 144

Figure 5.81 – Tension stress distribution for the pushover analysis in YY direction: a) before and b) after the retrofitting strategy. 144

Figure 5.82 – Transversal displacement vs load factor regarding the vertical load analysis.	145
Figure 5.83 – Longitudinal displacement vs load factor regarding the vertical load analysis.	146
Figure 5.84 – Transversal displacement vs load factor regarding the pushover analysis in the XX direction.	146
Figure 5.85 – Longitudinal displacement vs load factor regarding the pushover analysis in the XX direction.	147
Figure 5.86 – Transversal displacement vs load factor regarding the pushover analysis in the YY direction.	148
Figure 5.87 – Longitudinal displacement vs load factor regarding the pushover analysis in the YY direction.	148
Figure 5.88 – Tension stress distribution for the pushover analysis in XX direction: a) before and b) after the retrofitting strategy.	149
Figure 5.89 – Tension stress distribution for the pushover analysis in YY direction: a) before and b) after the retrofitting strategy.	150
Figure 5.90 – Transversal displacement vs load factor regarding the retrofitting strategy proposals through a pushover analysis in the XX direction.	151
Figure 5.91 – Longitudinal displacement vs load factor regarding the retrofitting strategy proposals through a pushover analysis in the YY direction.	151
Figure 5.92 – FRP retrofitting strategy in Via Roma San Pio, L'Aquila: a) placement of the FRP strips and b) final result (SismyGroup 2016).	153

Figure 5.93 – Possible layout of the FRP strips application for vault strengthening.

154

## LIST OF TABLES

### Chapter 4 Mallorca Cathedral

Table 4.1 – Material properties of the structural elements of the Mallorca Cathedral.	50
---	----

### Chapter 5 São Jorge Castle - Paço Real II building

Table 5.1 – Material properties.	104
Table 5.2 – Average error calculation after the numerical model calibration.	105
Table 5.3 – Thickness and specific weight of each layer which constitutes the terrace of the building Paço Real II.	108
Table 5.4 – Load induced by the terrace roof system over the vaults of the building Paço Real II.	109
Table 5.5 – Terrace roof load over the vaults after the removal of the two first layers and considering an accessible roof.	132





# CHAPTER 1

## INTRODUCTION

### 1.1 Motivation

The historical constructions are an important part of the world built heritage, architectural valued symbols of their cities, countries and cultures. Museums, monuments, castles, churches, cathedrals, among others, are particular buildings and sites that offer unique experiences as centres of knowledge. These historical buildings are valuable assets for the tourism sector, which can represent important economic resources for local communities. For these reasons, the society holds great technical and economical effort for the conservation and value of their historical and cultural heritage.

Overtime, since their construction until the present day, a historical building is exposed to several factors that could affect their state of conservation such as, the material

degradation and aging, architectural alterations, natural disasters with high return periods, destruction in occasion of conflicts, retrofitting actions, amongst others. Therefore, the assessment of historical constructions is a concerning issue, not only from the heritage safeguarding point of view, but also from the structural safety and durability.

The structural assessment is of full importance to identify the origin of existing damage and deformation and their effect over the equilibrium of the structure. With a correct and appropriate approach, it is possible to evaluate the structural capacity of historical constructions, define and validate retrofitting and strengthening strategies to assure and maintain the global behaviour of original structure.

## **1.2 Objectives**

The main focus of the dissertation is to evaluate the structural capacity of two historical constructions, the Palma Mallorca Cathedral (Mallorca, Spain) and One-story masonry arched building of the Castelo of São Jorge complex (Lisbon, Portugal).

This dissertation proposal includes the following objectives:

- i.** State of art review regarding the damage mechanisms and of existing numerical modelling approaches for the assessment of historical constructions;
- ii.** Numerical modelling of the case studies identified above using a finite element modelling software, considering the non-linear material behaviour;
- iii.** Development of a parametric study to understand the influence of material properties over the structural behaviour;
- iv.** Assessment of the structural capacity of the case studies and retrofitting strategies proposal.

### 1.3 Dissertation outline

The present document is divided into six chapters. In the present chapter (Chapter 1), is presented a brief reference to the importance of the structural analysis of historical constructions to validate future rehabilitation or retrofitting strategies as well as an introduction to the main goals of the present dissertation.

Chapter 2 covers a literature review of the most common damage mechanisms of the several macro-elements that may be present in a church or cathedral to recognise and understand the most probable damage mechanism for an accurate analysis and an correct and compatible future rehabilitation proposal.

Chapter 3 focuses on the structural analysis literature review and the reasons of the appearance of this type of analyses, the distinct possible methods of analysis as well as the main difficulties and constrains when we are in the presence of historical constructions. Still, in this chapter a brief reference is made to the numerical modelling software's used to perform the analyses.

As previously stated, in the present study it will be evaluated the structural capacity of two historical constructions: study of Palma Mallorca Cathedral (Mallorca, Spain) and in one-story masonry arched building of the São Jorge Castle complex in Lisbon, Portugal.

In Chapter 4 is described the first case study of Palma de Mallorca Cathedral (Mallorca, Spain) and the existing damages and defects, is presented the numerical model and is performed a sensitivity analysis followed with a discussion of results.

In Chapter 5, is exposed the history of the construction of the second case study and the existent damage and defects. It is presented and discussed the numerical models and the results for the proposed retrofitting strategies will close this chapter.

In the last chapter of this document, are listed the main conclusions from the work developed as well as future developments which may be considered to improve the present study.

## CHAPTER 2

### DAMAGE MECHANISMS OF HISTORICAL CONSTRUCTIONS

The stone masonry constructions represent the majority of the existing historical constructions in cities throughout Europe, classified most of them as World Heritage by United Nations Educational Scientific and Cultural Organization (UNESCO). These constructions require a special attention due to their historical, cultural and architectural value (Vicente, Parodi et al. 2011). Therefore, for an accurate analysis and a future rehabilitation or retrofitting proposal it is very important to recognise and understand the probable damage mechanisms that can occur in historical constructions, such as churches and cathedrals.

Regarding the assessment of historical constructions, originally, were identified and classified 28 frequent damage mechanisms, taking into account, a survey form

developed in Italy by Lagomarsino and Podestà (2004). This methodology was applied in the damage assessment of churches in Açores by Guerreiro, Azevedo et al. (2000), enabling a first perception of the viability of occupying damaged churches and an initial estimate of the rehabilitation costs (Guerreiro, Azevedo et al. 2000), however the method has not been made official by the Portuguese civil protection authorities. Over the last years, the method has experienced some changes, evolving, based on different studies, leading to a more complete document (LineeGuida 2006), the most recent publication and considered a main reference to evaluate the damage mechanisms of historical constructions.

LineeGuida (2006) is a document that provides all the necessary information for a suitable evaluation, mainly of the seismic risk, for the heritage safeguarding. This directive was established with the purpose to specify, as accurately as possible, a path of knowledge, the historical heritage seismic safety evaluation and consequently the definition of interventions to improve the seismic performance (LineeGuida 2006).

The systematic analysis of the damage suffered by churches, due to strong earthquakes, since Friuli in 1976 up to Salò in 2004, allowed to establish that the behaviour of this type of constructions can be interpreted through its division into architecture elements, macro elements as defined in Figure 2.1, characterized by an independent structural response of the church as a whole (LineeGuida 2006).

This guideline, LineeGuida, identifies twenty-eight damage mechanisms, listed and briefly exposed in the next sub-chapter, related to several macro-elements that may be present in a church or cathedral.

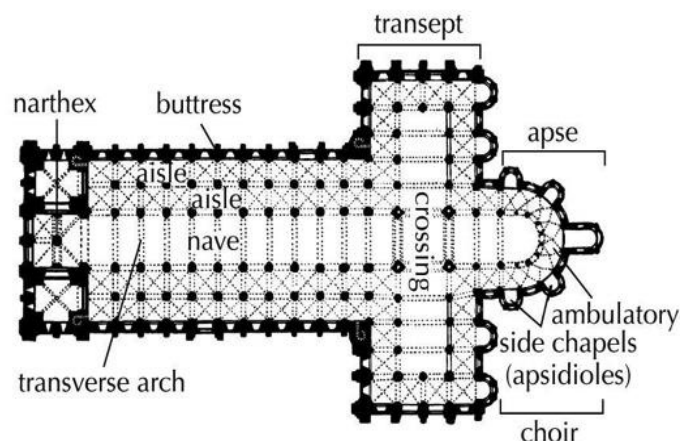


**Figure 2.1** – Principal macro-elements that define the church/cathedral structure.

## 2.1 Façade damage mechanisms

The façade of a historical construction such as churches and cathedrals is the significant exterior side of the building, generally the main front of the building. There are several damage mechanisms that can occur in the façade such as the façade out-of-plane rotation that could lead to the façade collapse (see Figure 2.2 a), the damage at the top of the façade (see Figure 2.2 b), the shear mechanisms presents in the façade (see Figure 2.2 c) and also damages in the narthex (see Figure 2.2 d). The narthex is an architectural element located at the west end of the nave opposite to the church's main altar, considered as an entrance (LineeGuida 2006).

The four major damage mechanisms are presented below:

- i. **Façade out-of-plane rotation** – it is possible to observe the disconnection between the façade and the sidewalls or signs of a possible façade out-of-plane rotation. This mechanism can be caused by some structural elements of the church, for example, the presence of elements that push the façade to out of their plan (arches and roof beams), the existence of large openings in the façade

(windows and doors) and also the poor connection among the façade and the side walls, in the quoin area (see Figure 2.2 a).

- ii. **Damage at the top of the façade** – mechanism stimulated by the presence of large openings in the top of the façade or by the existence of a heavy gable, which can cause the top of the façade to fall out. In this mechanism, the appearance of horizontal cracks at the frontispiece base is also very common (see Figure 2.2 b).
- iii. **Shear mechanisms in the façade** – the appearance of diagonal cracks is caused by the shear in the façade plane intensified by the presence of considerable openings and vertical elements with high slenderness, height/width ratio (see Figure 2.2 c).
- iv. **Damage in the narthex** – in the presence of portal frames or galleries in the façade, it is quite usual the appearance of cracks in the arches or in the connection gallery/façade. This cracking is caused, most of the times, by the high slenderness of the gallery elements (see Figure 2.2 d).

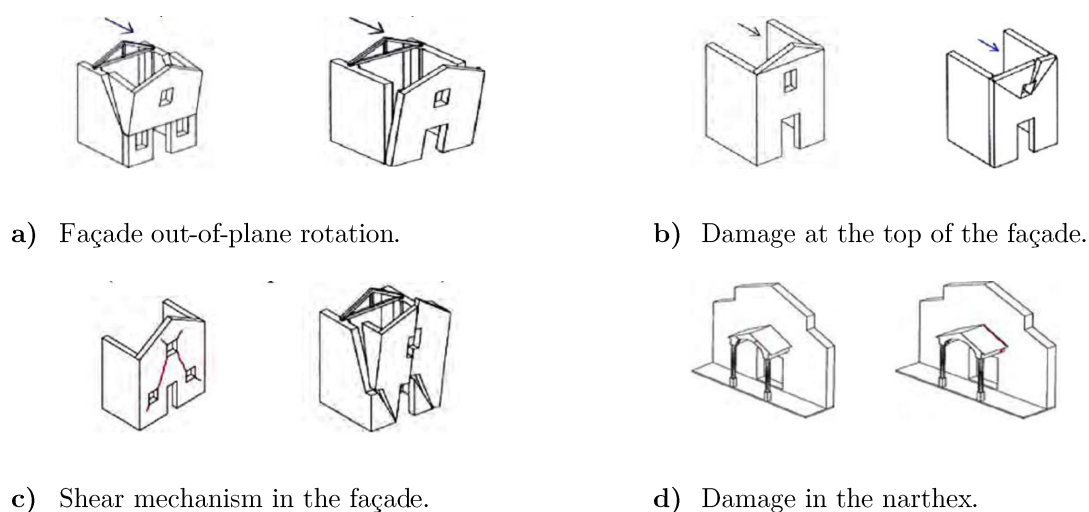


**Figure 2.2** – Façade damage mechanisms (LineeGuida 2006).



## 2.2 Nave damage mechanisms

The nave is the main body of a church, extends from the entry to the chancel and provides the central approach to the high altar, in other words is the central longitudinal space and it is usually flanked on its long sides by aisles which are separated from the nave by columns or piers (Medart 2015). In the case of the nave, it can mainly occur four damage mechanisms: transversal vibration of the nave, shear mechanisms in the side walls, longitudinal response of the colonnade and cracking in the vaults of the nave as well in the vaults of the aisles (LineeGuida 2006).

To properly understand these damage mechanisms, it is also important to identify the macro-elements vaults and aisles in a church. The vault is an arched form used to provide a space with a ceiling or roof and the aisle is an open area parallel to the nave and separated from it by columns or piers, made for walking with seat rows on either side or with seat rows on one side and a wall on the other (Medart 2015).

- i. **Transversal vibration of the nave** – this damage mechanism is characterized by the cracks opening in the transversal arches and the sidewalls rotation causes the appearance of cracking in the vaults by shear. This mechanism is affected by the typology and also by the conservation of the arches and vaults materials, the high slenderness of the walls influences, also, this damage mechanism (see Figure 2.3 a).
- ii. **Shear mechanisms in the walls** – the appearance of cracks with diagonal orientation and the cracking close to the sidewalls discontinuities features this damage mechanism. The existence of large openings, high loads from the roof and the longitudinal movement of the walls during an earthquake can lead to the cracking type of the present mechanism (see Figure 2.3 b).

- iii. **Longitudinal response of the colonnade** – this is a typical damage mechanism in the naves caused by the appearance of cracks in the arches or/and by damages in the connection between the vaults and the arches, heavy vaults in the central nave and roof with high self-weight. It is possible to also occur crushing or cracking at the base of the columns (see Figure 2.3 c).
- iv. **Cracking in the vaults of the nave or aisles** – this mechanism is defined by the cracking in the vaults of the nave and aisles and it is created due to the presence of openings, discontinuities and irregularities adjacent to the vaults or also because the existence of concentrated loads in the vaults roof. The possible inadequate thickness (high or insufficient) of the vaults is another reason that can stimulate this damage mechanism (see Figure 2.3 d and e).

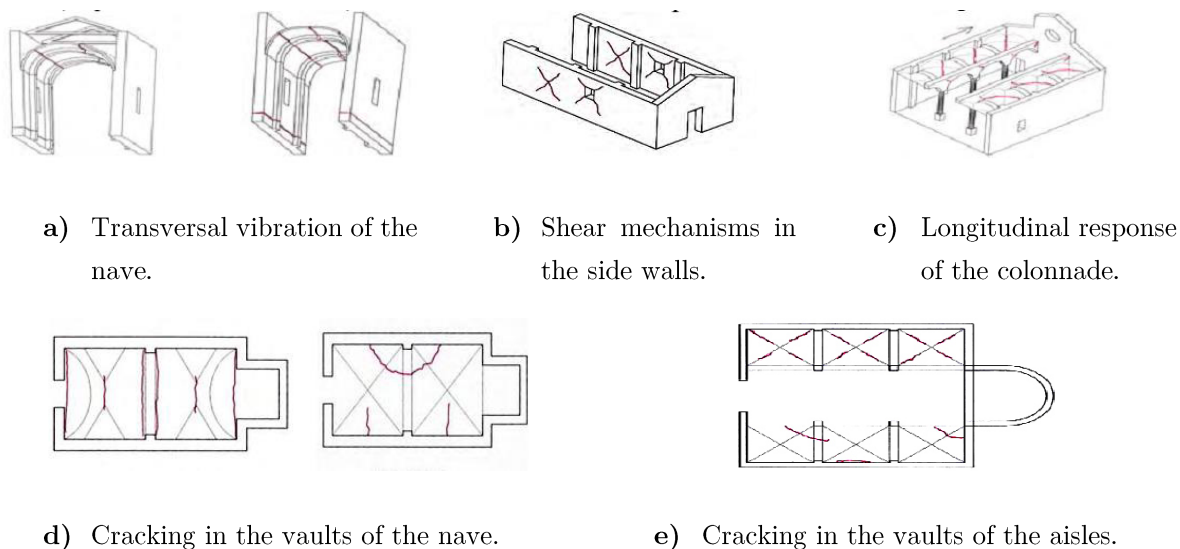


**Figure 2.3** – Nave damage mechanisms (LineeGuida 2006).

## 2.3 Transept damage mechanisms

The transept is an area with a rectangular shape, which divides across the main axis the church, in other words, sets crosswise to the nave. The transept gives the shape of a Latin cross and separates, frequently, the main area of the building from an apse at the end (Medart 2015).

The damage mechanisms that can occur in the transept are similar to other macro-elements such as the façade and also the nave. Similar to the damage mechanisms in the façade, also in the transept can occur the transept out-of-the plane rotation (see Figure 2.4 a) and the shear mechanism in the transept walls (see Figure 2.4 b) that are induced by the same reasons than the occurred in the façade, detailed above in the (i) and (iii) damage mechanisms of the sub-chapter 2.1 but in this case, the element in question is the transept. In this element, there are also another possible damage mechanism, the cracking in the transept vaults (see Figure 2.4 c) similar to the cracking in the nave vaults mechanism, (iv), described in sub-chapter 2.2 (LineeGuida 2006).

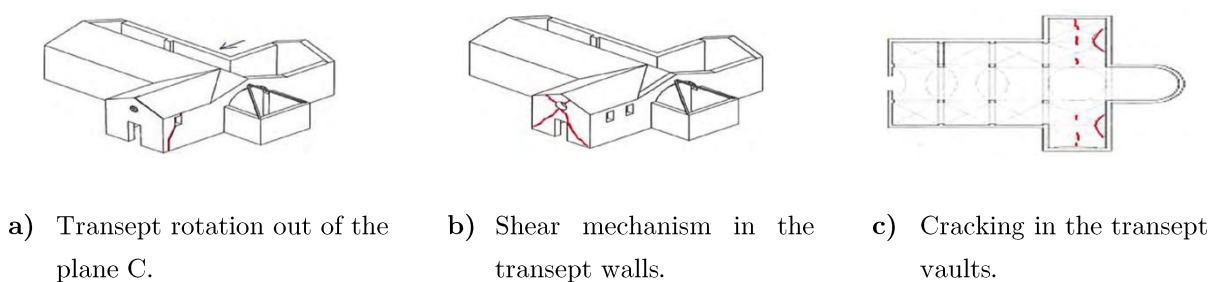


**Figure 2.4** – Transept damage mechanisms (LineeGuida 2006).

## 2.4 Triumphal arch damage mechanisms

The triumphal arch, is the main and principal arch and consists of two piers connected by an arch.

The structural weakness associated with the present macro-element is identified by the appearance of damage in the arch or crushing at the base of the columns, as evidenced in Figure 2.5. This mechanism can be caused by the presence of some macro-elements for example, domes and lanterns and also by a roof with heavy weight (LineeGuida 2006).

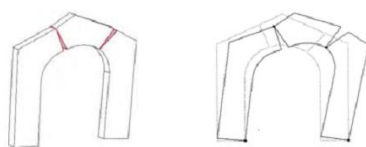


**Figure 2.5** – Triumphal arch damage (LineeGuida 2006).

## 2.5 Dome damage mechanisms

The dome is a hemispherical vault that resembles the hollow upper half of a sphere. When a dome is part of the structure of a church, cathedral or another historical it is quite usual the occurrence of cracks intensified by the existence of openings in this area (see Figure 2.6 a) and another damage mechanism associated to this element is caused by the rotation of the vertical elements and also by the countless openings in the skylight and your slenderness, as shown in Figure 2.6 b) (LineeGuida 2006). The skylight is a small structure with the circular or polygonal shape, with windows all around the base which opens above a larger tower or dome (Medart 2015).

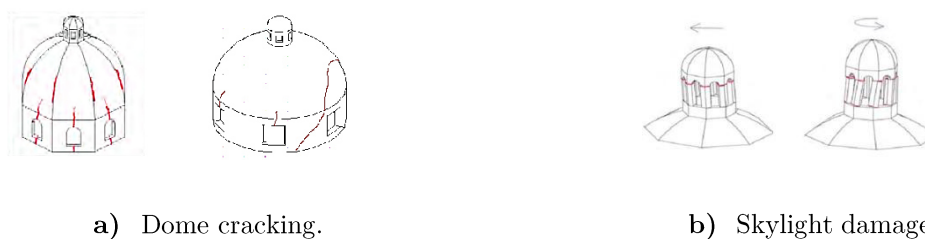


**Figure 2.6** – Dome damage mechanisms (LineeGuida 2006).

## 2.6 Apse damage mechanisms

The apse is a vaulted extension or projection, most of the cases from a chapel and usually with a shape circular or polygonal (Medart 2015). For this macro-element, there are distinct possible damage mechanisms, the first one is the rotation out-of-plane of the apse where is typical vertical or curvilinear cracks appearing in the apse walls, mainly in discontinuities areas. The presence of rigid elements in the perpendicular direction in contact with the apse walls can induce an impulsive effect on the walls causing their out-of-plane rotation (Figure 2.7 a).

The occurrence of shear mechanisms in comparison to the façade ((iii) of sub-chapter 2.1) and transept (sub-chapter 2.3) is also another possible damage mechanism that can occur in the apse. The presence of several openings and vertical elements excessively thin induces this mechanism through diagonal cracks (Figure 2.7 b).

Lastly, another probable damage mechanism is the cracking in the apse vaults, as shown in Figure 2.7 c), in the same way to what occurs in the nave. The presence of openings and irregularities, inadequate thickness of the vaults and concentrated loads in the roof are all structural characteristics that can cause this damage mechanism to occur (LineeGuida 2006).

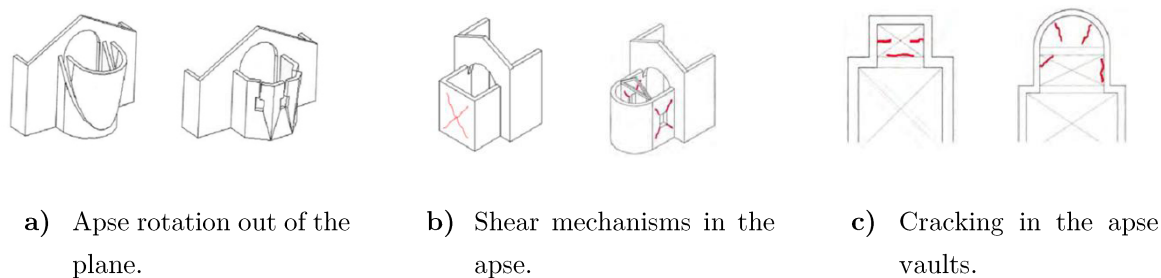


**Figure 2.7** – Apse damage mechanisms (LineeGuida 2006).

## 2.7 Roof damage mechanisms

The connection between the roof structure with any other macro-element - side walls, transept and apse - is a very vulnerable area of a church to horizontal actions causing an impulsive effect of the roof in the top of the walls. This impulsive effect creates horizontal cracks, which tend to spread by the discontinuities of the sidewalls, to the transept walls, as well as the apse walls as shown in Figure 2.8. Another reason that can induce these cracks is the fact that the roof has heavy self-weight and high loading condition. In other cases, these cracking, resultant of the interaction between the roof and the adjacent elements can cause movement of the walls, for example, their out-of-plane movement (LineeGuida 2006).

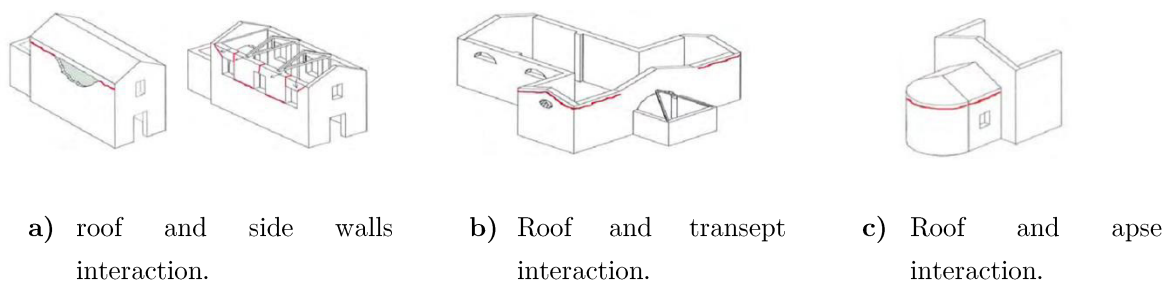


**Figure 2.8** – Roof damage mechanisms (LineeGuida 2006).

## 2.8 Chapel or adjacent constructions damage mechanisms

The damage mechanisms that can occur in the chapels or any adjacent constructions to the churches or cathedrals are also identical to others above described, such as, the out-of-plane rotation of the chapel walls (see Figure 2.9 a), the shear mechanism in the chapel walls (see Figure 2.9 b) and the cracking in the chapel vaults (see Figure 2.9 d).

These damage mechanisms, referred above, are similar to others that could occur in different macro-elements, such as, the façade, the transept and the nave. The out-of-plane rotation and the shear mechanisms in the chapel walls are similar to the (i) and (iii) mechanisms described in sub-chapter 2.1, respectively, and the cracking in the vaults of this macro-element identical to the (iv) mechanism described in 2.2 sub-chapter (LineeGuida 2006).

The height and/or walls thickness irregularities among adjacent constructions can induce another damage mechanism through the appearance of cracks in the connection between both, in the interaction area as shown in Figure 2.9 d.

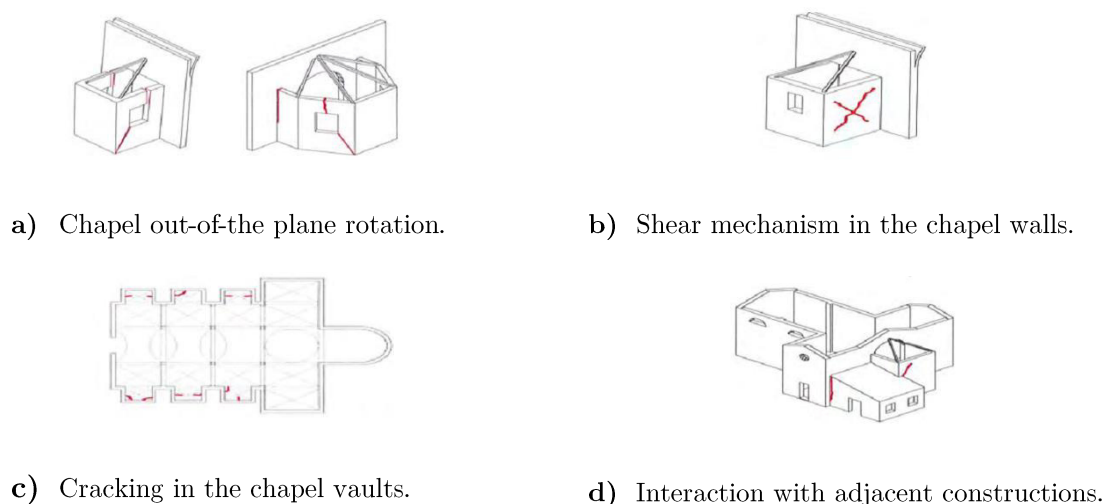


**Figure 2.9** – Chapel or adjacent constructions damage mechanisms (LineeGuida 2006).

## 2.9 Secondary elements damage mechanisms

In addition to the macro-elements already mentioned, there are several secondary elements that are part of the church or cathedral structure such as gable belfry, spires, pinnacles and statues. These secondary elements, usually, are very thin and asymmetric macro-elements which make them elements quite vulnerable, increasing the possibility of cracking, weakening them which may even lead to their projection and collapse as shown in Figure 2.10 and Figure 2.11 (LineeGuida 2006).

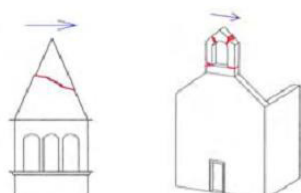


**Figure 2.10** – Projections of secondary elements such as gable belfry, spires and statues (LineeGuida 2006).

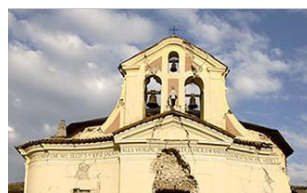


**Figure 2.11** – Damage in Santa Maria della Concezione Church near L'Aquila region (NYT 2009).

## 2.10 Bell tower damage mechanisms

The bell tower, as the name suggests, is a tower designed to hold one or more bells and in this element, is very common the appearance of some cracks in the connection between the tower with the church because the distinct behaviour of both the structures (LineeGuida 2006). The presence of large openings can induce also cracking in the bell tower through shear mechanisms (see Figure 2.12 and Figure 2.13).



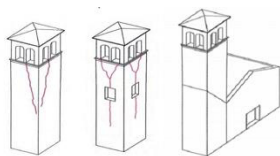


**Figure 2.12** – Bell tower cracking (LineeGuida 2006).



**Figure 2.13** – Damaged bell tower of San Bernardino Church (WSJ 2009).

## 2.11 Belfry damage mechanisms

The belfry has a similar function to the bell tower, is also a tower with one or several bells, but the name refer to the entire tower or building, in other words, it is a disconnected element of the church. Since there is no connection between the belfry with the church, cracking will not occur amongst these elements, in contrast to what occurs in the bell tower.

Therefore, the damage mechanism that can occur in the belfry is caused by the development of cracks in the arches or their rotation and also by the possible column fall (see Figure 2.14), these damages are caused due to the elements slenderness of the belfry (LineeGuida 2006).

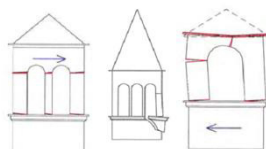


**Figure 2.14** – Belfry damage (LineeGuida 2006).

## 2.12 Final synthesis

The present chapter exposed the several and most probable damage mechanisms that can occur in historical constructions considering the distinct macro-elements that may be present in a church or cathedral, for example.

LineeGuida (2006) is a recent publication and the main reference to evaluate the damage mechanism of historical constructions, in which is provided all the necessary information for a suitable evaluation, mainly of the seismic vulnerability and risk, for the heritage safeguarding and preservation. Understanding the mechanisms of collapse of historical constructions allows a more accurate analysis identification of structural fragilities and consequently a more effective and acknowledgeable future rehabilitation or retrofitting proposals.

Analysing the distinct macro-elements and their associated damage mechanisms it is possible to conclude that for the several elements, there are common mechanisms such as the macro-element out-of-plane movement, shear mechanism and cracking.

# CHAPTER 3

## STRUCTURAL ASSESSMENT OF HISTORICAL CONSTRUCTIONS

Initially, the historical constructions were designed resorting to simple empiric rules based on past experience. This approach in spite of quite rudimental was used in constructions that nowadays represent an important part of the world heritage, such as cathedrals and bridges (Lourenço 2001).

Structural assessment arose due the necessity of the conservation and restoration of historical structures contributing to all the steps and activities as diagnosis, reliability assessment and design of possible strengthening interventions, as a way to ensure an efficient and proper conservation of monuments and historical buildings. In other words, the main goals of the structural assessment are the understanding of the original structural features of the constructions, identification of the actual causes of existing or possible damage, evaluation of the structural safety for different loading actions (as

gravity, wind, earthquake and soil settlements) and finally propose, if necessary interventions. (Roca, Cervera et al. 2010). Therefore, with more knowledge, later, began to be used methods based on limit analysis. For this analysis, is defined the structural safety of a construction, assuming that a structure is in collapse state and is compared with the real structure. The main advantages of this method is the use of a reduced or minimum number of necessary material properties, since this properties are associated to a high level of uncertainty, which is very difficult to find reliable information and also combine the knowledge about mechanisms and collapse loads with practical computation tools (Orduña and Lourenço 2001).

Due to the high and growing capacity of computational numeric problems resolution, it became possible simulate the material behaviour, as masonry (characteristic material of historical constructions), taking into account their nonlinear properties. Nowadays, the most used approaches for the assessment of masonry structures are advanced techniques based on finite element method (FEM), where the basic cell that characterize this method – finite element – usually doesn't represent a structural element but a subpart. In this field, there are also alternative procedures for this type of studies such as approaches based on discrete elements or macro-elements methods, most used in rock mechanics problems which in several cases are very similar to masonry. These methods are still very useful in the analysis of failure mechanisms in masonry structures. It is also presented other numerical techniques, such as discrete element method (DEM) that models the interaction between individual particles or blocks and boundaries to predict the behaviour of bulk solids.

However, there are some difficulties posed to all the analysis referred above, that are very challenging such as the description of the geometry, the characterization of the material, the internal morphology of the structural members, the definition of the actions experienced by the construction, the recognition of existing damages and

alterations and finally all the history of the building. These difficulties will be mentioned and discussed with more detail in the next sub-chapter and at the end of the present chapter regarding the historical constructions modelling.

### 3.1 Limit analysis

The limit analysis method assumes that a structure is in collapsing state and compares its behaviour with the actual condition, defining in this manner its structural safety (Silva, Guedes et al. 2010).

This method when applied to historical constructions, is based on three basic hypothesis defined by Heyman (1966) applied to ancient masonry structures with the aim to characterize the mechanical behaviour, further discussed below:

- i. **Masonry has no tensile strength.** Although masonry elements have tensile strength, the joints between them may be made with weak and unresisting mortar or be dry which causes that the tensile forces does not be transmitted through a mass of masonry. This assumption is justified by the low tensile strength and the quasi-brittle tensile failure of masonry. Nevertheless, this hypothesis is slightly conservative because a non-tension and continuum model corresponds more properly to non-cohesive materials, as sand, and its use for masonry buildings is questionable however acceptable.
- ii. **Masonry has an infinite compressive strength.** This assumption emerged due to the compressive stresses values are usually small compared with the corresponding strength which lead us to conclude that the probability of crushing failure can be often negligible. However, assuming this theory can be considered unsafe, since stress concentrations occur at collapse state and it would be more correct and realistic to consider that compressive stresses are limited.

- iii. Sliding effect cannot occur.** This is a simplification made by Heyman (1966) for his hand calculations, although it was recognised by him that sliding failures sometimes occur. This hypothesis, however can be assured by the existent friction mobilized at the interface level.

Heyman (1966), assumed one more hypothesis independent of the material but necessary for the application of the limit analysis, which is that the failure can occur for small displacements, therefore accepting this hypothesis, the variations in the external displacements depend on the variations of the internal strains, linearly. This assumption is usually accepted in structural analysis, however it must be noted that if significant displacements are expected before the failure, the results might be inaccurate and possibly unsafe.

### 3.2 Finite Element Method (FEM)

The finite element approach allows the modelling of structures by means of two (shell) and three-dimensional (solid) elements and offers a widespread variety of possibilities for describing masonry structures, especially for nonlinear analysis. These main features amongst others makes this approach as one of the most accurate and versatile tools available for the assessment of structures. In finite element models it is possible to request different modelling strategies depending on the level of accuracy and simplicity desired. These strategies are based on micro and macro-modelling, where the micro-modelling procedures can be summarized in: i) detailed micro-modelling where in masonry, units and mortar in the joints are represented by continuum elements and the unit-mortar interface represent by discontinuum elements (Figure 3.1 a) and ii) simplified micro-modelling where the continuum elements are the expanded units and the descontinuum elements are represented by the behaviour of the mortar joints and by the unit-mortar interface (Figure 3.1 b). In the macro-modelling strategy wherever

the units, mortar and unit-mortar interface are defined as discontinuum elements, as evidenced in Figure 3.1 c), (Lourenço 2008).

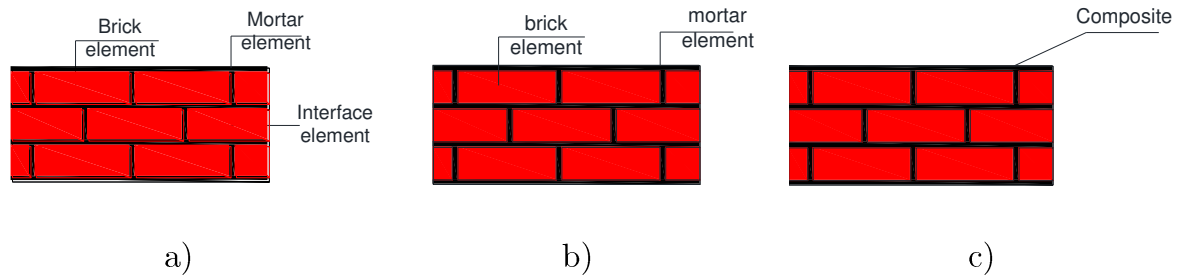


**Figure 3.1** – Numerical modelling strategies for masonry structures based on FEM: a) detailed micro-modelling, b) simplified micro-modelling and c) macro-modelling (Furtado, Rodrigues et al. 2015).

### 3.2.1 FEM based approaches: Macro-modelling

The macro-modelling approach is the most used and common approach, probably, due to its lower calculation demands and less difficulties in the definition of all material parameters. This approach, as referred above, considers the masonry as a fictitious homogeneous orthotropic continuum material, making none distinction between units and mortar joints. Comparing this method to more detailed approaches regarding the description of discontinuities, macro-modelling have significant practical advantages, more precisely, the finite element meshes are simpler once they don't have to accurately describe the masonry internal structure and the finite elements can have greater dimensions than the single brick units, which makes this type of modelling more valuable when needed a compromise between accuracy and efficiency (Roca, Cervera et al. 2010). This approach, macro-modelling, however features a drawback for its implementation to the assessment of masonry structures, such as, the intrinsic complexity when formulating the anisotropic inelastic behaviour. The macro models have been used, extensively, for analysing the seismic response of complex masonry

structures in several works, such as Pelà, Aprile et al. (2009) in arch bridges (Figure 3.2), Mallardo, Malvezzi et al. (2008) in historical buildings, and Roca, Massanas et al. (2004) and Murcia-Delso, Das et al. (2009) in churches and cathedrals (Figure 3.3).

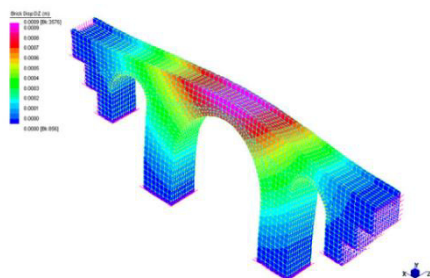


**Figure 3.2** – Dynamic on-site test of the S. Marcello Pistoiese Bridge, mode 1 (Pelà, Aprile et al. 2009).

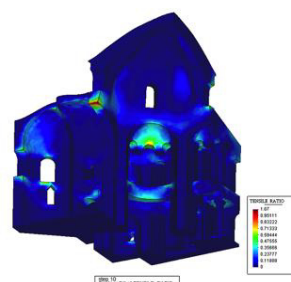


**Figure 3.3** – Distribution of tensile damage for the dead load in the analysis of Küçük Ayasofya Mosque in Istanbul (Roca, Massanas et al. 2004).

### 3.2.2 FEM based approaches: Micro-modelling

In the micro-modelling approach, the various components, namely the mortar, units and the unit/mortar interface should be clearly described. This strategy consists of a detailed numerical representation of masonry structures aiming at considering different failure mechanisms such as the cracking in the joints and units and also the sliding and crushing of masonry (Roca, Cervera et al. 2010). Micro-modelling leads to a structural response with high sensitivity to the definition of the masonry mechanical properties, since this approach is based on individual modelling of each masonry component and its interaction. In the detailed micro-models, the units and the mortar at the joints are defined as continuum finite elements and the interaction between these two components represented by means of discontinuous elements accounting for potential crack or slip planes (Roca, Cervera et al. 2010). To compute the accurate behaviour of masonry (especially for describing local response), detailed micro-modelling is probably the most



effective tool but with high computational costs, where should be realistic taken into account the elastic and inelastic properties of unit and mortar. Due to the detailed description of the models, detailed micro-modelling demands high computational resources, which simplified micro-modelling exceeds partly this drawback (Roca, Cervera et al. 2010).

The simplified micro-modelling approach follows a similar procedure as the detailed one, where the continuum elements represented by the expanded units are used to model both the materials (units and mortar), while the unit/mortar interface and the behaviour of the mortar joints are lumped to the discontinuous elements. In both of micro-modelling approaches, the nonlinearity of the material is focused usually on the interface elements once they present a weaker behaviour. Since the micro-modelling approaches are capable of capturing the main failure mechanisms of masonry structures, it is considered a trustworthy tool for the study of the behaviour of this type of structures (Lourenço 1996). Nevertheless once again, the high level of refinement required leads to an intensive computational effort which limits the applicability of the micro-models to the analysis of small elements or structural details (Roca, Cervera et al. 2010). Micro-modelling approaches are used in distinct researches, overtime, since Lotfi and Shing (1994), Lourenço and Rots (1997) and Sutcliffe, Yu et al. (2001), for example.

### **3.3 Discrete Element method (DEM)**

The discrete element method corresponds to an alternative methodology of modelling apart the FEM, which shows promising results. This method was originally applied by Cundall (1971) in the field of rock mechanics, therefore useful in the modelling of the materials such as masonry, very similar to rocks in several characteristics.

The application of the discrete element method to masonry structures was based on rigid or deformable elements (blocks) which interact among them by means of contact constraints designated “soft contact”, where the stresses are obtained from the relative displacement between blocks not overlooking the normal and tangential properties adopted. There are also another contact constraints called “rigid contact”, that can be found in the research work of authors as Jean (1995), Acary and Jean (1998) and Casolo (2004a).

In the discrete element method, the masonry modelling can be made at micro level, as well as, macro level such as in the finite element method. In the micro-modelling field, the main difference between DEM and FEM, focus in the modelling of the contact between the different elements, so in the finite element method it was considered an interface surface while in the discrete element method, the contact is made through constrain points allowing analysis with large displacements. However, besides the differences between these two approaches, due to the constant evolution, they complement each other existing already hybrid-modelling solutions, called finite/discrete element method.

Regarding to macro-modelling approach, the material discretization using the discrete element method it would make no sense, since besides the necessity of finite elements in the modelling, the discrete element software capacities are limited in this field when compared to the finite element ones. The discrete element method, in the macro-modelling field, features advantages when used approaches as the proposed by Siro Casolo in (Casolo 2004b), who presented a simplified discrete element model aiming at simulating the behaviour of masonry structures. The approach falls into the category of rigid body spring model which is based on the assemblage of rigid bodies by means of elastic springs where two orthogonal springs and one additional spring are placed at

the edges of each rigid block aiming at simulation its interaction with adjacent elements.

### 3.4 Main difficulties and assumptions in historical constructions modelling

Nowadays, analysing ancient constructions is still a challenging task and investigations on historical structures must be integrated with complementary activities involving detailed historical researches for obtaining different approaches and sources of evidence (Roca, Cervera et al. 2010).

As stated in the introduction of the present chapter, in addition to all the advantages and possibilities that structural analysis allows, there are some difficulties that appears in the beginning of any referenced analysis which are an obstacle that must be overcome. The main difficulties are associated with the following aspects: definition of the geometry, the characterization of the material, the internal morphology of the structural members, the definition of the actions experienced by the construction, the recognition of existing damages and alterations and finally all the history of the building, all these further explained below (Roca, Cervera et al. 2010):

- i. **Geometry** – Historical constructions and also their elements are frequently characterized by a very complex geometry, which is the case of arches, flying arches, vaults, domes, fillings, pendentives, among others. However, the existing numerical methods such as FEM, makes geometry one of the least, yet still significant, challenges to be faced.
- ii. **Material** – The materials used in historical constructions such as earth, brick, stone and wood are very heterogeneous causing a difficult characterization of their mechanic and strength properties, except for wood. The use of non-

destructive tests and minor destructive tests solve in part the problem of material characterization where only limited and partial data can be collected, where assumptions must be done for the model elaboration regarding the material properties and their morphology.

- iii. **Morphology** – This problem is related with the characterization and description of the internal morphology of structural members and their connections and constitution such as material layers, metal connectors, fillings, cavities, among others. The modelling of this connections and morphology can be highly demanding from a computational point of view and also very difficult to physically characterize them by non-destructive testing.
- iv. **Actions** – The historical constructions experienced since the moment they were erected and overtime, different type of actions such as the effects of gravity forces in the long term, earthquakes, environmental effects and anthropogenic actions (intentional destructions, architectural alterations, etc.).
- v. **Damage and alterations** – The structural response of the constructions may be affected significantly by the existing and general alterations over time. These changes should be modelled to assure a more realistic behaviour and accuracy in the prediction of the real performance and capacity.
- vi. **History** – The history of the constructions should be taken into account and integrate the model. The construction process, architectural additions and alterations, destruction in occasion of conflicts, natural disasters and long-term decay are some effects associated to the overall history of the constructions that must be considered and the study of these actions allows a better understanding of the construction performance and strength.

Although the scientific and technological progress allows the achievement of analysis more and more complex in a shorter period of time, most often, increasing the model detail and size can difficult the analysis of the structures behaviour and consequently the analysis of the obtained results, implying a lack of objectivity for the end-user, obtaining therefore more information although no specific and detailed (Silva 2008).

Given the high number of factors necessary for an historical construction assessment and the associated uncertainty and lack of knowledge on buildings connection and material properties, it is neither appropriate nor correct to propose a single method of analysis, therefor the correct approach is to propose the analysis with several methods, comparing the results of each method increasing in this way the confidence of the obtained results. Also, It is very important to validate the complex models with simple analytical calculations, such as, for example, the simple calculation of the structural element weight and compare the reactions obtained with the numerical model (Silva, Guedes et al. 2010).

### **3.5 Numerical modelling software**

Nowadays, for the analysis of historical constructions behaviour there are countless computational tools based on distinct theories and strategies, resulting in several levels of complexity, different calculation time involving obviously different costs. When selecting the most appropriate software it must have clearly defined the type of analysis required, the main goals and know, with no doubt, the advantages and the limitations of the available tools, not forgotten that more complex analysis are not necessarily synonymous with greatest results (Lourenço 2002).

In the numerical modelling it is important select, considering the reasons mentioned above, three separate pieces of software within a typical finite element system, the pre and post-processor for creation of the finite element model and for the presentation of

results, respectively, and the solver for the finite element equations assembly and solution.

### 3.5.1 GiD Software

The software GiD (2015) is a general pre and post-processor for numerical modelling in the science and engineering fields. This software answers to all the required needs of the numerical simulations such as: geometrical modelling, definition of analysis data, meshing, data transfer to analysis software and also the visualization of numerical results (Figure 3.4). GiD (2015) can be applied in several areas, including most situations in solid and structural mechanics, fluid dynamics, electromagnetics, heat transfer, geomechanics, among others, using finite element and volume, boundary element, finite difference, meshless or particle based numerical procedures. This software reduces time and consequently the costs associated with numerical analysis with high performance data input and post-processing, high speed and quality meshing (GiD 2015).

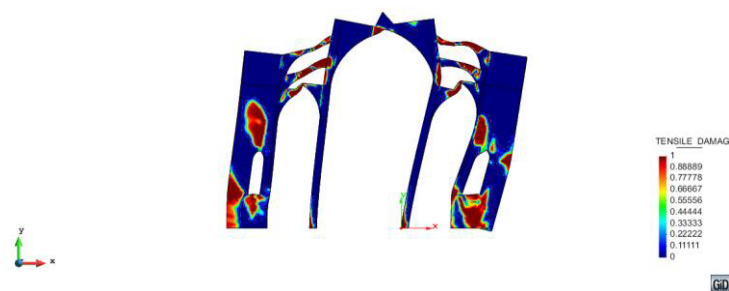


**Figure 3.4** – Tensile damage results of a seismic analysis of Mallorca Cathedral in GiD.

GiD (2015) has been developed by the International Center for Numerical Methods in Engineering (CIMNE), a research organization created in 1987 in the Universitat Politècnica de Catalunya (UPC) based in Barcelona, Spain, as a partnership between

the Government of Catalunya and UPC. The main aim of this international center, CIMNE, is the development of numerical methods and computational techniques for advancing knowledge and technology in engineering in applied sciences (CIMNE 2015).

### **3.5.2 COMET Software**

Besides GID software, also COMET is a program developed at CIMNE and it means COupled MEchanical and Thermal problems solved by the finite element method. COMET is a modular program intended to encompass a wide range of applications and to be used as a practical tool both in industrial and research environments. The COMET finite element library includes classical displacement-based elements, mixed displacement/pressure elements to deal with the incompressibility constraint and mixed stress/displacement formulations to reach the greatest stress-accurate response in highly non-linear analysis. The constitutive law library includes visco-elasticity, small and large strain plasticity, damage models, among others. The equation solver library ranges from direct to iterative solvers (COMET 2015). COMET is a program that may perform the following finite element analysis (Cervera, Saracibar et al. 2002):

- i. **Mechanical** – 2D or 3D problems subjected to static, quasi-static or transient dynamic conditions;
- ii. **Thermal** – 2D or 3D problems subject to transient or steady state conditions;
- iii. **Thermal/Mechanical** – 2D/3D problems in transient or steady state conditions.

### **3.5.3 MIDAS FEA Software**

The main focus of MIDAS includes civil, structural and mechanical engineering software development along with analysis and design support. The several programs of MIDAS have been developed since 1989 and used commercially since 1996, their

consistency has been established applying the software's over a innumerable number of real projects wherein the main strengths is to respond extremely fast to the needs of the practicing engineers (MIDAS 2016). As referred above, MIDAS holds solutions in several fields such as bridge, building, geotechnical and mechanical engineering.

MIDAS FEA is an advanced nonlinear and detail analysis system for civil and structural engineering applications, it is specialized for refined method analysis and hold unique capabilities that make possible efficiently complex structures models with plate and solid elements instead using 1D elements to simplify the model. Consequently, MIDAS FEA will be able to perform local analysis for elements and obtain in-depth and highly accurate calculations that are necessary for projects that involve refined method analyses (MIDAS 2016).

Since this solution is specialized for detailed and nonlinear analyses of civil structures, MIDAS FEA support several analysis including linear static analysis, construction stage analysis, modal analysis (Figure 3.5), transient analysis, cracking analysis, reinforcement analysis, geometry nonlinearity analysis, heat transfer analysis, among others (MIDAS 2016).

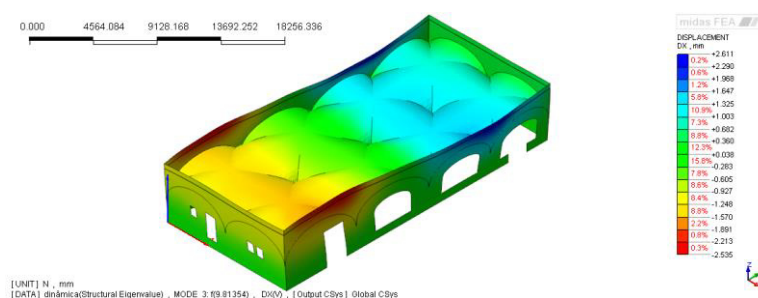


**Figure 3.5** – Mode 3 of structural eigenvalue analysis of Paço Real II by Midas FEA.



### 3.6 Final synthesis

The need of conservation and restoration of historical constructions caused the appearance of the structural analysis. In this chapter were presented the several methods of structural analysis, being the first one based on limit analyses where it is defined that a structure is in collapse, comparing those results with the real state of the structure. Due to the high computational capacity, it became possible to simulate the non-linear properties of the material, turning out the most used approaches for the assessment of masonry structures methods bases on finite element method, where there is a basic cell that represents a subpart of the structural element. Moreover, other methods based on discrete elements or macro-elements are used. However, in addition to all the advantages of structural analysis, there are some difficulties and limitations that need to be overcome.

It is important highlight that the choice of the most adequate approach for structural analysis should be based on the cost, the necessity of an experienced user, the use of the results and on the purpose of the structural analysis. It is possible conclude that, generally, advanced modelling is appropriate for understanding the behaviour and the existent damage and deformation of historical constructions and simplified modelling as limit analysis is adequate for overall structures, as buildings for example.

The evaluation of the structural capacity of historical constructions implies the need to overcome some difficulties such as, the geometry definition, the material characterization, the internal morphology of the structural members resorting to non-destructive testing, as was done for the case study of the building Paço Real II, extracting core samples (detailed in chapter 5), the actions definition, the identification of existing damages and deformations and the chronologic history of the building in analysis.

The next case studies, presented in the next chapters, have resourced to the referred software. GID software and COMET where used for the first case study – Mallorca Cathedral and MIDAS FEA was used for the second case study – One-story masonry building.

## CHAPTER 4

### MALLORCA CATHEDRAL

Designed in a Gothic style, the cathedral of Santa Maria in Palma de Mallorca, also known as La Seu, is one of the most emblematic monument in Spain, located in the city of Palma, Mallorca Island and it is classified as Cultural Heritage of National Interest (Mohamed 2015). The cathedral was constructed progressively over a period of 300 years, from 1306 to 1600 and presents typical features of the Catalan Gothic style such as, the high lateral naves, the chapels between massive buttresses and also the extremely slender octagonal piers (Pelà, Bourgeois et al. 2014).

In the present chapter will be exposed, summarized, the history of construction of the Mallorca cathedral, the description of the building and the existing damage and deformation. After this introduction to the case study, it will be introduced the

numerical model, relating essential parameters such as geometry, material, loading and boundary conditions and the mesh definition. Following, a sensitivity analysis is carried out in respect to the compressive strength, elastic modulus, fracture energy and tensile strength variation with a discussion of the results obtained.

## **4.1 History of construction**

The history of Mallorca cathedral construction can be divided in five distinct phase's since the beginning of its construction until the present days: from 1300 to 1370; 1371 to 1601; 1602 to 1851; 1852 to 1888; and from 1889 to the present. Notwithstanding the great efforts made by historians, there are still uncertainties and debates about the exact date of the conclusion of each part of the cathedral (Mohamed 2015).

### **i. Period from 1300 to 1370**

This first period is called the royal construction, the king Jaume II provided the financial support for the Trinity chapel construction (see part 1 of Figure 4.1) and in its crypt were lodged the tombs of the royal family. In this period, the apse of the Trinity chapel, named the Real chapel was concluded (part 2 Figure 4.1) and also the construction of six lateral chapels, three on the south side and more three on the north side of the cathedral (see part 3 of Figure 4.1).

### **ii. Period from 1371 to 1601**

It was in this period that the cathedral full construction was carried out, starting with the first bay of the nave in the year 1374 (see part 4 of Figure 4.1) followed with the conclusion of the second bay and two lateral chapels by the year 1385 (see part 5 of Figure 4.1). By the end of the XIV century,

it was built the “Portal del Mirador” (west entrance) and the adjacent chapel (see part 6 of Figure 4.1), continuing with the construction of the third bay with the two lateral chapels and the fourth bay (see part 7 and 8 of Figure 4.1, respectively). In spite of the difficulties of the fifth bay construction due to the span increasing, it was finished around 1560 along the three chapels on each side (see part 9 of Figure 4.1). The remaining three bays of the nave were easily constructed in the next years due to economical funding’s (see part 10 of Figure 4.1), concluding the full structure of the cathedral with the construction of the “Portal Mayor”, west façade (see part 11 of Figure 4.1)

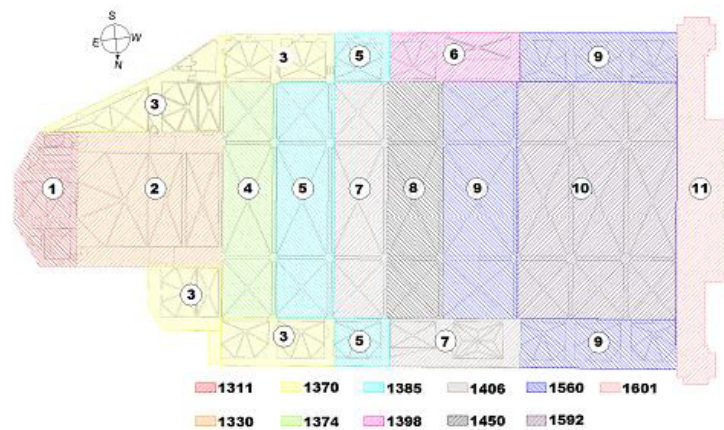


**Figure 4.1** – Progress of Mallorca cathedral construction from 1306 to 1601 (Mohamed 2015).

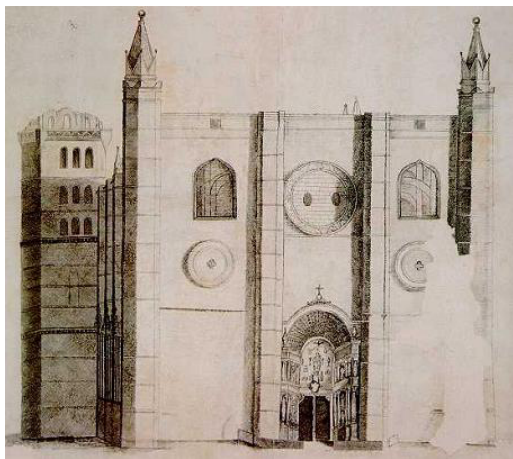
### iii. Period from 1602 to 1851

This period can be designated as the reconstruction period, in which the first structural problem occurred. In this period, several parts of the cathedral or failed or manifested severe cracking, leading to the decision of dismantling and rebuilding again. In the 17<sup>th</sup> and 18<sup>th</sup> century, some of the vaults and

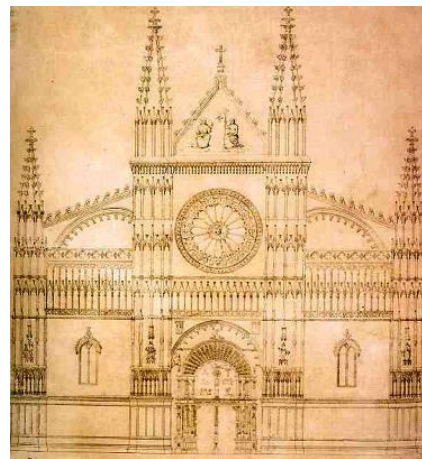
arches suffered severe deformations furthermore some of them collapsed and were reconstructed. It should be noted that the earthquake of 18<sup>th</sup> March in 1660 also compromised the structural safety of the Mallorca cathedral, resulting directly in the failure of two arches and lead to the west façade out-of-plane overturning.

#### iv. Period from 1852 to 1888

This period focused mainly in the reconstructing of the west façade and the new architect chosen, Juan Peyronnet Baptist, presented the new design in 1854. The new façade presented several differences from the previous and also from the rest of the cathedral, presenting a flamboyant neo-Gothic style (see Figure 4.2).



a)



b)

**Figure 4.2** – Comparison between the original west façade a) with the new design b) of Mallorca cathedral.

#### **v. Period from 1889 until the present**

This last period, since 1889 until the present includes several interventions, such as the carried out by Gaudi with the collaboration of other architects between 1904 and 1914, moving the Gothic choir from the central nave to the presbytery. In addition, during the last decades, the Mallorca cathedral experienced continuous repair and maintenance works including the restoration of the west and south façades about ten years ago.

### **4.2 Description of the building**

The Mallorca cathedral is made of limestone masonry obtained from the local quarries of Santanyi, Mallorca (Das 2008). The most resistant limestone available in the island was used to build the piers, the rest of the members, as the vaults and the buttresses were built using poorer limestone, comparatively. Regarding the vaults, the lateral ones were filled with a lightweight pottery although the central vaults, except for the resistant backing in the lower region, do not present any filling (Roca, Cervera et al. 2013).

The structure of the cathedral can be divided in two distinct parts through the plan and the longitudinal sections (see Figure 4.3 and Figure 4.4, respectively), the main nave forms the first body and the second includes the choir and the surrounding chapels. In more detail, the first body is composed by the central and two lateral naves and it is bordered by eight heavy buttresses lodging between the lateral chapels. The second body includes the Royal chapel, a single nave of Gothic construction and the Trinity chapel.

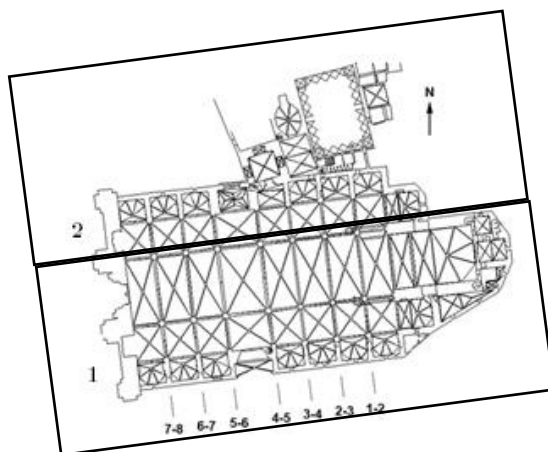


**Figure 4.3** – Plan at roof level of Mallorca cathedral (Roca, Cervera et al. 2013).

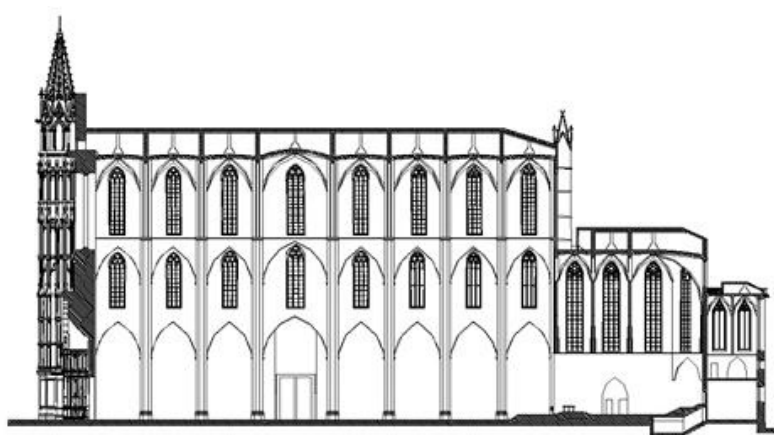


**Figure 4.4** – Longitudinal section of Mallorca cathedral (Roca, Cervera et al. 2013).

The Mallorca cathedral has a length and width of 120 and 55 meters, respectively, and it is formed by three parts in the longitudinal direction from the east side to the west side, which are a small apse, the Trinity chapel (see K in Figure 4.5), a choir in the shape of single nave Gothic construction, the Royal chapel (see J in Figure 4.5) and the main nave surrounded by the lateral chapels, as shown in 1-18 Figure 4.5 (Das 2008).

As referred above, the main nave is composed by the central nave that spans around 20 meters and reaches 43.9 meters at the vaults keystone and by two collateral naves



surrounded by several lateral chapels built in between the buttresses, the referred naves are sustained by octagonal shape piers with a circumscribing diameter of 1.6 or 1.7 meters and a height of 22.7 meters to the springing of the vaults (Das 2008). The cathedral exhibits certain particularities that show the importance of the different structural elements placing. As seen in Figure 4.6, the double flying arches were placed with the main aim to transfer the lateral thrust offered by the central vault towards the buttresses (Das 2008).

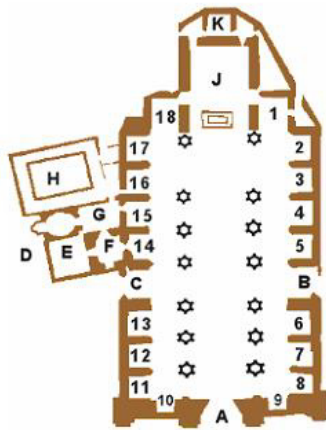


**Figure 4.5** – Mallorca cathedral interior arrangement (Das 2008).



**Figure 4.6** – Double battery of flying arches of Mallorca cathedral (Das 2008).

Another detail is the presence of some necessary overloads in the shape of triangular masonry masses to guarantee the cathedral stability, on the transversal arches (see Figure 4.7 a) a symmetrical triangular wall reaching its maximum depth at the key of the arch and on the keys of the vaults, the overload occurs as a pyramid of square bases (see Figure 4.7 b), these overloads are essential due to the fact that the vaults are not filled with rubble masonry but only with a light structure composed of slender stone wallets and slabs (Mohamed 2015).



**Figure 4.7** – Additional overloads of Mallorca cathedral: a) over the transversal arches key and b) over the vaults keys.

### 4.3 Existing damage and deformation

Mallorca cathedral shows a satisfactory conservation condition notwithstanding some damage and deformation revealed by local inspection. This damage and deformation is present in several parts of the cathedral, more specifically in the piers, buttresses and flying arches (see Figure 4.8), being some of these cracks repaired during restoration works (Roca, Cervera et al. 2013).

The cracks visible in the piers appears close to the corners of the octagonal section and could be caused, probably, by compression forces. The piers also reveals, remarkable curvature and lateral displacement especially along the direction transverse to the nave, however this deformation is progressing at a very low rate, fact justified by the monitoring during the last years (Roca, Cervera et al. 2013).

The flying arches, predominantly those of the upper battery, exhibit some deflection that can be caused by the overall deformation of the structure and by the outward rotation of flying arches. It should be noted that, non-mechanical effects, can contribute to this deflection, such as the later loss of mortar in joints due to chemical problems (Roca, Cervera et al. 2013).



a)



b)



c)



d)

**Figure 4.8** – Existing damage and deformation of Mallorca cathedral: a) at the top pf the pier, b) cracks at the base of the pier, c) cracks in a buttress following the perimeters of a false window and d) deformed flying arches.

The Mallorca cathedral, from a structural point of view, is an outstanding case of exemplar construction and holds highly optimized members, at least against the gravitational action. This dead load is not a problem in the short term, however, creates some concern when it is considered in long term as the continuous progression of deformation along geometric nonlinear effects. Considering the seismic capacity of Mallorca cathedral, the existence of transverse arches, robust external buttresses and light vault filling contribute in a favourable way to the seismic response of the cathedral, however, some structural features as slender piers and large spans can induce seismic weakness to the cathedral, leading to the possible need of a detailed seismic assessment (Roca, Cervera et al. 2013).

#### 4.4 Numerical model

Around one century ago, (Rubió 1912) carried out a pioneering structural assessment and since then, a relevant number of studies have been realized on the Mallorca cathedral which include aspects such as the history of construction, the damage and deformation assessment and analysis, the characterization of building materials, the seismic safety assessment, the static and dynamic monitoring, amongst others (Mohamed 2015).

The model adapted for the numerical analyses of the present case study is based on continuum damage mechanics theory. The mechanical damage in masonry in the presence of cracking and crushing is described by the Tension-Compression damage model (Faria, Oliver et al. 1998), under elastic regime, based on the theory of effective stress tensor  $\bar{\sigma}$  related to strains  $\varepsilon$ , being  $C$  the isotropic linear-elastic constitutive tensor:

$$\bar{\sigma} = C : \varepsilon \tag{4.1}$$

Since there is a different mechanical behaviour between tension and compression, it was introduced a slip of the effective stress tensor into tensile and compressive components,  $\bar{\sigma}^+$  and  $\bar{\sigma}^-$ , respectively:

$$\bar{\sigma}^+ = \sum_{i=1}^3 \langle \bar{\sigma}_i \rangle p_i \otimes p_i \quad \text{and} \quad \bar{\sigma}^- = \bar{\sigma} - \bar{\sigma}^+ \quad (4.2)$$

where  $\bar{\sigma}_i$  represents the  $i^{\text{th}}$  principal stress value from tensor  $\bar{\sigma}$ ,  $p_i$  denotes the unit vector associated with its respective principal direction and the symbol  $\langle . \rangle$  is the Macaulay brackets, if  $x \geq 0$ ,  $\langle x \rangle = x$  and if  $x < 0$ ,  $\langle x \rangle = 0$  (Roca, Cervera et al. 2013).

Once defined the variables of internal damage,  $d^+$  and  $d^-$ , connected with the sign of the stress and consequently with tension and compression, the constitutive equation is the following:

$$\sigma = (1 - d^+) \bar{\sigma}^+ + (1 - d^-) \bar{\sigma}^- \quad (4.3)$$

It should be noted that when the material is undamaged the internal damage variables are equal to zero and when the material is completely damaged the variables assume the value (Roca, Cervera et al. 2013).

For masonry, different damage criteria are assumed for tension and compression stress states in order to describe different failure mechanisms, for example cracking and crushing for the material, being the damage functions defined as:

$$\phi^{\pm}(\tau^{\pm}, r^{\pm}) = \tau^{\pm} - r^{\pm} \leq 0 \quad (4.4)$$

representing  $\tau^{\pm}$  the scalar positive quantities, designated as equivalent stresses and defined with the intention of compare different stress states in two or three dimensions (Roca, Cervera et al. 2013):

$$\tau^{\pm} = [\bar{\sigma}^{\pm} : \Lambda^{\pm} : \bar{\sigma}^{\pm}]^{1/2} \quad (4.5)$$

The tensors  $\Lambda^{\pm}$  define the shape of each damage criterion. In the present work, particularly with masonry, it is assumed that  $\Lambda^{+} = p_i \otimes p_i \otimes p_i \otimes p_i$ , which corresponds to the Rankine criterion in tension, while  $\Lambda^{-} = C/E$  represents the compression case, where  $E$  is the Young's modulus. For the two-dimensional model case, Figure 4.9 represents the composite damage criterion for masonry, where  $\bar{\sigma}_1$  and  $\bar{\sigma}_3$  are the principal stresses for the direction 1 and 3, respectively.

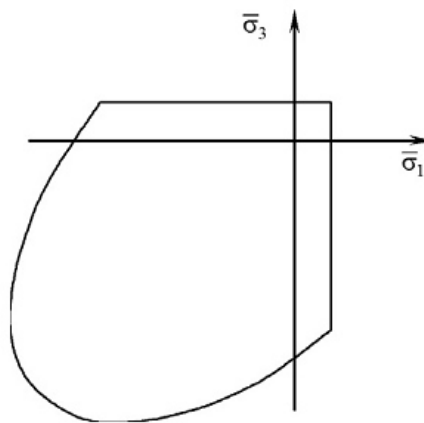


**Figure 4.9** – Composite damage surface adopted for masonry (Roca, Cervera et al. 2013).

The variables  $r^\pm$  characterize the internal stress like variables representing the current damage threshold and their values control the expanding damage surface size. The initial values of the damage are  $r_0^\pm = f^\pm$ , where  $f^+$  is the uniaxial strength in tension and  $f^-$  in compression (Roca, Cervera et al. 2013). The analyses presented in this chapter were carried out with COMET, a FE software developed at the International Centre of Numerical Methods in Engineering (CIMNE). The pre and post-processing was carried out with a software also developed at CIMNE, GiD. The 2D numerical model was prepared for the sensitivity analysis, to carry out a simulation of long-term deformation and a seismic load analysis. Subsequently it will be presented the numerical model definition from geometry, material properties, loading and boundary conditions to mesh definition. In the present work, the numerical model exclusively used in order to perform the sensitivity analysis, since there are several broader studies which focus in the Mallorca cathedral assessment and structural analysis, such as (Rubió 1912), (Mark 1982), (Maynou 2001), (Salas 2002), (Clemente, Roca et al. 2006), (Pelà, Cervera et al. 2011) and (Roca, Cervera et al. 2013), amongst others (Figure 4.10 to Figure 4.13).

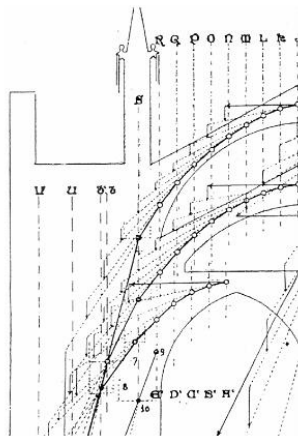


**Figure 4.10** – Static graphical analysis of the Mallorca cathedral (Rubió 1912).



**Figure 4.11** – Photo elastic analysis with the distribution of internal forces (Mark 1982).



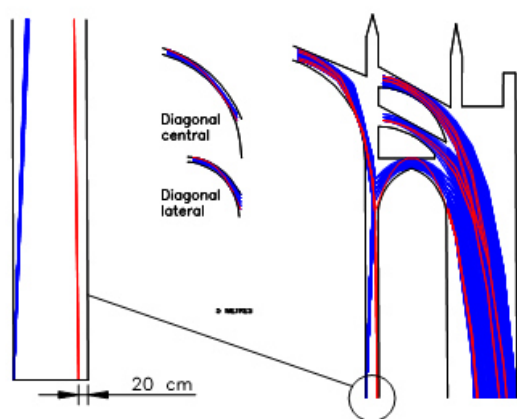


**Figure 4.12** – Analyses by line pressures of Mallorca cathedral (Maynou 2001)

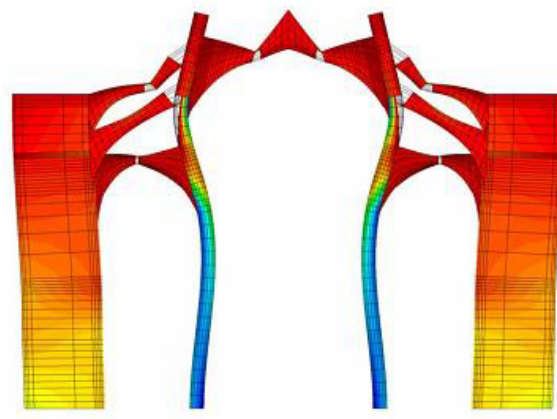


**Figure 4.13** – Collapse mechanism of Mallorca cathedral (Salas 2002).

#### 4.4.1 Geometrical configuration

The numerical model was prepared in two dimensions, as referred, through a geometry created by (Roca, Cervera et al. 2013) which is based on a single typical bay including piers, buttresses, flying arches, nave vaults and aisles (see Figure 4.14). Note that the false window existing in the buttresses has been modelled as a real opening characterized by a reduced thickness.

A plane-stress finite element model equivalent to the 3D model of the bay has been prepared by preserving the weights of different structural elements. Plane stress is a state of stress in which the normal stress,  $\sigma_z$ , and the shear stresses  $\sigma_{xz}$  and  $\sigma_{yz}$  directed perpendicular to the  $xy$  plane are assumed to be zero, this is assumed because the geometry of a body is basically that of a plate with one dimension much smaller than the others, regarding the loads that are applied uniformly over the thickness of the plate. The plane stress is the simplest and common form of behaviour for continuum existent structures.



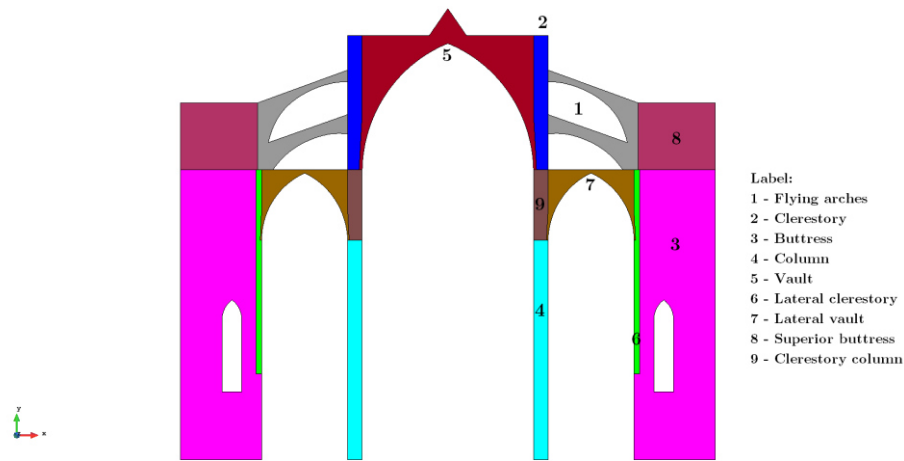


**Figure 4.14** – Different structural elements in the two-dimensional FE model.

#### 4.4.2 Material properties

Results of the in-field survey allowed the definition of the structural elements properties, the non-structural element such as infills, pinnacles and stone pyramids over the vaults have not been included in the model however their weight was applied on the rest of the structure (Roca, Cervera et al. 2013).

The model has been calibrated taking into consideration that the weight of all the members is identical to the corresponding one in the three dimensional model, as can be seen in the Figure 4.15, it should be noted that the structural elements with the same colour either in the 2D and 3D model have the same weight.

Furthermore, the thickness of the elements in the two dimensional model was modified in a manner that after a linear elastic analysis, the 2D and the 3D models produce equivalent deformed shapes (Roca, Cervera et al. 2013), the material parameters of the structural elements adopted for the numerical analysis are described in Table 4.1.

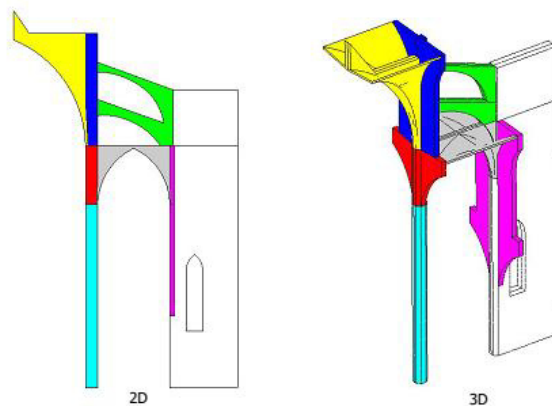


**Figure 4.15** – Equivalence between the 2D and the 3D models.

**Table 4.1** – Material properties of the structural elements of the Mallorca Cathedral.

	$\gamma$ (kg/m <sup>3</sup> )	E (MPa)	$\nu$	$f_t$ (MPa)	$f_c$ (MPa)	$G_r^+$ (J/m <sup>2</sup> )	$G_r^-$ (J/m <sup>2</sup> )
<b>Flying arches</b>	2400	8000	0.2	0.4	8.0	100	40000
<b>Clerestory</b>	2500	2000	0.2	0.1	2.0	100	40000
<b>Buttresses</b>	2100	2000	0.2	0.1	2.0	100	40000
<b>Columns</b>	2400	8000	0.2	0.4	8.0	100	40000
<b>Vault</b>	2130	2000	0.2	0.4	8.0	100	40000
<b>Lateral clerestory</b>	4200	2000	0.2	0.1	2.0	100	40000
<b>Lateral vault</b>	6060	2000	0.2	0.1	2.0	100	40000
<b>Superior buttress</b>	2100	2000	0.2	0.1	2.0	100	40000
<b>Clerestory column</b>	2220	8000	0.2	0.4	8.0	100	40000

The masonry compressive strength was estimated through previous experience for comparable materials and the tensile strength was presumed equal to 5% of the

compressive strength. The structural identification procedure described in (Martínez 2007) allowed the assessment of the Young modulus. Regarding the fracture energy, since it is not possible to measure experimentally this parameter, the value was assumed based on previous experience (Roca, Cervera et al. 2013).

#### **4.4.3 Loading and boundary conditions**

The structural analysis of the Mallorca cathedral is divided in two distinct sections. The first, focuses on a gravitational analysis simulating a long-term deformation and the second a seismic load analysis. As referred in the sub-chapter 4.4.1, both analyses were carried out on a plane-stress FE model. Regarding the boundary conditions, the displacements in the XX and YY directions were blocked, more specifically reactions at the base of the structure.

For the long-term deformation, vertical load analysis, only one loading condition was applied, the gravitational load. This load is vertical, being increased step by step, gradually, up to the structure failure. The seismic load analysis of the representative bay was assessed by a pushover analysis involving a gradual application of lateral equivalent static forces onto the structure. In this analysis, two loading conditions have been applied in consecutive phases, in the first step was applied the gravity load, following with the application of lateral forces proportional to the mass distribution, increased gradually (500 steps) until reaching failure.

#### **4.4.4 Finite element meshing**

After the previous phases, from the definition of geometry, material properties, loading and boundary conditions, several analyses with distinct meshing with the main purpose to differentiate areas where it would be most convenient to refine the size of the mesh elements. The areas with a higher concentration of stresses end up

having to be the areas with more elements leading to a refined mesh, such as the base of the window in the buttress, the base of the piers, the connection between the pier and the clerestory and the joining area of the buttresses with the clerestory (see Figure 4.16). These referred areas have relatively high gradients of stresses, where the damage is localized thus being convenient a more refined mesh.

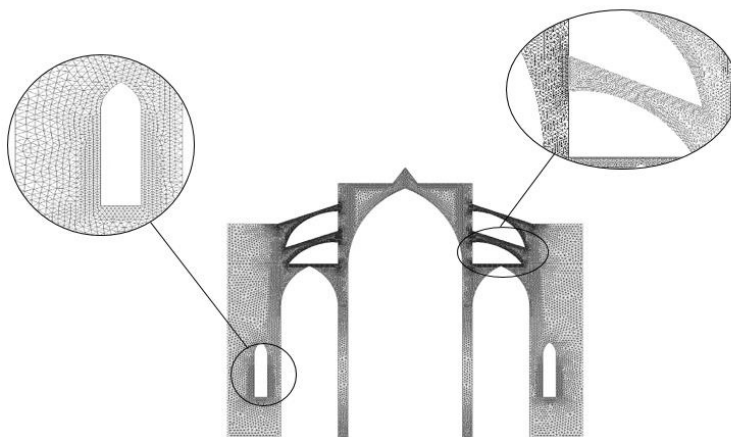


**Figure 4.16** – Finite element mesh adopted for the analysis.

The entire bay structure has been discretized by a finite element mesh composed by 32858 triangular elements and 17628 nodes. The number of integration point per element is one, this integration is performed through the Gauss method.

## 4.5 Sensitivity analysis

The purpose of a sensitivity analysis is to understand the influence of a certain parameter in the global response of a structure. This study also allows to understand the importance of the uncertainties included in some intrinsic properties of the numerical model. In the present work will be studied the influence of four important parameters in the material characterization, which are: (i) compressive strength; (ii) elastic modulus; (iii) fracture energy, (iv) tensile strength. The variation of this

material properties was studied either for the gravitational (vertical load) either for the seismic assessment (pushover analysis) and as previously stated, both analyses were carried out in a two dimensions' numerical model. In each analysis, the structure is analysed with a load increment until the failure, and when a parameter is varied the other parameters remain constant, thus assessing the influence of each one individually. For the vertical loads the displacements were obtained for the centre of mass (node number 12360) and for the seismic analysis was analysed a lateral node (node number 17628) as shown in Figure 4.17.

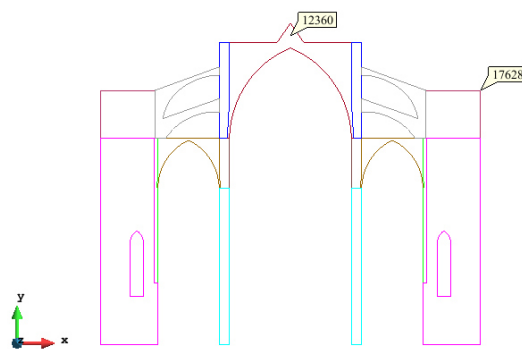


**Figure 4.17** – Location of the analysed nodes for the vertical load analysis and seismic assessment.

It is important to highlight that the type of damage mechanisms for both analysis do not change with any variation either the value or the parameter. In Figure 4.18 and Figure 4.19, it is possible see the damage mechanism for the vertical load analysis and for the seismic analysis, respectively.

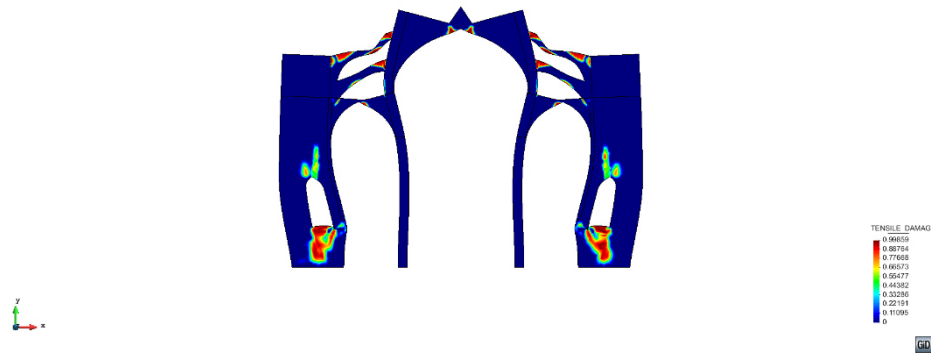


**Figure 4.18** – Damage mechanism with half of the tensile strength value for the vertical load analysis.

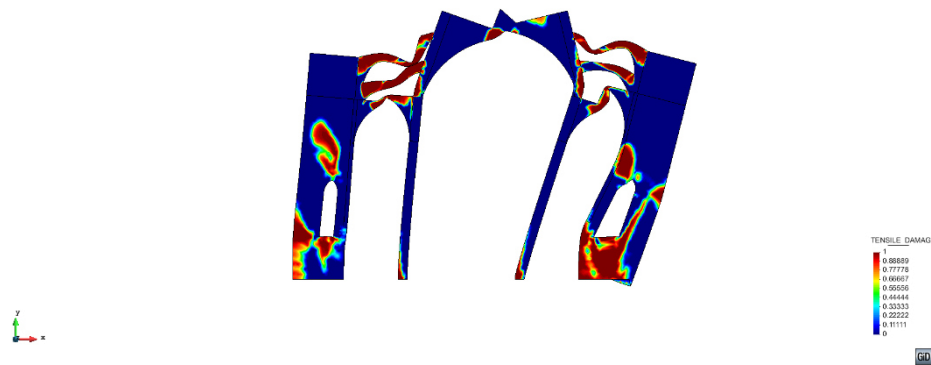


**Figure 4.19** - Damage mechanism with double of the elastic modulus value for the seismic analysis.

#### 4.5.1 Compressive strength

Compressive strength is the maximum compressive stress that under a load, applied gradually, a material can sustain without reaching the failure. Departing from the original model, were performed several analyses with the purpose to understand the influence of the variation of this parameter over the structure. Therefore, the initial compressive strength was multiplied by the factors 0.5, 0.75, 1.4 and 2.

### a) Vertical load analysis

Regarding the results for the vertical (considering only the dead load) analysis of the compressive strength variation, as can be seen in the Figure 4.20 and Figure 4.21, it is obtained a linear relation. When doubled the value of the compressive strength it is obtained a strength increase of 50% and when it reduces to half of the value a decrease of the compressive strength is around 47%. This linearity is caused due to the ultimate load factor being directly proportional to the compressive strength of the material, this occurs because the collapse of the structure is triggered by the complete rupture of the buttress in the window area and in this area crushing damage that is caused by excessive compression. It is important to highlight that all the produced damage mechanisms for all the analyses are similar, exhibiting material crushing close to the windows area and in some areas of the flying arches.

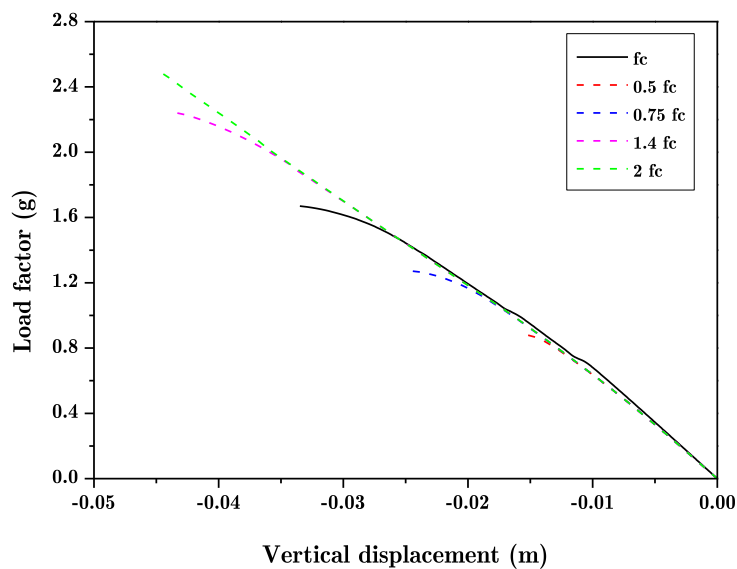


**Figure 4.20** – Vertical displacement vs load factor regarding the compressive strength variation  
– vertical load analysis.

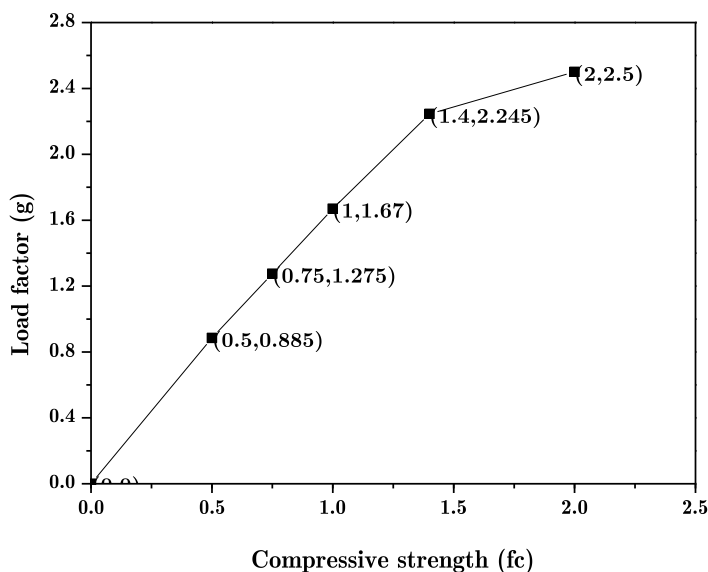


**Figure 4.21** – Relationship between the compressive strength variation with the collapse load factor– vertical load analysis.

### b) Seismic assessment

As referred above, the seismic assessment has been evaluated through a pushover analysis with a gradual application of horizontal forces onto the structure.

The influence of the compressive strength variation is slightly different when it is performed a pushover analysis instead of a long-term deformation analysis. As can be seen in the figures below, Figure 4.22 and Figure 4.23, the decrease of the compressive strength has more impact on the overall behaviour of the structure than its increase. For a reduction of 25% of the value of this parameter there is a strength decrease up to 43%, nearly half, but when it is increased the compressive strength in the same proportion (25%), the strength of the structure is improved about 30%.



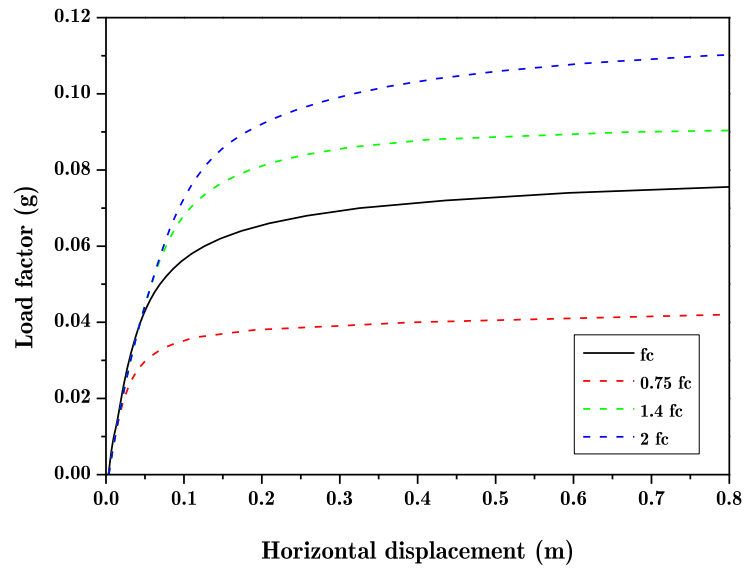


**Figure 4.22** – Horizontal displacement vs load factor regarding the compressive strength variation – seismic assessment.

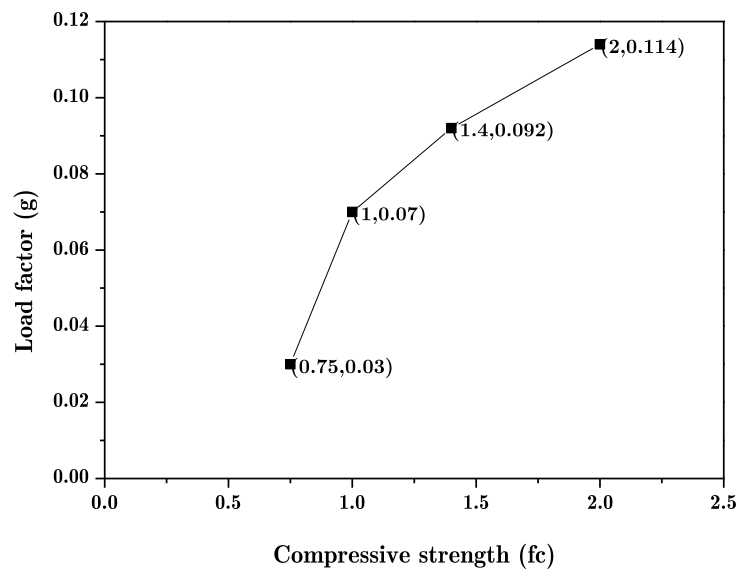


**Figure 4.23** – Relationship between the compressive strength variation with the collapse load factor – seismic assessment.

#### **4.5.2 Elastic modulus**

The elastic modulus also known as modulus of elasticity, tensile modulus and Young's modulus is a value that measure's the resistance of a material to be deformed, elastically, when subjected to loads, in other words, is a measure of stiffness of an elastic material. This parameter is defined as the ratio of stress, force per unit area, along an axis to strain, ratio of deformation over initial length, along that axis.

The masonry modulus of elasticity is related as a factor over the compressive strength. To understand the effect of the elastic modulus variation of a material, it was analysed the effect of the duplication of this parameter and also its reduction to half and quarter of the value.

##### **a) Vertical load analysis**

Either doubled or halved the elastic modulus, the collapse load factor increases and decreases 5%, respectively, being possible to conclude that is a linear relation, however very slightly (Figure 4.24 and Figure 4.25). The vertical displacements variation is more significant, predominantly when the elastic modulus decreases, as can be shown in the Figure 4.24, the 50% and 75% reduction of this parameter leads to an increasing of the vertical displacements of 3 centimetres and 8 centimetres, respectively. With this results it is possible to conclude that the higher the elastic modulus, more stiff the material is, in other words, the elastic modulus increase leads to a smaller elastic deformation, as expected. The collapse mechanism is not changed with the elastic modulus variation, in fact remains the same as the previous case analysis for the compressive strength variation.

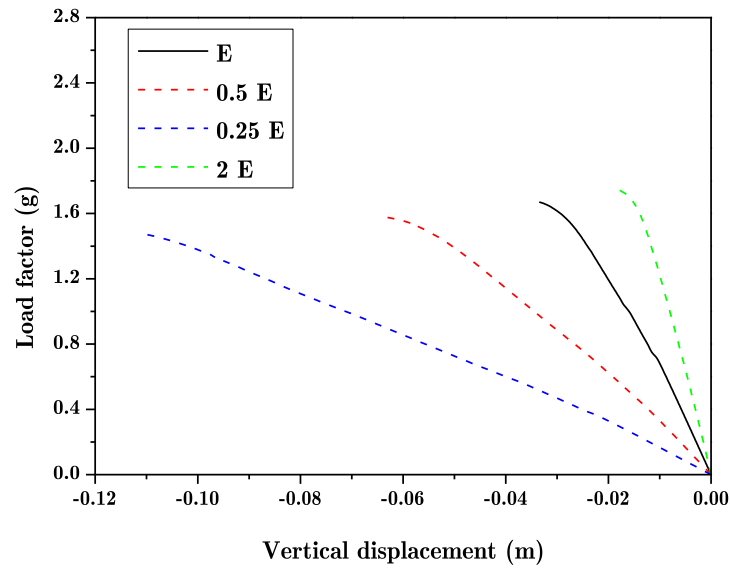


**Figure 4.24** – Vertical displacement vs load factor regarding the Elastic modulus variation – vertical load analysis.

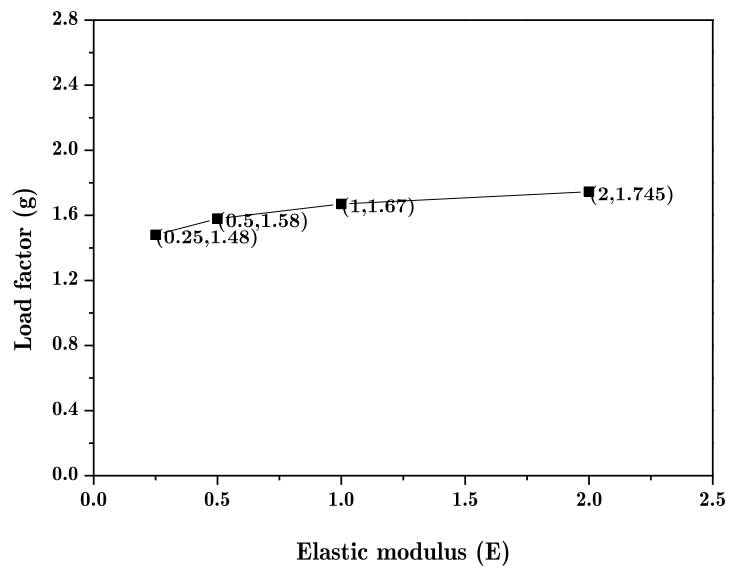


**Figure 4.25** – Relationship between the elastic modulus variation with the collapse load factor– vertical load analysis.

**b) Seismic assessment**

Regarding the pushover analysis, similar to the previous parameter analysis, the elastic modulus reduction causes more effect over the structure response than its increase. Wherein the elastic modulus assumes half of its value, it is reduced the strength about 33% however when the value of this parameter is doubled there is only an increase of the strength of 14% (see Figure 4.26 and Figure 4.27).

The variation of the elastic modulus has more influence on the seismic assessment than the vertical load analysis due to the material stiffness, being the reduction more effective over the structure response than the increase of this parameter.

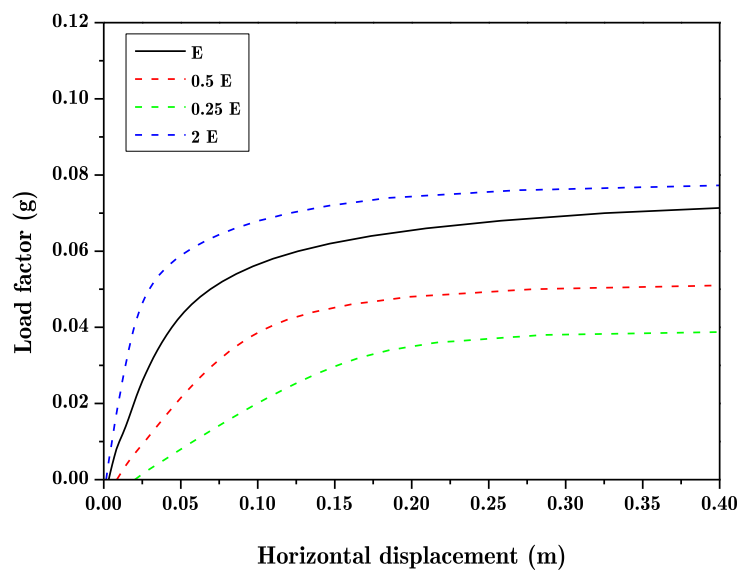


**Figure 4.26** – Horizontal displacement vs load factor regarding the elastic modulus variation – seismic assessment.

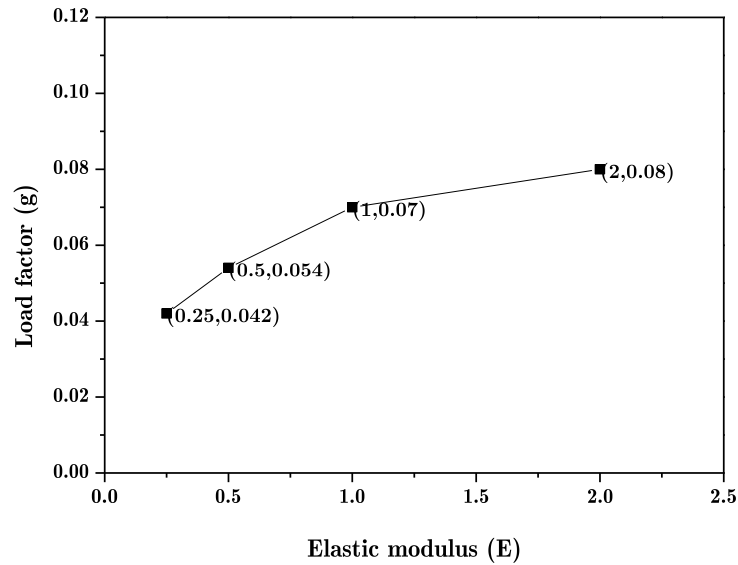


**Figure 4.27** – Relationship between the elastic modulus variation with the collapse load factor – seismic assessment.

### 4.5.3 Fracture energy

The fracture energy or energy release rate is the energy dissipated through the fracture per unit of a fractured surface area. In other words, the fracture energy is defined as the amount of necessary energy to create an area unit of crack. To define the softening behaviour, it was introduced the fracture energy concept, being softening the gradual decreasing of the mechanical resistance resulting from a continuous deformation increasing imposed on a material or a structure.

The lack of appropriate tests for the determination of this parameter leads to an empirical estimation. In the present work, will be studied two distinct and opposite cases, a practically perfect fragile behaviour ( $0.1 G_f$ ) and a practically perfect plastic behaviour ( $1000G_f$ ).

**a) Vertical load analysis**

From the analysis of the Figure 4.28 it is shown that a more fragile material decreases, significantly, the collapse load factor multiplier attained by the structure. More particularly, for the most fragile case ( $0.1 G_f$ ), fails for only 21% of the necessary load for the initial conditions. When the fracture energy is increased to  $1000G_f$ , a resistance increase of 20% is attained, so in other words, reducing this parameter reveals to be much more influent on the global response of the structure than its increase. It is expected that the models with lower fracture energy collapse in an earlier stage, since in these cases there is a faster energy dissipation, leading to a faster transmission of stresses by the damage elements to the surrounding ones, thereby accelerating the process of structural deterioration. Nevertheless, the damage mechanisms of the structure are practically independents of the fracture energy value selected or used.

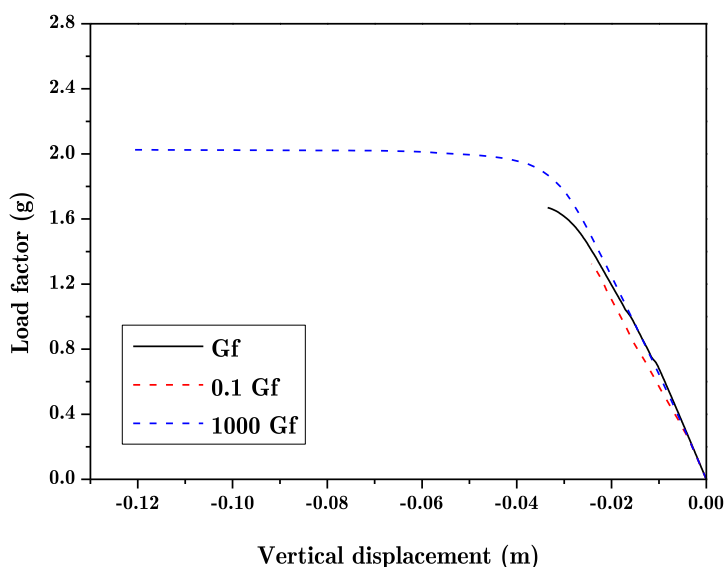


**Figure 4.28** – Vertical displacement vs load factor regarding the fracture energy variation – vertical load analysis.

## b) Seismic assessment

Analysing the results of Figure 4.29, it is easily noticeable that the reduction in 10 times of the fracture energy causes more influence in the global response of the structure than the 1000 times increase of this parameter. Once again, along what occurs in the structure with the variation of the parameters discussed before, the reduction of this value is more significant. The decrease of the fracture energy will implicate a drastic reduction in the amount of necessary energy to create an area unit of crack to more than half, and the opposite does not happen when the value is increased. This happens due to the non-linearity of the material and also with the main collapse mechanism of the structure in the case of this 2D model section.

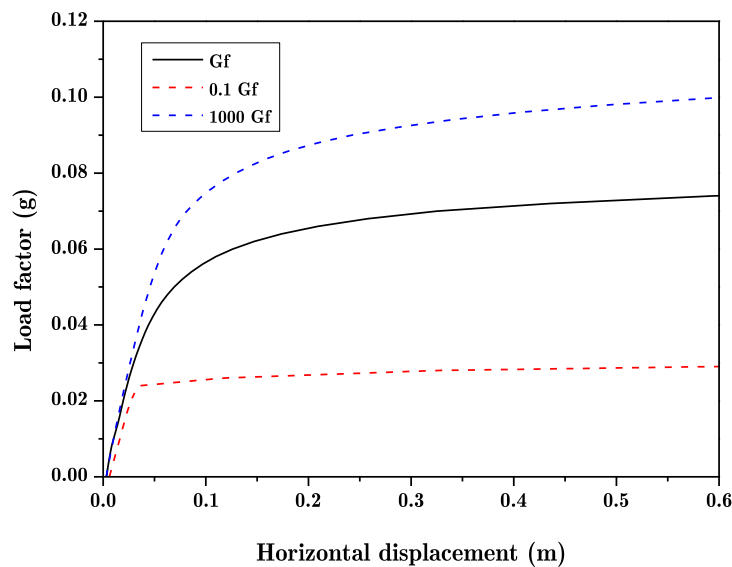


**Figure 4.29** – Horizontal displacement vs load factor regarding the fracture energy variation – seismic assessment.

#### **4.5.4 Tensile strength**

The tensile strength is one of the most difficult material parameters to estimate for the historical constructions. However, the tensile strength takes very low values for masonry due to the weak connection between the units and the mortar, in fact, there are several cases wherein it is assumed a null value of tensile strength. In general, in masonry, this parameter is not more than 10% of its compressive strength. It is important to assess the influence of the tensile strength on the overall strength of the structure since the structural damage that occurs in most structures is mainly associated with damage through tension, for example bending and tensile cracking.

For this material parameter, it was performed the sensitivity analysis with 3 values for reduced strengths, 10%, 25% and 50%. It was also increased this value to the double and also five times more.

##### **a) Vertical load analysis**

The analysis of the tensile strength variation, as shown in Figure 4.30 and Figure 4.31, allows to conclude that there is a direct relationship between the collapse load multiplier and the tensile strength of the material. The reduction by half of this parameter leads to a strength loss around 45% of the original structure and an increase to the double of the initial tensile strength lead to a strength increase of about 49%.

It should be noted that the increase of this parameter to more than double revealed a very slight influence as shown in Figure 4.31.



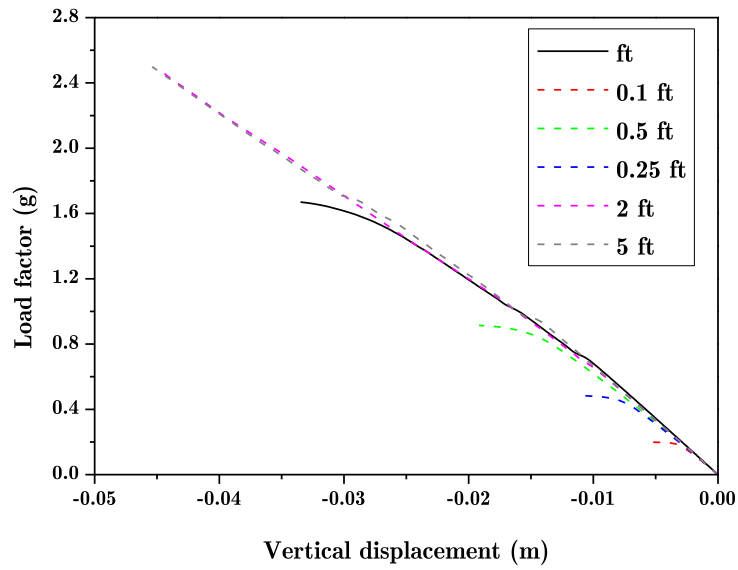


**Figure 4.30** – Vertical displacement vs load factor regarding the tensile strength variation – vertical load analysis.

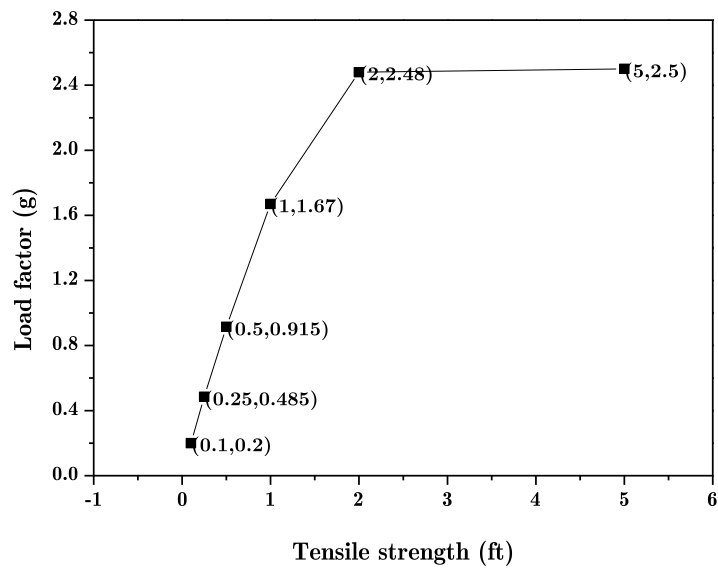


**Figure 4.31** – Relation between the tensile strength variation with the collapse load factor – vertical load analysis.

## b) Seismic assessment

For the study of the tensile strength variation, regarding a seismic assessment, it was only possible to evaluate the influence of this parameter increase. Once for this analysis, first was applied the gravity load and only then applied the lateral forces proportional to the mass distribution, the reduction of the tensile strength led to the failure of the structure yet in the vertical load analysis thus making it impossible to analyse that effect in the presence of a pushover analysis. As shown in the Figure 4.32 and Figure 4.33, when the value of the tensile strength is duplicated, there is an increase of the strength in the global response of the structure of about 30%, however when this parameter is increased 5 times, the strength increases to 58% which leads us to conclude that, eventually, the increase of the tensile strength several times will not highlight significant influence over the structural response.

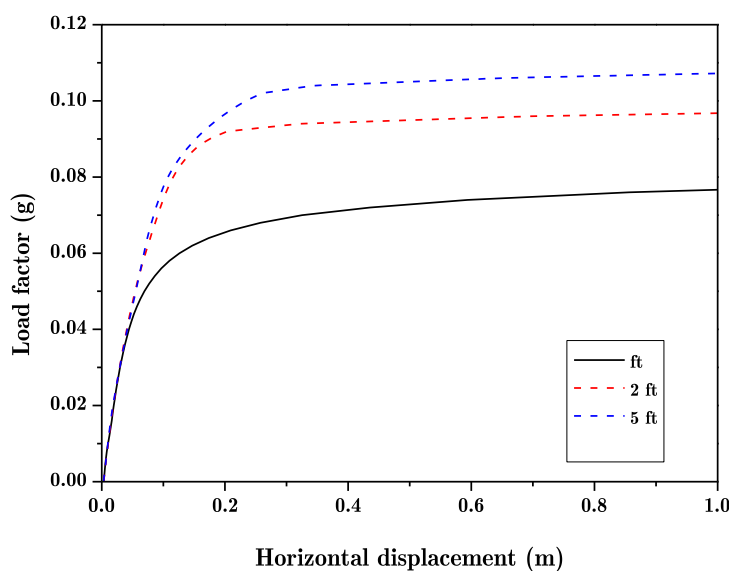


**Figure 4.32** – Horizontal displacement vs load factor regarding the tensile strength variation – seismic assessment.

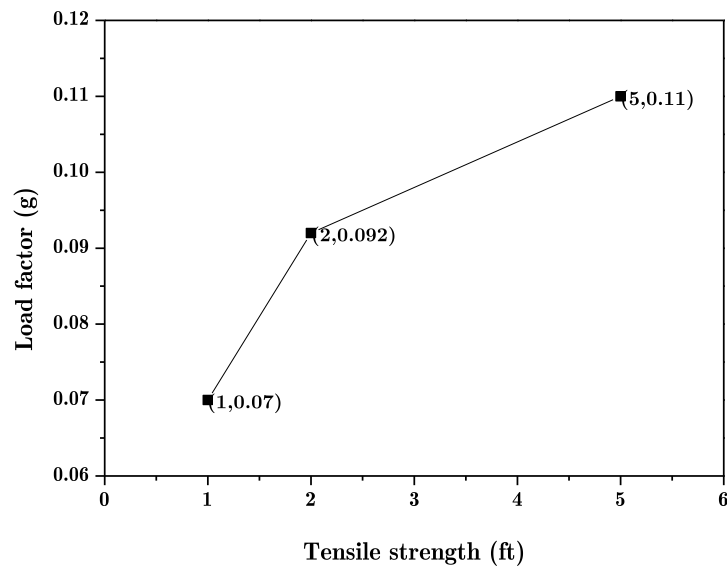


**Figure 4.33** – Relationship between the tensile strength variation with the collapse load factor – seismic assessment.

## 4.6 Final synthesis

The focus of this chapter is understanding the influence of the variation of a certain parameter over the global response of a structure, in this case, the Palma de Mallorca Cathedral.

Firstly, it is easily perceptible that whatever may be the variation of the several parameters analysed the effects are more noticeable in the seismic assessment than in the vertical load analysis.

It is possible to conclude, through the sensitivity analysis, that reducing the value of a parameter causes more effects on the global response of the structure than its increase, specifically in the case of the pushover analysis since in the long-term deformation either reduced or increased the value, the parameter variation impact

over the overall behaviour/response of the structure is very similar. It is the variation of the compressive and tensile strength that causes more effect over the structure.

Regarding the damage mechanism, it is also important to highlight that the damage mechanism of the structure remains the same regardless of the parameter and variation, only changing as expected with the analysis performed.

## CHAPTER 5

### SÃO JORGE CASTLE – PAÇO REAL II BUILDING

The building in study, Paço Real II, is located in the classified area of São Jorge castle, Lisbon, rising up in a dominant position on the highest hill of the historic centre offering one of the most beautiful views of Lisbon and the Tejo River. The building Paço Real II is part of the panoramic tour, next to Paço de Alcáçova tower with a preponderant orientation North/South. The fortification was built in the mid-11<sup>th</sup> century by the Moors and it was the last defensive stronghold for the elite who resided on the Citadel, the palaces and homes of the Moorish governor and of the elite city are still visible in the archaeological area (CasteloSãoJorge).

In the current chapter, it will be presented an introduction to the case study, as done with the previous case study, exposing the history of the construction, the description of the building and the existing damage and deformation. Following the theoretical framework of the case study, it will be detailed the dynamic identification “in situ”

required for the model calibration, the core sampling for the material identification, introducing then the numerical model and the obtained results and their discussion. The retrofiting strategies proposals will close this chapter with a brief conclusion.

## 5.1 History of construction

The building under study, Paço Real II, as referred is part of the classified area of São Jorge Castle situated near to the Torre do Paço (see Figure 5.1). Since XVII century there are several plans with distinct configurations of the building. Analysing in detail a plan dated from 1650 it is possible conclude that there was already construction in the actual Paço Real II location at that time although with a distinct perimeter configuration (Gésero 2011).



**Figure 5.1** – Location of the building, Paço II, through an aerial view of the city (Google earth, 2016).

The plan executed in 1761, which shows the building before the 1755 earthquake, shows a walled perimeter with a construction similar to the actual building, being divided by the Torre do Paço (SIPA 2016). In the beginning of the 90<sup>th</sup> century, around 1807, the representation of the building introduces the connection between the Paço II with the Torre do Paço and also a larger built perimeter. It should be noted that in this plan,

the ravine representation was made until the built borders which is not the current situation (Silva 1898). A few years ago, in 1825, it is possible to identify a connection between the ground floor and the Castelejo which is represented in plant until 1938 along the representation of the raved slope described above (SIPA 2016).

In the plan of 1893, the castle and the building Paço Real II arose connected at the level of the first floor. Comparing this plan with the available of 1944, it is notorious that occur a reduction in the volumetry of the building, disconnecting with the castle. It is, especially in the year's 1939 and 1940, which the major interventions occur in the building, as demolition works with the aim of restore the castle image.

Several plans from 1938, show a construction perimeter involving the Torre do Paço and the existence of two distinct volumes with independent roofs associated, being one of them the case study of the present work. It is possible conclude, through this plans, that the building with two floors is connected by the first one to the Torre do Paço, however at the floor level there are a partition wall forming an interior hall which it is currently an uncovered passageway.

Through the available historical information of the next two decades, it is possible to conclude that the building has no longer two floors but instead an accessible terrace identical to the present, however back then the terrace area was larger. Through the plan of 1960, it can be seen that the building is quite identical to the actual, with the windows and doors with the same configuration. It is also represented the exterior staircase that allows the terrace access, but with another attached to the same façade, with bigger dimensions, facing south, that nowadays does not exist. The inside of the building also presents some notorious differences in the kitchen and is also represented the bar counter and the fireplace, however the latter as a decorative element since there was no chimney.

## 5.2 Description of the building

The São Jorge Castle, as a national monument is installed within the area of the old Citadel or fortress of Lisbon, being nowadays the village of Castelo, which includes the Castelejo or Fortaleza implanted northwest, the Praça de Armas in the south direction, the Praça Nova and the Núcleo Arqueológico do Castelo implanted east, a viewpoint is developed along the west side of the Castelejo and in a direction north/south is implanted the study case, Paço II, in the Paço Real de Alcáçova (see Figure 5.2). It should be noted that the northern area of the Castelejo and the area east of the Praça Nova it is a circulation zone which was part of the old fortress or Citadel, although nowadays does not belong to civil and urban areas of the village (Cruz 2013).

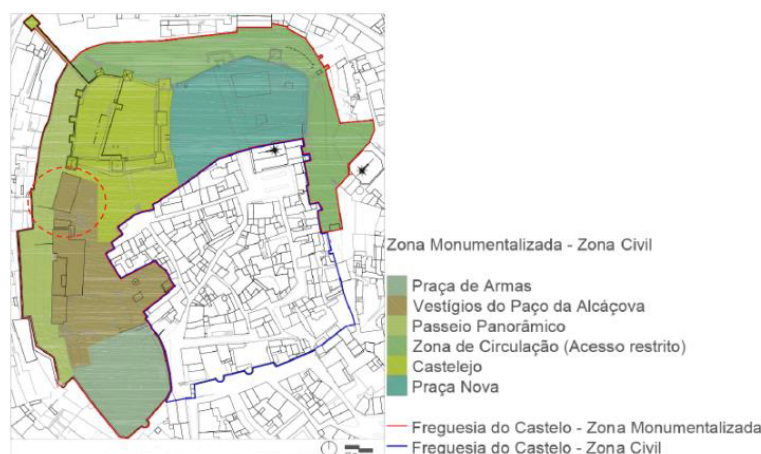


**Figure 5.2** – Distribution of the ancient fortress of Lisbon areas (Cruz 2013).

Looking with more detail into the building in study, Paço Real II, this currently has a deployment area of 365 m<sup>2</sup> with a coverage terrace with access from the outside by a limestone staircase (see Figure 5.3).



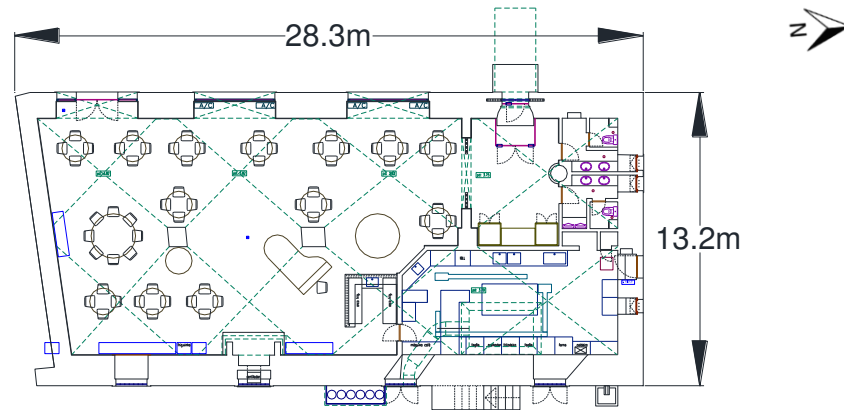


**Figure 5.3** – Ground floor plan of the Paço Real II, Casa do Leão restaurant.

The building has only one floor with a plan development especially in the North/South direction. It is important to note that almost all the façades are partly buried as the northern façade, which has an exterior part with a descendent slope in the direction South/North, being the lower part of the façade located south. The south façade has no openings and is mostly buried with an adjacent second system of walls and also with a narrow tunnel (see Figure 5.4 and Figure 5.5).

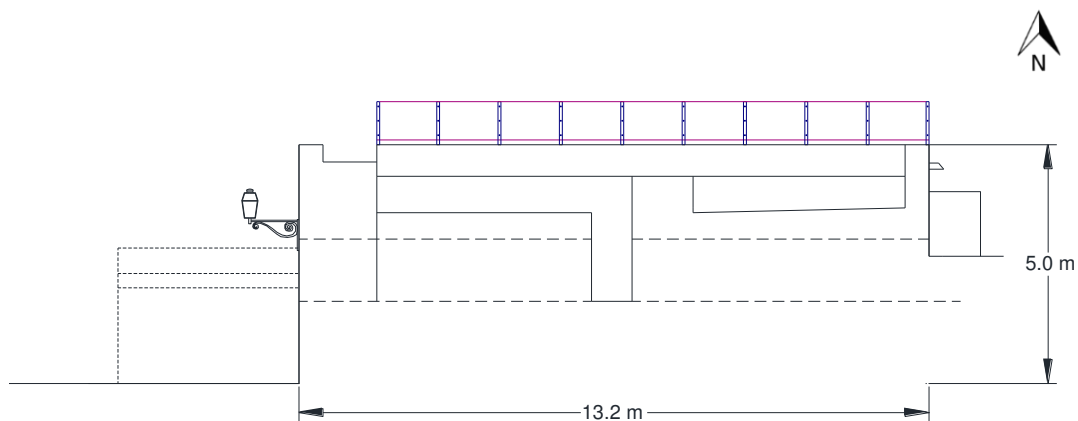


**Figure 5.4** – South elevation of the Paço Real II.

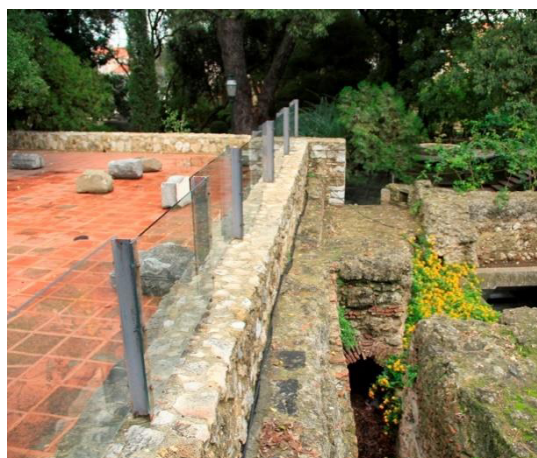


**Figure 5.5** – Detail of the south façade of Paço Real II.

The entire perimeter of the terrace has a wallet with a height of around 40 cm, this protective height is complemented by a translucent tempered glass guard with one meter on the south façade (see Figure 5.6).



a)



b)

**Figure 5.6** – Roof top view of Paço Real II: a) surrounding wallet of the terrace b) detail of the translucent tempered glass guard on the south façade.

Currently the building presents the inside surface rendered, the ceilings in vaults supported by thin walls of brick and also a longitudinal and centralized alignment of brick columns (see Figure 5.7).

The inner surface of the walls of the room are covered to middle-height by a tile wainscot with floral and figurative motifs in blue and white, there is a fireplace but only as a decorative element of the room (see Figure 5.8).



**Figure 5.7** – Interior of the building Paço Real II, Casa do Leão restaurant.



**Figure 5.8** – Interior details of the building Paço Real II: a) fireplace (only as a decorative element)  
b) tile wainscot that cover a part of the wall.

The external structural façade walls are composed lime stone, fragments are of several types of limestone, porous stones and ceramics such as bricks and roof tiles debris, bonded with hydraulic lime mortar. The walls have an average thickness of 80 cm and are not rendered on the outside. Vieira da Silva in 1948, describes this method of construction, with earth, as a complement to the masonry walls construction of the São Jorge Castle and also refers that the walls are constituted by two leafs of stone masonry filled with earth grounded nucleus, fact confirmed during the demolition process that occurred in the 1940 decade of the XX<sup>th</sup> century (Silva 1948).

The height of the building is 3.80 meters at the highest point of the vaults, being lower in the service areas due to the presence of the false ceilings. The ground floor slab is covered with red ceramic tiles with dimensions of 0.3 x 0.3 m<sup>2</sup> and the terrace roof of the building is also finished with red ceramic tiles, accessible and used until recently for cultural activities, and now is not accessible.

### **5.3 Existing damage and deformation**

A recent inspection and diagnosis of the building, carried out by the Civil Engineering Department of Aveiro University, allowed the identification of the actual defects and also the recognition of possible causes that lead to such damages.

Nowadays, the building in study, Paço Real II, exhibits several structural damages such as external wall cracking, deformation of the roof structure and also non-structural damages such as infiltration and moisture problems inside the building, efflorescence and painting detachment, detachment of the ceramic tiling on the inside surface, stone external and façade walls mortar disintegration and corrosion of metallic elements, amongst others.



### 5.3.1 Generalized Cracking

The cracking is a damage very present in the building Paço Real II, it is possible to identify longitudinal cracking in the roof tiles of the terrace, in the interior face of the masonry vaults and on both faces (interior and exterior) of the façade walls.

On the roof was observed a longitudinal cracking almost in the middle and develops over the entire length of the building, wherein is divided into two parallels cracks spaced around 30 centimetres in a southern area, that corresponds possibly to the columns alignment (see Figure 5.9).

Another evident cracking appears inside the building, longitudinally in the middle of the masonry vaults, appearing from this principal crack smaller. It is also worth noting some cracking in the arch that divides the entrance lobby to the restaurant, in the wall and in the connection of the vault in that area (see Figure 5.10).

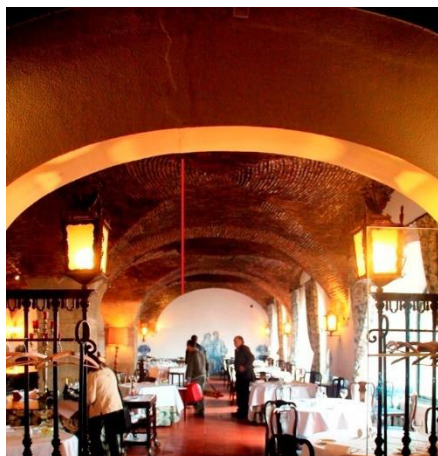


a)

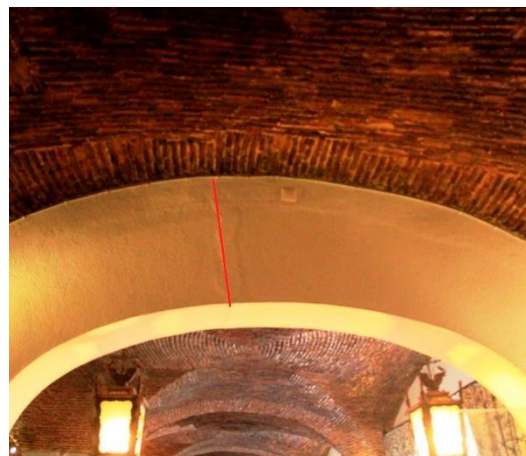


b)

**Figure 5.9** – Longitudinal cracking on the roof: a) longitudinal alignment of the crack b) cracking detail of the terrace.



a)



b)

**Figure 5.10** – Longitudinal cracking inside the building: a) longitudinal alignment b) cracking detail in the arch.

There is also cracking in other areas however less severe and with smaller amplitude such as, the cracking that appears in the connection between the vault arch and the wall (see Figure 5.11), in the lower part of the wall below the window sills and also in a façade window arches (see Figure 5.12).

It is also important to highlight the cracks in the northeast wall that covers the entire wall, breaking the window sill stones (see Figure 5.13). In addition, the crack between the staircase that gives access to the terrace roof with the façade wall confirms that these were later built, showing no signs of interconnection among the elements (see Figure 5.14).

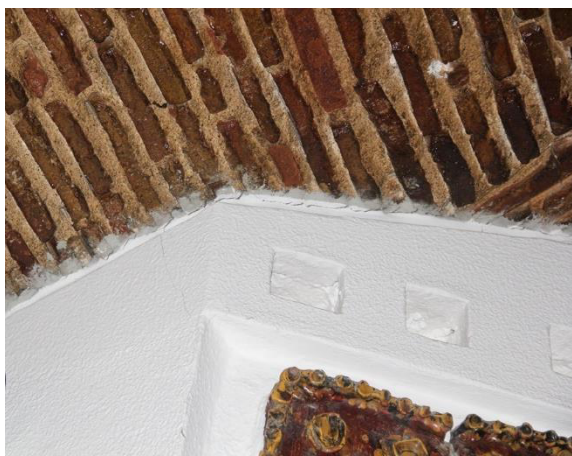


**Figure 5.11** – Cracking in the connection between the vault and the wall.



**Figure 5.12** – Cracking in the tiles in the lower part of the wall below the window.



**Figure 5.13** – Cracking in the exterior northeast wall.



**Figure 5.14** – Cracking between the staircase and the northeast wall.

### 5.3.2 Terrace roof and masonry vaults deformation

The presence of stains and signs of water puddles in the terrace revealed some areas that are not consistent with the needed slope for rain water flow. The roof tiling as well as the vaults, inside the building, exhibits a longitudinal cracking with the same orientation and with a maximum amplitude of about 5 mm (see Figure 5.15). This



cracking can represent a diffused cracking having a diffuse configuration, in some areas, with significant amplitude.



**Figure 5.15** – Longitudinal cracking inside the building: a) continuous longitudinal alignment b) cracking detail of the masonry vault.

### 5.3.3 Exterior walls deformation

The principal façade of the building, west oriented, reveals several cracks which are perceptible particularly in the openings areas as windows and steel glass frames and some elements out-of-plumb (see Figure 5.16 and Figure 5.17), as well as the tile cracking near the windows sills. From the outside, the deformation is more noticeable at the openings areas by the loss of mortar and stone fragments under the windows sills.





**Figure 5.16** – Linearity break along the spans in the west façade.



**Figure 5.17** – Plumb of some elements around the span in the west façade.

#### 5.3.4 Floors deformation

Considering the interior of the building, it is visible an unlevelled ground floor and some cracking and degradation of the floor tiles mainly near the windows areas. It is also noted a very irregular exterior stone pavement, predominantly in the surrounding areas of the building and also big trees most notably near to a pine tree situated around 2.5 meters from the west façade (see Figure 5.18 and Figure 5.19).

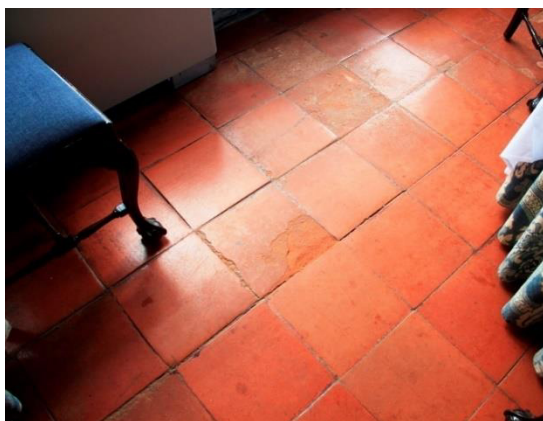


**Figure 5.18** – Floor tile cracking inside the building.



**Figure 5.19** – Irregular stone pavement outside the building.

### 5.3.5 Partial rotation of the exterior wall

The partial rotation of the exterior wall oriented to the north is identified in the northeast area of the corner angle, that presents a out-of-plumb at the top wall in relation to its base and also a diagonal cracking in the east façade that affects the total length of the wall and its full height. The out-of-plumb described above can be seen in the corner angle area either in the north or east direction (see Figure 5.20 and Figure 5.21).



**Figure 5.20** – Cracking in the east façade.



**Figure 5.21** – North façade out-of-plumb, visible on the north and east direction.

### 5.3.6 Non-structural damage

In addition to the structural damage described above, the building under analysis, Paço Real II, features non-structural damage regarding for example the inefficient rainwater drainage and the waterproofing system (see Figure 5.22), infiltrations and interior moisture problems, efflorescence's and painting blistering (see Figure 5.23), degradation of the interior covering materials (vaults and arches), desegregation of the façade materials (stone and mortar) due to the absence of external rendering, presence of black

films and stains that aggravate to stone cracking, lichens and metallic element corrosion.



**Figure 5.22** – Inefficient rainwater drainage and the waterproofing system.



**Figure 5.23** – Efflorescence and paint blistering on the south wall.

## 5.4 Dynamic identification in situ

All the structures hold characteristics of stiffness, mass and damping which define their dynamic behaviour, this fact is translated by the dynamic equilibrium equation:

$$M\ddot{u} + C\dot{u} + Ku = f(t) \quad (5.1)$$

In the above equation,  $M$ ,  $C$  and  $K$  are the mass matrix, damping and the structural stiffness, respectively and  $\ddot{u}$ ,  $\dot{u}$  and  $u$  are the acceleration, velocity and displacements vectors resulting from the exterior dynamic actions provided by the vector  $f(t)$ , respectively (Lopes 2009).



The dynamic identification test, as referred, are capable to provide information on the global dynamic behaviour of the building, including information on natural frequencies, damping and modal shapes. This tests, as in the case of the present work, have special importance for the updating and validation of structural models, since the results are directly related to the physical and structural parameters of the structure, such as the geometry, the stiffness and the boundary conditions. The dynamic identification can be carried out through accelerometers, by combining different accelerometers setups or by radar interferometer (D10.4-NIKER 2012).

Regarding historical structures, the dynamic identification tests are carried out to achieve the following aims (D10.4-NIKER 2012):

- obtain information on the global dynamic behaviour of the structure, including natural frequencies, modal shapes and damping coefficients;
- validate and update a structure's numerical model by comparing experimental and numerical natural frequencies and mode shapes;
- assess the level of connection between different parts and identify weak structural features;
- appraise the influence of major damage on the structural response;
- evaluate the effect of possible repair and strengthening solutions by comparing the dynamic parameters before and after the intervention and hence improving the design for future applications in other similar structures;
- allow monitoring before and after the intervention by repeating periodically the dynamic tests and comparing the results;
- study of the influence of environmental parameters in the case of buildings sensitive to them, as in particular earthen structures.

To obtain, experimentally, the dynamic characteristics of a structure are available two distinct methods: force vibration testing (FVT) and ambient vibration testing (AVT) (Cantieni 2005). It will be present a brief description regarding the method FVT, since the used in the present dissertation was the ambient vibration testing.

#### 5.4.1 Ambient vibration testing (AVT)

The dynamic identification of the present work is based on the ambient vibration testing (AVT), in this test no artificial excitation is used, instead the response of the structure to ambient excitation is measured. In respect of civil engineering, the ambient excitation can be the wind, traffic, seismic micro-tremors, among others. Comparing with the FVT, the information resulting from the force input signal  $x_i(t)$ , with FVT method is replaced with the information resulting from the response signal  $y_r(t)$  measured in a reference point,  $R$ , with the following calculation of the matrix  $H$ , as can be seen in a) of Figure 5.24 (Mohamed 2015).

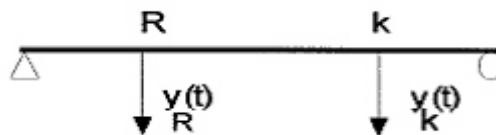


**Figure 5.24** – Ambient vibration testing scheme (Cantieni 2005).

The ambient vibration testing offerings more economical advantages and facility in the tests execution. In fact, the use of mechanical vibrators entail costs that do not exist when it is used the ambient vibration, in addition the forced vibration involves several difficulties in carrying out the tests. AVT also permits the dynamic assessment of structures without disturbing their normal operation. Furthermore, as the structures

are characterized using real conditions, in case of presence of nonlinear behaviour, the obtained results will be related to realistic levels of vibration. On the other hand, as the level of excitation is low it is necessary be used very sensitive sensors with very low noise levels and even so, one should expect much lower signal to noise ratios that the ones visible in the forced vibration tests (Magalhães and Cunha 2011).

Attending to the random characteristics of the actions involved in the ambient vibration tests, its independent character and to the fact that several of these actions act simultaneously, it is usual admit that the structure excitement under these conditions is a broadband process also called white noise. A white noise corresponds to a signal with spectral density of constant power, in other words, an excitement that combines with a white noise holds energy content similar for all the frequencies.

#### **5.4.2 Acquisition and signal processing**

In the monitoring of civil engineering structures are used, frequently output signals transducers of the analogue type that possess diverse characteristics. The role of acquisitions systems is based on the transformation of the transducers output signal in to a digital signal, suitable for the interpretation of the structural response.

Initially, the analogue signal is converted to be interpreted by the other components of the acquisition system. The operations of response linearization, signal amplification or attenuation, conversion of a quantity to another and organization of bridge circuit, application of anti-aliasing filters are examples of common operations. In the next phase, occurs the signal A/D conversion, wherein the analogue continuous signals from the transducers are transformed into discrete series in time and amplitude, by sampling and quantization processes, respectively. This series should describe the analogue signal with adequate accuracy in the frequency, amplitude and phase fields (Pimentel 2008). After these phases, the output digital signals are prepared to be stored and processed

in the own unit or then transmitted directly to a computer as it usual in the integrated acquisition board of computers by USB connection or PCI interface.

#### 5.4.2.1 Sampling frequency and acquisition time

The sampling frequency represents the velocity that the A/D converter scan the signal, in other words, the signal is sampled spaced in time, depending this spacing on the sampling frequency.

The ideal sampling frequency must be high enough for understanding the response framed in the interest frequencies, however should be take into account the costs associated to the storage and processing of the information (Pimentel 2008).

In the following equation, the sampling theorem of Shannon is described, where  $f_s$  represents the sampling frequency,  $f_{max}$  the maximum frequency and  $f_{Nyq}$  the Nyquist frequency.

$$f_s = \frac{f_{max}}{2} = f_{Nyq} \quad (5.2)$$

The acquisition time is a preponderant parameter in ambient vibration testing for the identification of the dynamic properties of the structures. The data acquisition in this type of tests is performed, mainly, through a dynamic response register of the structure over a range with finite and pre-defined time, as seen in the equation below, where  $T$  represents the acquisition time, in seconds, and  $f_{min}$  the value of the lower frequency of the structure (Lopes, Guedes et al. 2010).

$$T \geq \frac{1000}{f_{min}} \quad (5.3)$$

#### **5.4.2.2 Errors**

In the measurement process is always present the uncertainty factor, associated to the equipment's uncertainty, a group of malfunctions and errors connected with the acquisition and processing of the signal. They will be briefly discussed some common errors are the analogue noise, tendencies, dropouts (signal loss), signal saturation, leakage and aliasing.

##### **a) Analogue noise**

The analogue noise is a random phenomenon that disturbs the interest content of a signal and is characterized by bring up some peaks in the signals (Figure 5.25). This error can be caused by several components of the acquisition system, by influence of external factors as the frequency of the electricity distribution network and also derive from the real vibrations, without interest for the analysis, but that can be captured at high frequencies due to the equipment's sensitivity (Pimentel 2008).

The analogue noise can be minimized through digital filters as band-stop, placed around the frequency bands where the noise is more dominant, this is only possible in well-defined bands (Pimentel 2008). This type of error also can be prevented through the proper assembly of the entire system acquisition setup, in particular the connection and the quality of the cables (Lopes 2009).



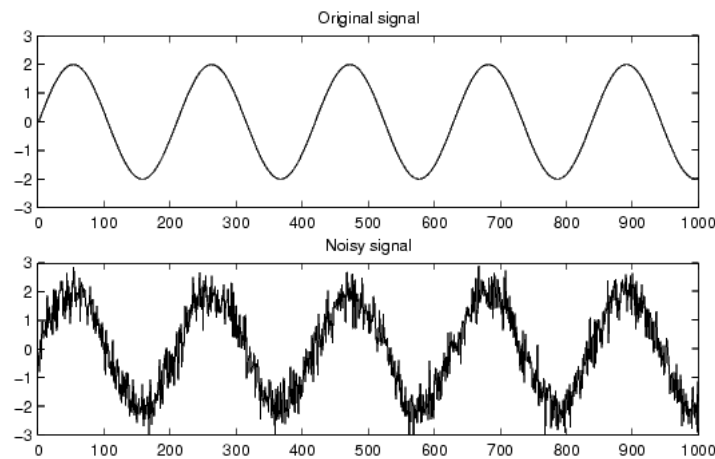


**Figure 5.25** – Original signal vs a signal with noise (WaveletToolbox 2016).

### **b) Tendencies**

A tendency is reflected in the slow variation of a signal, being like this a common phenomenon and its interpretation should be performed with special attention. This error can be instigated through others parameters in the sensors, temperature effects, malfunctioning equipment or static components of the response. To eliminate this unwanted tendencies, it is usual apply high-pass filters with a crossover frequency near zero or in basic cases, by subtracting a curve obtained by the interpolation of time series (Pimentel 2008).

### **c) Dropouts**

The signal loss consists in a rapid breakdown of the signals that can be momentary or permanent. The momentary break is triggered by a malfunction caused by a transducers saturation, while the permanent can be caused due to a power failure of the transducers or conditioners (Rodrigues 2004).

#### d) Signal saturation

The signal saturation is characterized by cutting the signals values corresponding to the minimum or maximum input in the acquisition system and results in the information loss for certain periods of time (Figure 5.26). This error can be perceptible through a simple observation of the time records and easily detectable in signals of the random or periodic type and more difficult in transient signals.

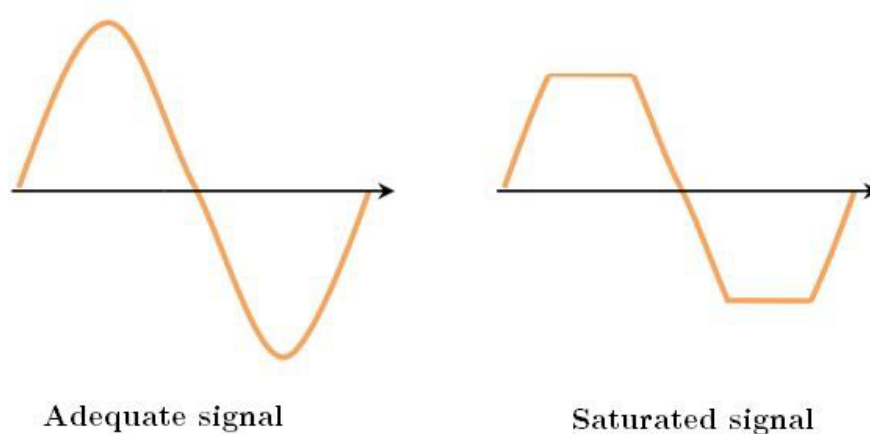


**Figure 5.26** – Effect of the signal saturation.

This problem may occur due to the excessive sensitivity of the transducers, excessive gain in the signal conditioners, to the incorrect definition of the measurement range given by the expected amplitudes of the response or to the lack of devices correction, common phenomenon in accelerometers. It should be noted that is not possible the correction or even the attenuation of this error (Pimentel 2008).

### e) Leakage

In the signals analysis in the frequency domain it is usually applied the discrete Fourier transform (DFT) through the Fourier fast transform (FFT) algorithm and is based on the periodic repetition of the signal highlighting the border areas (Figure 5.27). The leakage appears when the signal, infinite in the time domain is distorted due to the non-existence of a periodic content, with an integer number of cycles in the signal, limited in the time domain (Pimentel 2008).

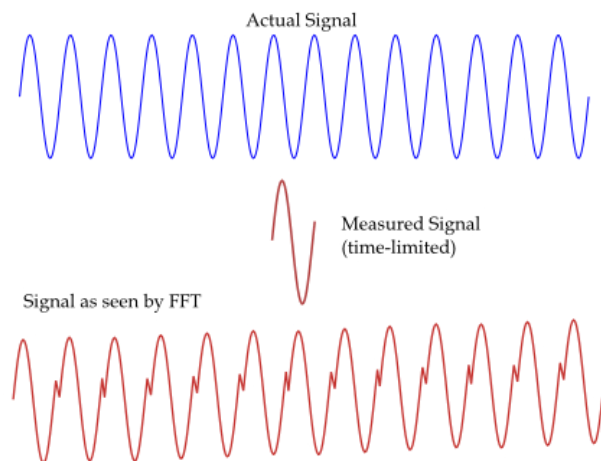


**Figure 5.27** – Impact of observation interval on FFT (GaussianWaves 2016).

In order to minimize this errors, the observation times can be increased or otherwise, apply non-rectangular data windows and eliminate any existing discontinuities in the temporal records, *Hanning* is the windows more used and efficient in the processing signal of the random type (Caetano 1992).

#### f) Aliasing

This error is manifested by the appearing of energy associated to frequencies higher than the *Nyquist* ones (Figure 5.28). It is an error instigated by the discretization operation of the continuous signal in the time domain, causing the origin of the *Shannon* sampling theorem which is sometimes referred as *Nyquist* theorem.

To eliminate this type of error are applied analogue filters as low-pass anti-aliasing immediately at the output transducers, this filters will eliminate the signal components with frequencies higher than the *Nyquist* frequency (Lopes 2009).

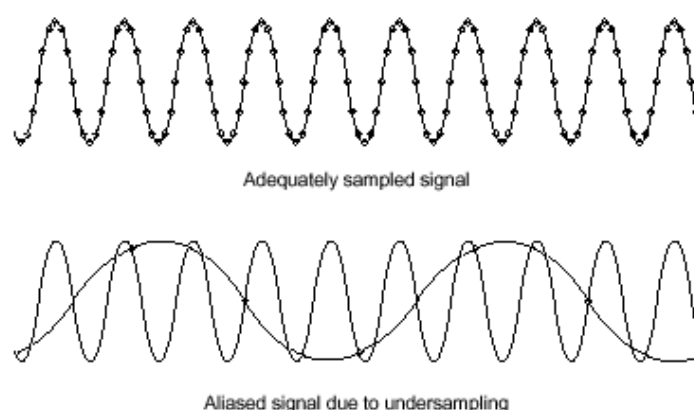


**Figure 5.28** – Adequate and inadequate signal sampling through aliasing effect (Corporation 2016).

#### 5.4.3 Modal identification

As mentioned in the previous chapters, the experimental modal identification can be made through forced vibration testing, ambient vibration testing and response measurements testing of the structure in free vibration.

There are several modal identification methods that allow the identification of the dynamic characteristics of the structure through measurements made in the testing's

referred above, in this case, by means of AVT. These methods can be distinguished in to major groups and by the type of data used to identify the required parameters, being them mainly, the methods based in the time domain, applying response time series of the structure and the methods based in the frequency domain which are based on estimates of the spectral response of the structure.

#### **5.4.3.1 Analysis in the frequency domain**

The technique of analysis in the frequency domain is based on the transformation of the response series measured in different points of the system to the frequency domain by applying the FFT (Fast Fourier Transform) algorithm. When the number of vibration modes to identify and respective frequency range are limited best results are achieved when compared to the technique of analysis in the time domain (Caetano 1992). They will be briefing presented, the two methods of modal identification, selecting peaks method (PP – Peak Picking) and the decomposition method in the frequency domain (FDD).

##### **a) Peak Picking**

The Peak Picking method, also called basic method in the frequency domain (BFC), was the first method to be used for dynamic identification of structures from the measurement of their responses to ambient actions such as traffic, wind, among others. It is a method frequently used in civil engineering applications through the reliability of the results obtained, the relative facility of implementation and by providing a clear interpretation (Tavares 2013).

There is a strong possibility of these actions, since they have environmental features, will be not possible to measure. Hereupon, it is assumed that the excitation represents

a Gaussian stochastic process of the type white noise with null mean for purposes of modal identification. Under these circumstances, it can be seen that the spectral density functions of the response exhibit amplitude peaks in the frequencies near the natural frequencies of the structure for the usual values of the damping coefficients and vibration modes with separate frequencies (Tavares 2013).

The PP method uses the signal analysis techniques based on estimates of the functions of spectral density, calculated using the FFT algorithm. In order to be able to identify the vibration modes of the systems, it is necessary that these modes have well-spaced frequencies, reduced damping and that the excitation forces have spectral density approximately constant. In this method, are defined the deformation modes operating instead of the expected vibration modes. In practice a deformation mode operating relates to the deformation of a structure subject to a purely harmonic excitation, however in theory, corresponds to the combination of all vibration modes. Only the vibration modes that exhibit frequencies closer to the excitation frequency contribute significantly to the deformation operational mode. It is possible conclude that these modes will reflect the superposition of several vibration modes when the modes have closer frequencies, thus explains the difficulties in obtaining good results with this method.

An additional limitation of the peak picking method is related to the finite frequency resolution of the spectral density functions estimates, evaluated through the FFT algorithm. Nevertheless, the advantages previously described that makes this method the more suitable in the stochastic modal identification field of civil engineering structures leading to the most required method to make an initial information analysis collected in modal identification testing's based in the ambient vibration (Rodrigues 2004).

**b) Frequency domain decomposition method (FDD)**

The frequency domain decomposition method is based on the peak picking method and for that reason is considered as an extension of PP method (Tavares 2013). In this method it is introduced an “diagonalization” operation in the spectral density function matrix, with the ability to decompose the matrix in to a range of systems with one degree of freedom, each one corresponding to a vibration mode of the system. This operation consists in the application of decomposition algorithms for eigenvalues or singular values, being equivalent for the matrix of response spectral density functions (Rodrigues 2004).

The spectral density function of each vibration mode can be identified in the singular values spectrum and be considered to adjust the estimates of the frequency and modal components, achieved by the selection of a resonance peak and the respective singular value (Pimentel 2008). In the presence of cases wherein the modes have closer or even coincident frequencies and are geometrically orthogonal between them, each singular vector corresponds to a not null singular value leading to a good estimate of the modal components. Nevertheless, that if the modes are not geometrically orthogonal between them, it is possible obtain good estimates for the modal components related to the dominant mode, however, in the non-dominants modes that is not possible (Rodrigues 2004).

Concerning the execution times, the frequency domain decomposition method is quite fast, there are only a time increase necessary to realize the diagonalization operation. Besides this benefit, the FDD method offers improvements at the identification level with closer frequencies allowing the resolution of the problem with the multiple modes with equal frequency. Should be noted that in the FDD method are identified vibration modes in contrary to the PP method where are identified deformation operation modes.

In 2001, was presented by (Brincker, Ventura et al. 2001) the enhanced frequency domain decomposition (EFDD) which is based in the FDD method. However, were performed several improvements that allowed the estimation of the modal damping coefficients and the identification, more rigorously, the natural frequencies and the modal configurations of the structure (Rodrigues 2004). In this enhanced method, is made a transformation to the time domain of the spectral density function to each vibration mode through the application of the inverse fast Fourier transform (IFFT). Thus, it is obtained the auto-correlation function of a system with one degree of freedom, associated to each vibration mode, from which it is possible estimate the system frequency by the instants of zero crossing and the damping coefficient through the algorithm decay (Lopes 2009). With the information for all the selected area for each mode and with a weighted average of the singular vectors it is possible obtain the modal components in the instrumented places (Rodrigues 2004).

#### **5.4.3.2 Analysis in the time domain**

The analysis in the time domain will be briefly discussed since the present work only uses techniques in the frequency domain.

This method is a parametric technique that consists in the adjustment of the models regarding two types of database, mainly, the adjustment of the own response temporal series and the adjustment of the estimates of the response correlation functions of the structural systems (Ferreira 2013).

The modal identification of dynamic systems which are based on information in the time field appears to be advantageous when the natural frequencies of the structure are distributed in an amplitude high range and the vibration modes to identify is elevated.



The major disadvantages of this technique are the impossibility of consider the residual effects of the vibration modes located out of the range previously referred and the fact that only is possible to identify vibration modes in the selected frequencies range for analysis (Caetano 1992).

#### **5.4.4 Data acquisition system**

The instrumentation used in the dynamic test of the Paço Real II, the case of study, comprising:

- six piezoelectric unidirectional accelerometers, *PCB Piezotronics®* model 393B31, with 1000 mV/g of sensibility, frequency measuring range of 0.5 Hz to 2000 Hz and with a range of accelerations between -5g and 5g (see Figure 5.29);
- six cables brand *PCB Piezotronics®*, model 024R10, to connect the accelerometers to the acquisition board;
- six extension cables;
- a data acquisition system with four channels, with 24 bits' resolution which includes a signal conditioner and analogue filters for aliasing error correction that automatically adjusts the frequency acquisition used;
- Uninterruptible power supply, brand *Phasac ®*, model 9420
- six metal plates for the accelerometers placement;
- Megapoxy PF resin, brand *Vivacity Engineering*, with a tensile strength of 25000 MPa, compressive strength of 65000 MPA, fracture strength of 18000 MPa and shear strength of 10000 MPa;
- a laptop computer with the software LabVIEW that allows the test data control and acquisition.



**Figure 5.29** – System and piezoelectric unidirectional accelerometers.

#### 5.4.5 Test setup

To evaluate the dynamic behaviour of the case study to ambient vibration, two measurements were made with 300 seconds each

The dynamic test performance included six piezoelectric unidirectional accelerometers, whereas two of them served as reference, remaining therefore in the same location for all the measurements, particularly in the upper right and left corner of the east façade.

The remaining accelerometers were placed in different points of the structure always at the same level of the reference accelerometers, in order to capture mainly, the accelerations for the transversal, longitudinal and torsional modes. For this, were defined two setups, schematised in the following figures (see Figure 5.30 and Figure 5.31). The reference accelerometers are fixed in both setups in order to make it possible to correlate the readings made.

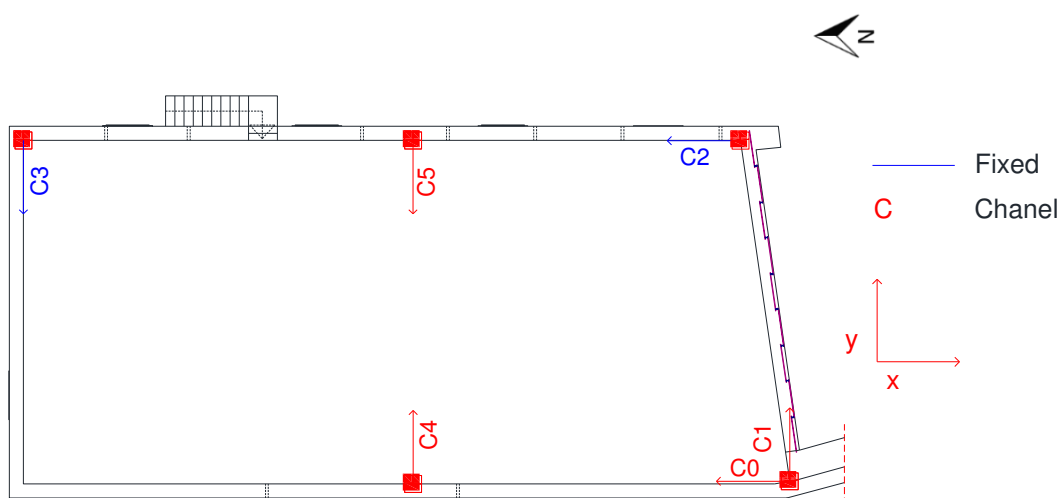


**Figure 5.30** – Representative scheme of the setup 1 relative to the dynamic test.

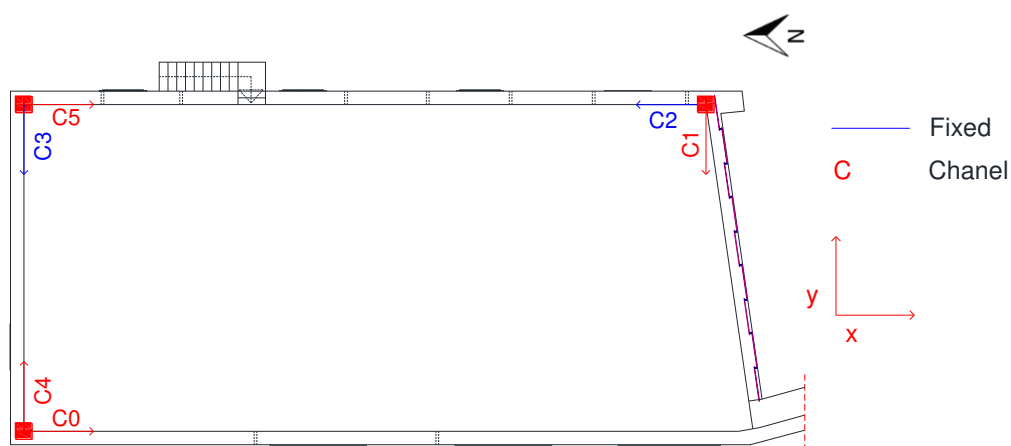


**Figure 5.31** – Representative scheme of the setup 2 relative to the dynamic test.

No measurements were performed in the vertical direction, since the purpose of this tests was to characterizing the structure response in terms of horizontal modal displacements whose frequencies are closer to the frequency range of the seismic action.

#### 5.4.6 Results

Performed the tests, were obtained results that were further processed through the software *ARTEMIS Extractor*®, 2011 version.

The first step was focused in changing the extension of the file obtained (.lmv) to mother type (.asc) in order to be able to open the file in the software and thus perform the signal processing. Then, a very basic geometry, a representative structure of the Paço Real II through the definition of points and surfaces was defined, after the signals processing, it was possible to construct the modals deformed.

Converting the recording for the frequencies domain, based on the FDD technique was the succeeding step. This technique consisted, initially, in the calculation of the matrices of eigenvalues of the power spectral density response obtained from the auto-spectrum and cross spectra of each test (Neves, Costa et al. 2004). At the same time, there were some connection procedures of the signal processing, to reduce or even eliminate the leakage and aliasing errors through the application of Hanning and low-pass filters, respectively (Lopes 2009).

This was followed by the selection of the peaks of the spectrum of these eigenvalues, through the PP technique (see Figure 5.32), allowing the identification of the natural frequencies of the structure and the respective vibration mode, being the first three, transversal global modes, and the fourth a longitudinal global mode, as shown in Figure 5.33.

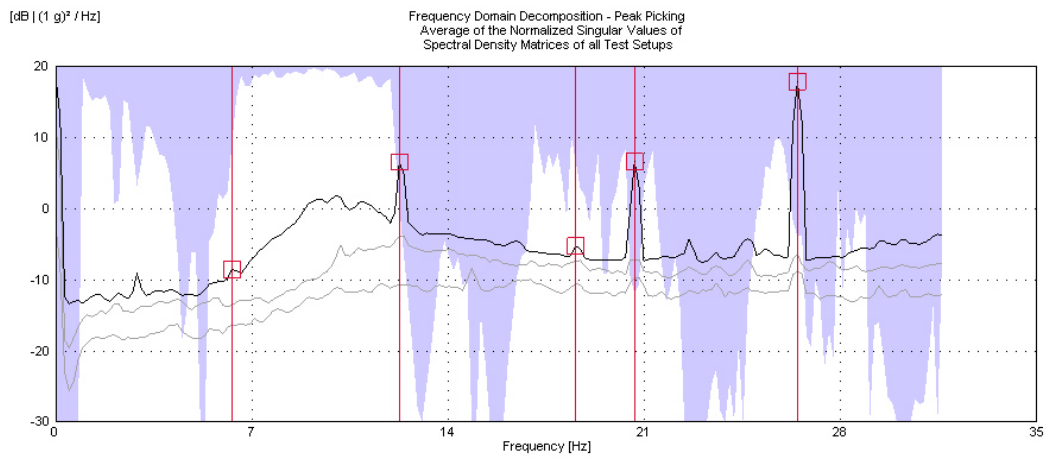


**Figure 5.32** – Spectrum peaks identification through the PP technique.

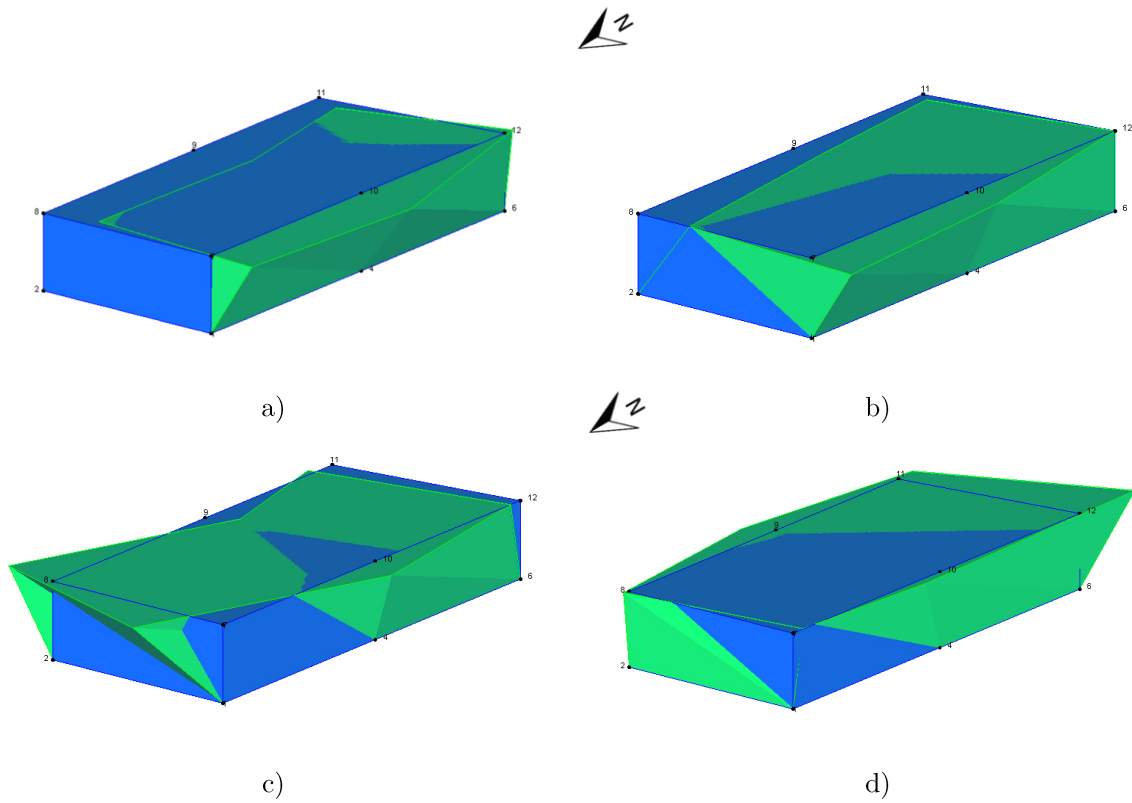


**Figure 5.33** – Vibration modes representation of the a) 1<sup>st</sup> mode – 6.29 Hz; b) 2<sup>nd</sup> mode – 12.26 Hz; c) 3<sup>rd</sup> mode – 18.55 Hz and d) 4<sup>th</sup> mode – 20.65 Hz.

## 5.5 Numerical model

The evaluation of the structural capacity of the present case study was carried out resorting to the software Midas FEA, that also allows the pre and post-processing.

The 3D numerical model was prepared with shell elements and a linear and non-linear analysis was performed. Subsequently, it will be presented the numerical model geometry, material properties, loading and boundary conditions and mesh definition. In the present work, the numerical model, after performed the analyses, focus is given on the evaluation of the structural capacity of the building Paço Real II for a continuous model and also for a model that simulates the actual and principal cracking pattern of the masonry vaults, lastly the retrofiting strategies proposals are the final purpose of this work.

### 5.5.1 Geometrical configuration

As referred above, the numerical model was prepared in 3 dimensions and is based on vaults and walls. After the detailed in situ assessment it was concluded that the type of vault that best suits and simulates the existent in the building Paço Real II is the groin vault. This vault is formed by the joining of two barrel vaults making a cross among them, they were originally created by the Ancient Romans and were used in the side aisles of medieval churches and in Renaissance loggias and arcades (TheNationalGallery 2016).

The geometry was designed using the software Rhinoceros, starting with the design of a single vault (see Figure 5.34) until attaining the final geometry of the building as shown in the Figure 5.35 and Figure 5.36.



**Figure 5.34** – Single groined vault by Rhinoceros 3D.



**Figure 5.35** – Group of groined vaults by Rhinoceros 3D.

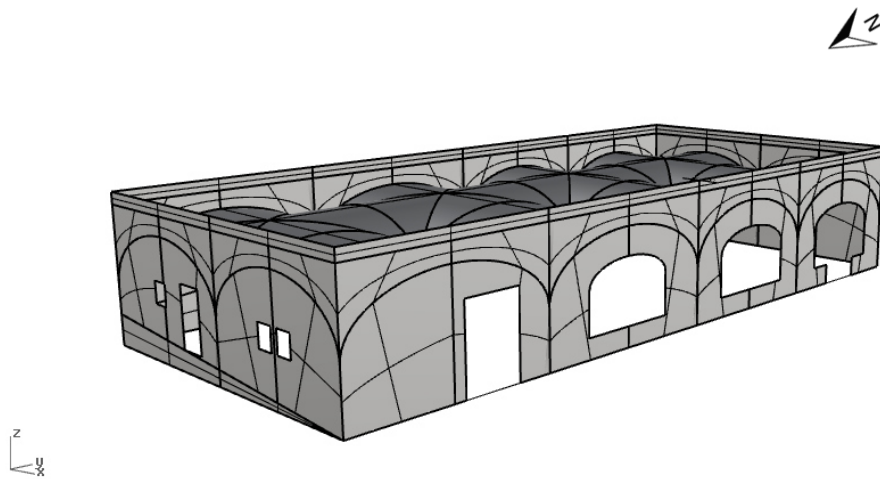


**Figure 5.36** – Final geometry of the building Paço Real II by Rhinoceros 3D.

It should also be noted that all the existent openings were introduced in the numerical model, as well as the wall south oriented that exhibits a geometrical configuration different from the others, that is, thicker and with variable height. Furthermore, it was also taken into account that the north and east façades are semi buried.

### 5.5.2 Material properties

To define the material properties (see Table 5.1), a literature survey was made to obtain reference values for the numerical model. Two distinct materials to characterize the existing structural masonry were considered, red brick masonry for the vaults and for the remaining structural elements (walls and wallet) of irregular two leaf stone masonry based on the table C8.A.2.1 of the Italian standard NTC 2008 which specifies the physics, mechanical and elastic properties of different masonry typologies (NTC 2008).

**Table 5.1** – Material properties.

	$\gamma$ (kg/m <sup>3</sup> )	E (MPa)	$\nu$	$f_t$ (MPa)	$f_c$ (MPa)	$G_f^+$ (J/m <sup>2</sup> )	$G_f^-$ (J/m <sup>2</sup> )	e (m)
<b>Vaults</b>	1600	3950	0.3	0.4	8.0	100	40000	0.25
<b>Walls</b>	2100	1200	0.49	0.4	8.0	100	40000	0.80
<b>South wall</b>	2100	1200	0.49	0.4	8.0	100	40000	1.45
<b>Wallet</b>	2100	1200	0.49	0.4	8.0	100	40000	0.6

For the numerical model calibration, it was modified the vaults rigidity, represented by shell finite elements, varying the elastic modulus, E, wherein the present case study was increased until attaining a first fundamental vibration frequency obtained through the model is similar to the value taken from the dynamic test described in the subchapter 5.4.

In Table 5.2, is indicated the deviation between the first fundamental frequency measurement of 6.29 Hz and the first frequency obtained from the numerical model of



6.22 Hz. From the obtained frequency through the dynamic identification in situ, associated to a first mode very pronounced by the behaviour of the walls with higher dimensions, it is possible to conclude that the numerical model is slightly less rigid.

This calibration was possible by turning the vaults stiffness, since due to the filling layers overlying the red clay bricks of the vaults to the upper face of the terrace, confer much higher axial stiffness than the value defined for masonry of this type. These filling layers were accounted in the numerical model through the application of a uniform distributed load on the terrace roof, as will be explained in the sub-chapter 5.5.3.

**Table 5.2** – Average error calculation after the numerical model calibration.

Frequency obtained through the dynamic identification in situ (Hz)	Frequency obtained through the numerical model (Hz)	Deviation (%)
6.29	6.22	1.11

### 5.5.2.1 Core sampling

In order to identify the constitution layers of the vaults it was carried out a core sampling on the terrace of the building Paço Real II. The cores were executed in two distinct points and those points were chosen in order to characterize the vault at the highest point and near a column, obtaining a vertical profile of the vault up to the terrace tiling.

For the cores sampling it was used the equipment *Bosch GDB 2200 WE* with a 55 mm diameter crown (see Figure 5.37 a) and, since the vault thickness is considerable it was necessary to copulate metal extenders with 500 mm of length (see Figure 5.37 b), thus

allowing the bore hole from the top surface (terrace) to the interior of the building, identifying completely the materials and their thicknesses along the hole length.



a)



b)

**Figure 5.37** – Core sampling on the terrace of the building Paço Real II: a) equipment used before starting the extraction with a 55mm crown, b) bore hole execution resorting to metal extenders of 500mm.

After the two cores sampling it was verified that both have a similar typology, only with a thickness variation of the filling layer (agglomerate of sand and small stone pebbles) to the vaults brick layer (most inner layer). The first core, near the masonry column, was not executed throughout the entire thickness, in order to prevent more damage to the vault, presenting only a 59 cm of length (see Figure 5.38). The second core, in the highest point of the roof, was executed completely through with the length of 72.5 cm, allowing in this way to identify all the layers that constitute the vault up to the terrace filling.



**Figure 5.38** – The two cores samples extracted, representing the layers.

In both cores, from the terrace surface to the interior, the roof presents a first layer of red clay followed by a filler layer of mortar, an asphaltic membrane, a filling layer of concrete, a layer of limestone, a filling layer (sand and small stone pebbles) and finally a red brick layer as the interior vault surface. It should be noted that the filling layer of sand is leached during the drilling process (see Figure 5.39).



**Figure 5.39** – Filling layer of sand leached during the extraction process.

The terrace roof constitution will allow a more reliable estimation and calculation of the load on the vaults through the thicknesses and specific weight of each material layer. These parameters were defined based on technical data taken from literature (Brasão Farinha and Correia dos Reis 1993). For the calculation of the load it was taken into account the layers of red clay bricks, concrete, limestone and an agglomerate which comprises the filling layers (see Table 5.3). This agglomerate has a variable thickness along the vaults prefill, in contrast to the other layers and since features a considerable thickness, therefore instead of calculate a medium thickness it was decided to divide the vault into two distinct areas, the central strip and the lateral strips.

**Table 5.3** – Thickness and specific weight of each layer which constitutes the terrace of the building Paço Real II.

	Red clay bricks	Concrete	Limestone	Agglomerate (central area)	Agglomerate (lateral area)
<b>e (m)</b>	0.015	0.163	0.100	0.097	0.597
<b><math>\gamma</math> (kg/m<sup>3</sup>)</b>	18	18	24	15	15

### 5.5.3 Loading and boundary conditions

To simulate the real situation of the case study, it was applied the gravity load in the -z direction simulating a long-term deformation and also the load from the several layers that constitutes the roof, which loads the masonry vaults.

The constitution of the roof, through the cores sampling allowed the estimation of the load acting over the vaults based on the thickness and self-weight of each layer, being this last one defined using the reference values presented in the technical literature, as stated before. This load was divided in two distinct areas (see Figure 5.40), the central

and the lateral areas regarding the vaults, consequently obtaining two different values for the active load over the vaults, as shown in Table 5.4.

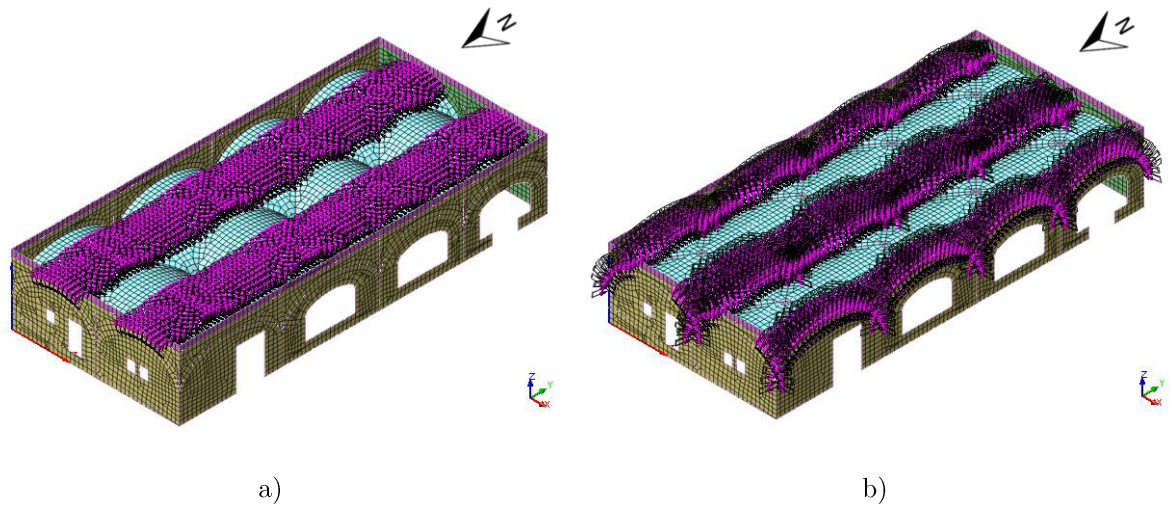


**Figure 5.40** – Applied load on the vaults induced by the terrace roof layers over the brick vaults: a) central strip area; b) lateral strip area.

**Table 5.4** – Load induced by the terrace roof system over the vaults of the building Paço Real II.

$P_{sd}$ central strip area (kN/m <sup>3</sup> )	$P_{sd}$ lateral strip area (kN/m <sup>3</sup> )
7.35	16.35

For the purpose of seismic analysis, it was applied, also, the gravity in the horizontal direction, either in the longitudinal direction either in the transversal direction of the building, Paço Real II.

Regarding the boundary conditions, in the case of the masonry external walls, at the base of the walls, translations and rotation in all the directions were constrained, simulating the foundations. In order to simulate the buried area of the east and north façade it was applied transversal constraints on the surface intersection, blocking the

translations only in that direction. Still about the boundary conditions, with the purpose of simplifying the numerical model, it was introduced constraints simulating the existing columns, similar to the foundation, where the translations and rotations were constrained.

#### 5.5.4 Finite element meshing

For the definition of the finite element mesh it was considered quadrangular shell elements, with a dimension of approximately 0.30 m for all the structural elements, vaults, walls and wallet, shown in the Figure 5.41.

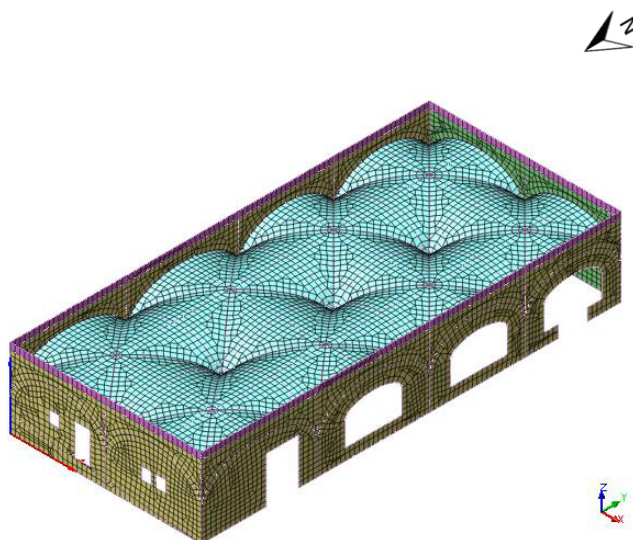


**Figure 5.41** – Finite element meshing of the numerical model.

## 5.6 Results

After the definition of the geometry, material properties, loading and boundary conditions, and finite element meshing, the numerical model is prepared to run the analysis. At this point, it will be analysed the results of the linear and non-linear models, still with the possibility of the model considered continuous or damaged, to simulate in the latter the current structural conditions of the building.



For a damaged numerical model, the most prominent cracks were simulated, located longitudinally that appear in the middle of the masonry vaults (see Figure 5.42). This simulation was made by the changing of some element parameters in the area where the cracks are situated, thereby drastically reducing the elastic modulus value down to 0.001 MPa, preserving the remaining properties, only changing in this way the stiffness of those elements.

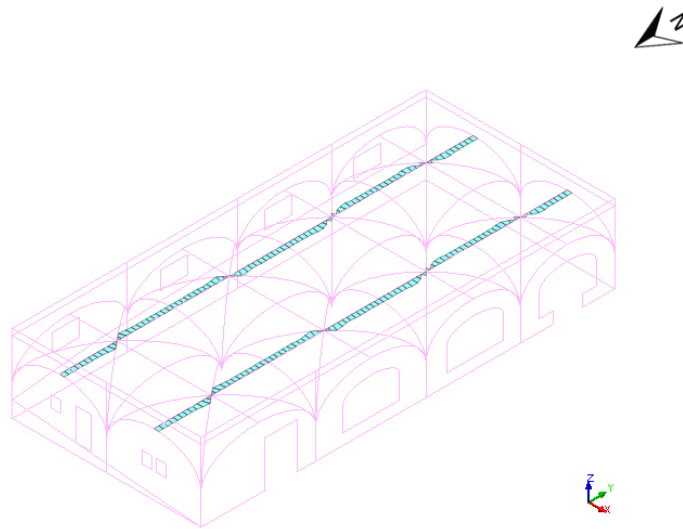


**Figure 5.42** – Location of the changed elements simulating the existent vault cracks.

As referred above, the results will be obtained for two distinct limit situations: a continuous and damaged model. As it is not possible to simulate, accurately, the actual structural condition of the building, it was considered on one hand that the building does not exhibit cracks, condition obtained after the treating and consolidating of the masonry (for example, through crack injection), discussed in the next sub-chapter, and on the other hand, a cracked model, where it is simulated a situation in which the existent cracks were not filled through a retrofitting strategy.

Regarding the non-linear analysis, it was used a total strain crack model type, it is also important to mention, that the functions used for the simulation of the non-linear

behaviour of the materials, was the Hordijk function for tension and the parabolic law for compression (see Figure 5.43) where it was necessary to define the tensile and compressive strength ( $f_t$  and  $f_c$ , respectively), the tensile and compressive fracture energy ( $G_f$  and  $G_c$ ) and the characteristic element length ( $h$ ), these properties were chosen taking into consideration other similar existing research studies.

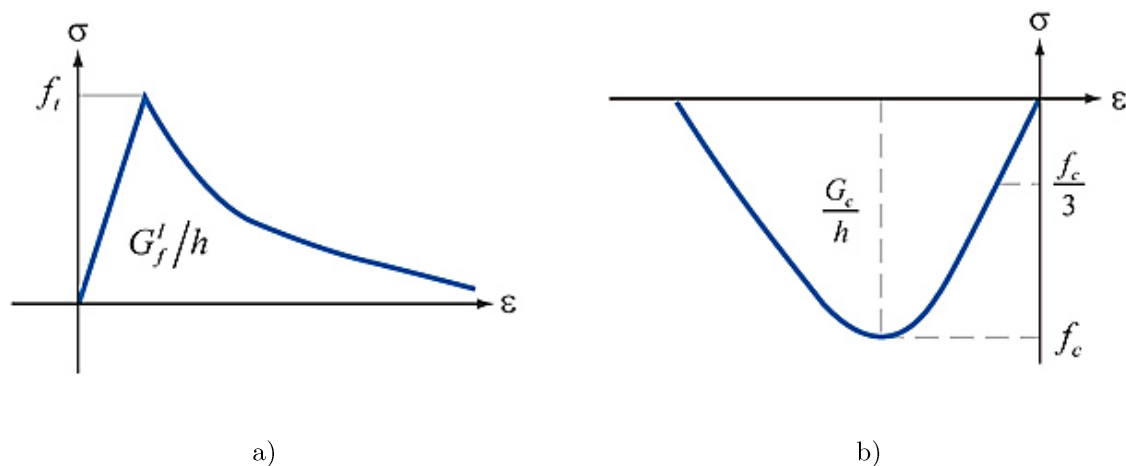


**Figure 5.43** – Non-linear behaviour functions: a) Hordijk function in tension; b) Parabolic function in compression (ManualMidasUser 2016).

The main results that will be presented discussed using the linear analysis with the continuous and damaged model situation will be the principal stresses and the displacements in the 3 directions. For the non-linear analysis, once more with the continuous and damaged numerical model, will be presented the displacements (transversal and longitudinal) regarding the load multiplier for the vertical load analysis (gravitational) and for the pushover analysis in XX and YY direction.

### 5.6.1 Linear analysis with a continuous undamaged model

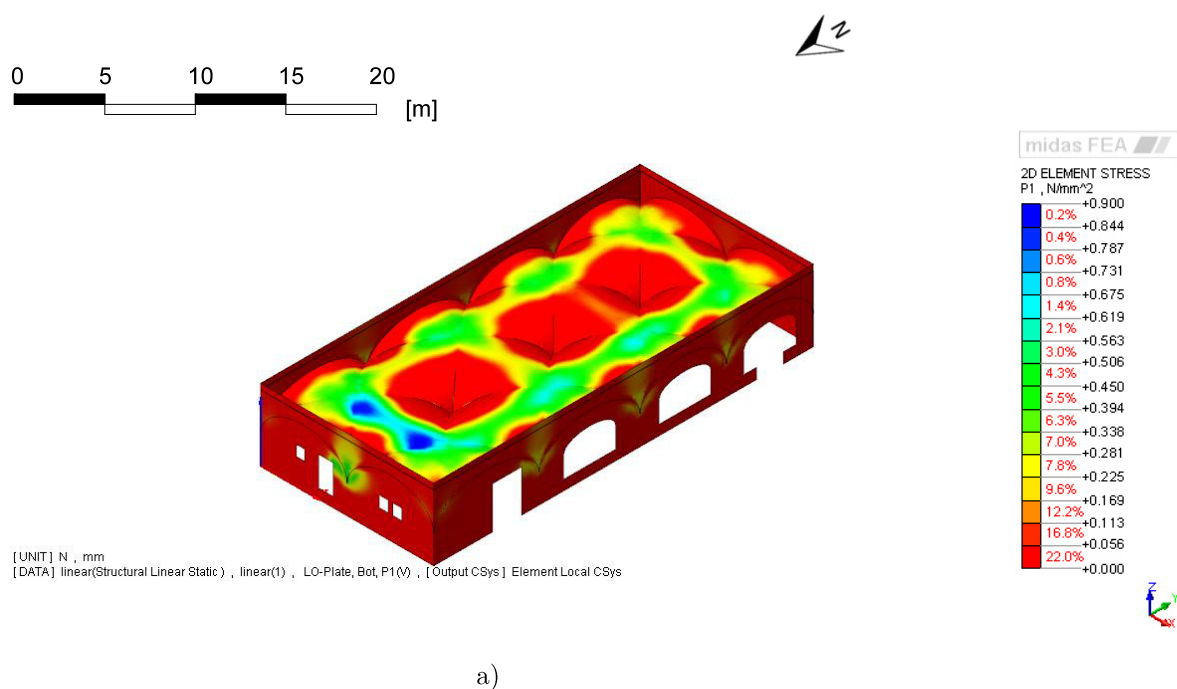
The following results were obtained through a linear analysis with a continuous model. The results that will be presented are the maximum principal stresses for tension and compression and the displacements for the permanent loads in all directions.

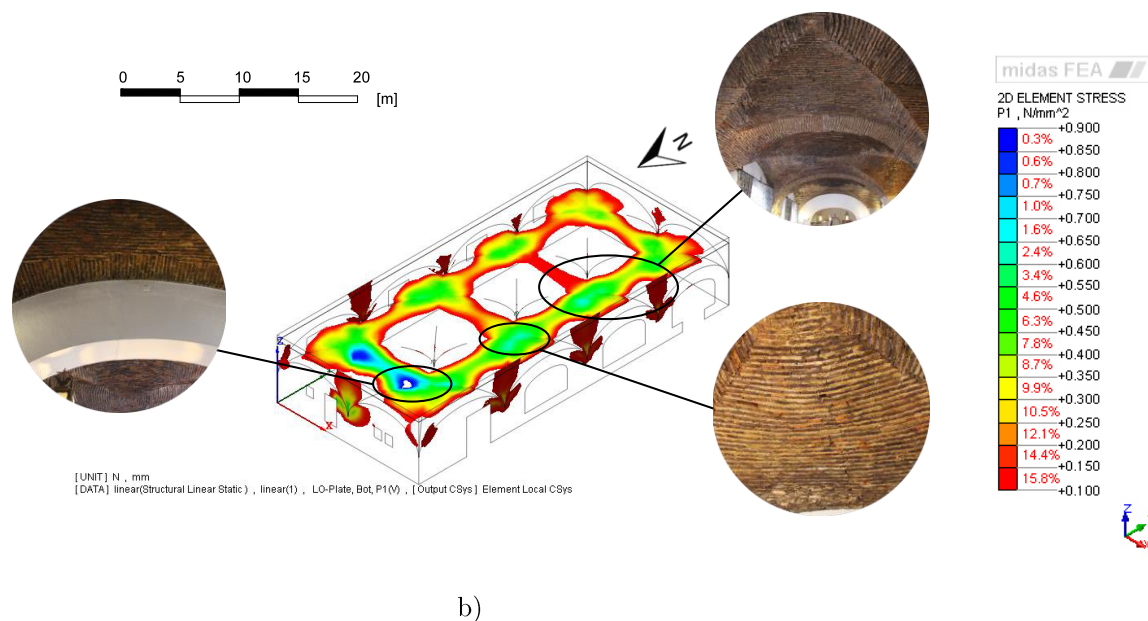


The maximum principal stress for tension for the loading conditions defined occurs in the lower fibres of the shell elements used to simulate the vaults as shown in Figure 5.44 a), with a value of 0.9 MPa and, as expected, appears in the central area of the vaults and in the closure area between the vaults and the walls or columns. It should be noted that lower stresses are obtained near the south wall, since this wall is thicker than the others.

From Figure 5.44 b) analysis, it is possible to conclude that there are areas that exceed the value of the yield stress, theoretically defined, regarding the tension,  $\sigma_t$ , of 0.1 MPa, value associated with the mechanism of joint fracture and indicated in the literature work (Milani, Milani et al. 2008) and (Szolomocki 2009).

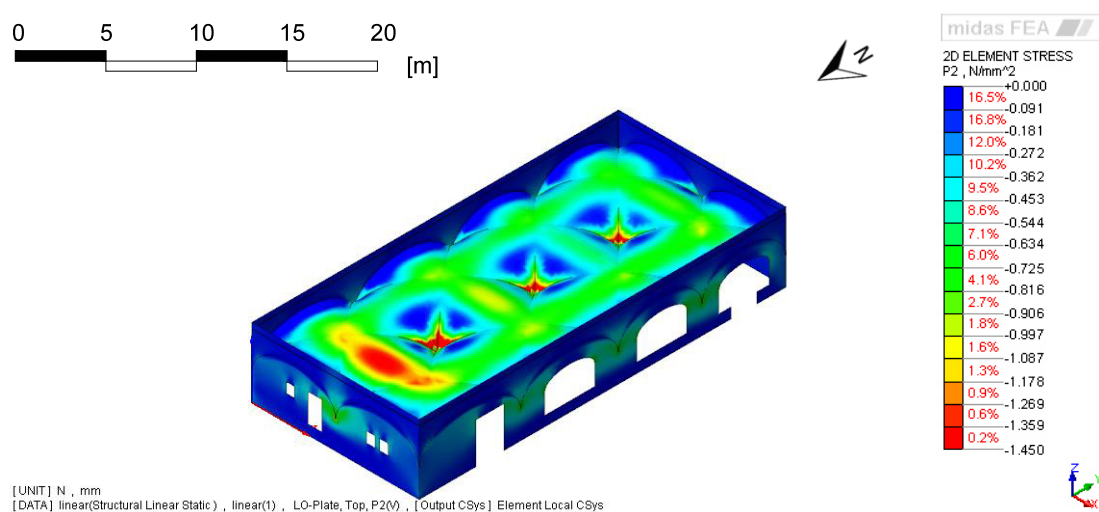
The stresses distribution of the model are well correlated with the pattern of the existing longitudinal cracking along the vaults observed. Due to the fact that the east and south walls are semi-buried makes these stiffer, thus presenting lower values of tension stresses.





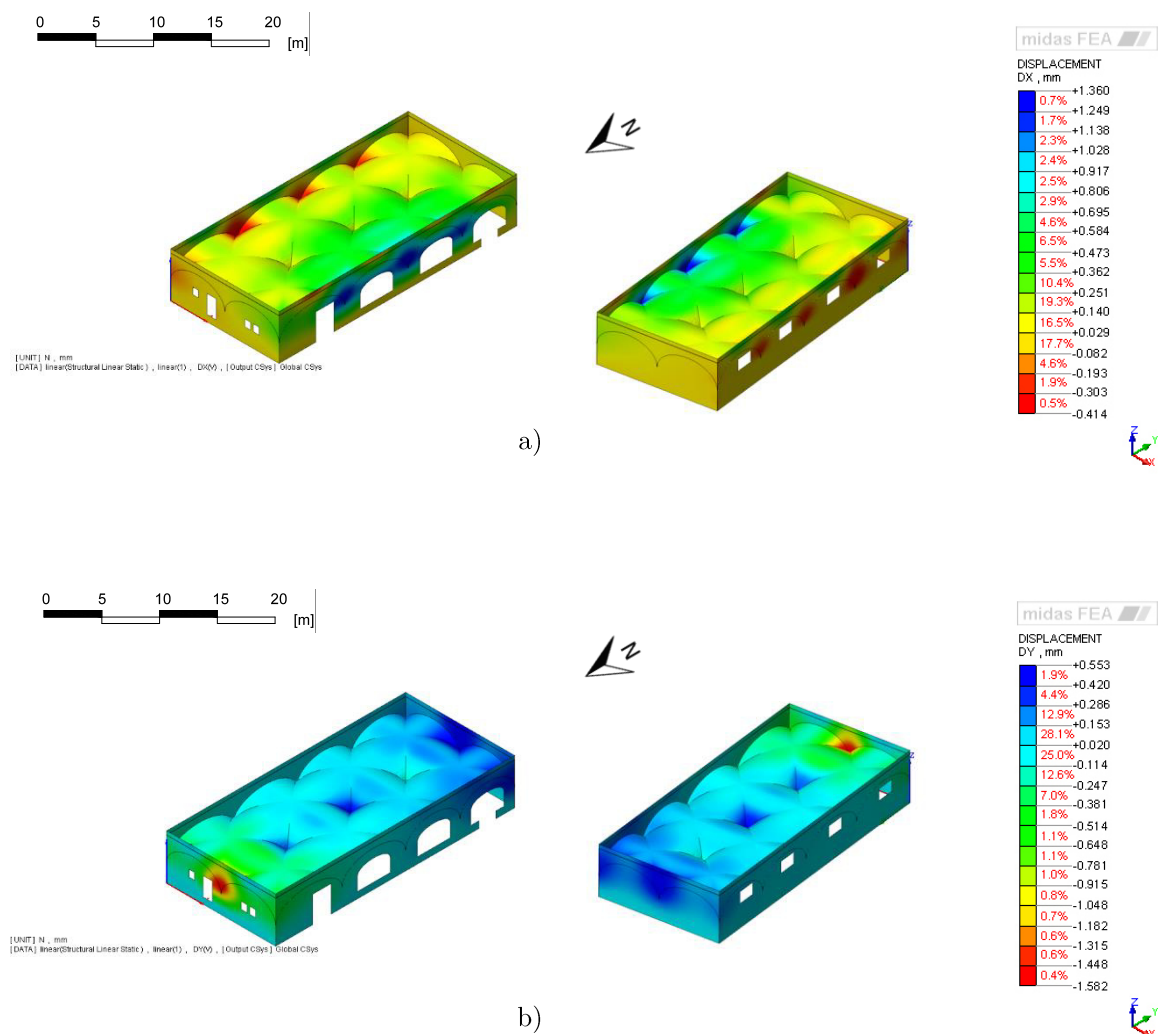
**Figure 5.44** – Maximum principal stresses for a) tension and b) tension higher than 0.1 MPa.

Regarding the maximum principal stress for compression, Figure 5.45, presents the greatest value of around 1.45 MPa and this higher values are located in the vaults (upper fibres) close to the columns and also in the vaults adjacent to the north wall, demonstrating a higher level of the vaults decompression consistent with the mapping of the maximum principal stresses for tension previously shown.



**Figure 5.45** – Maximum principal stresses for compression.

Considering the obtained displacements of the present linear analysis, as can be shown in Figure 5.46, in the XX and YY directions the maximum displacements occur in the connection area between the vaults and the masonry walls, being the maximum value approximately 1.4 mm and 1.6 mm for the XX and YY direction, respectively. The vertical displacements, in the ZZ direction, arise mainly in the vaults located near the north façade, indicating a decompression in the central area.



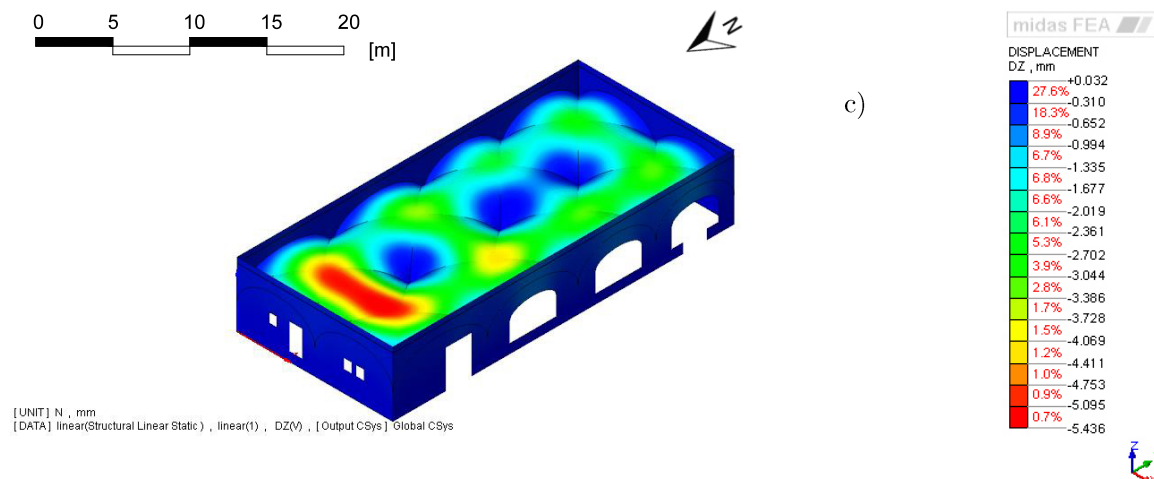


**Figure 5.46** – Displacements in the direction a) XX; b) YY and c) ZZ.

### 5.6.2 Linear analysis with a damaged model

Still following the linear analysis, but now with a damaged model, simulating in this way the condition state of the building (existent cracks at the present moment) it will be presented the maximum principal stresses for tension and for compression and the displacements in the XX, YY and ZZ direction.

Similar to the results of the linear analysis with a continuous model, also in this case, as demonstrated in Figure 5.47 a), the maximum principal tension stress appears in the lower fibres of the shell elements used to simulate the vaults in the connection area of the vaults with the walls or columns and also in the central areas of the vaults, standing out the areas near the north façade, being the maximum principal stress for tension, 1.02 MPa, slightly higher value comparatively to the obtained for the continuous model.

As stated in the previous case, it was defined for tension a yield stress,  $\sigma_t$ , connected with a joint fracture mechanism a value of 0.1 MPa, and in Figure 5.47 b) it is possible to identify the exceeding areas to this value. Predictably, the areas that exceed the

yield stress of 0.1 MPa trail the cracking simulated along the vaults and also, in the vaults and walls jointing.

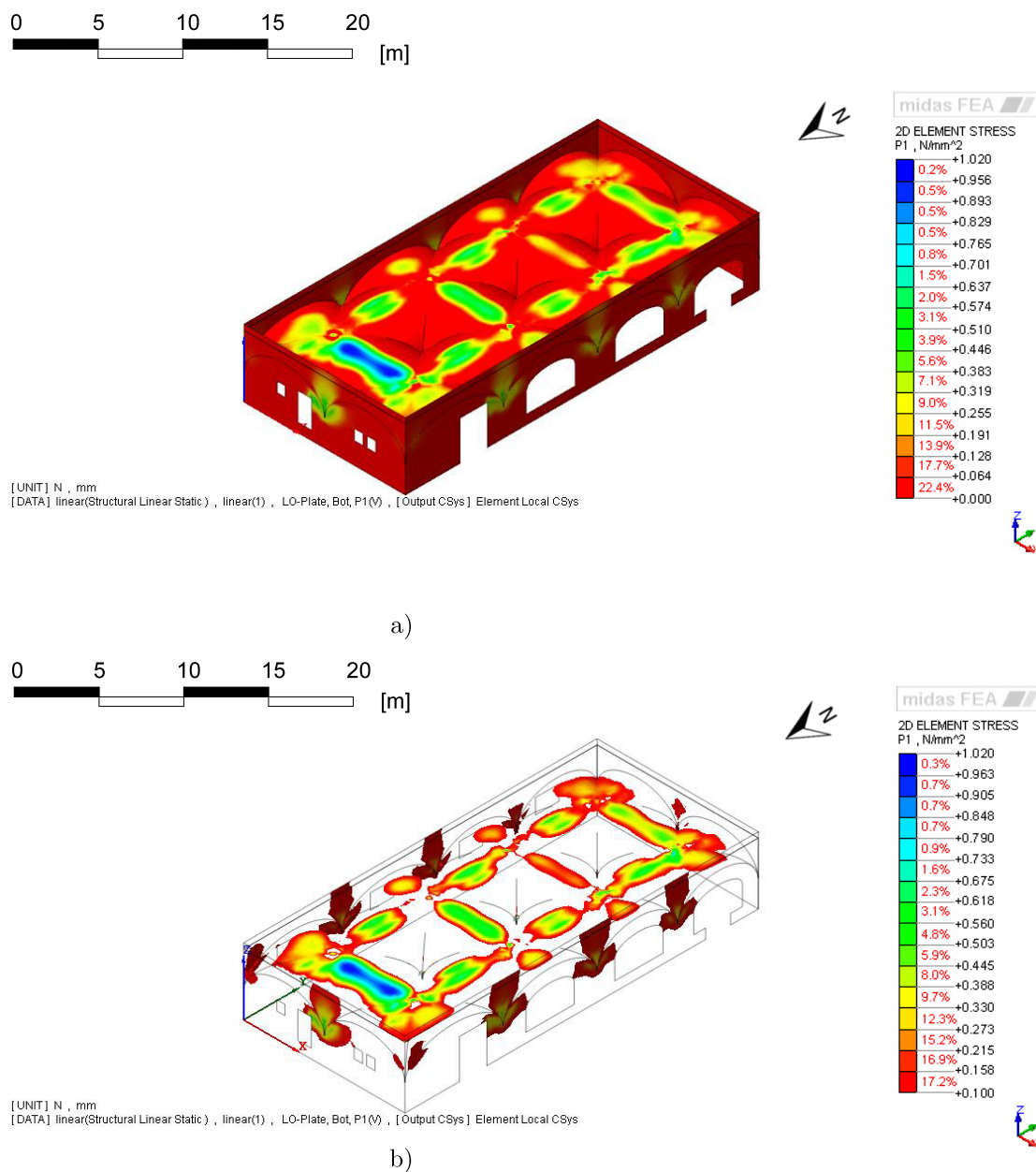


**Figure 5.47** – Maximum principal stresses for a) tension and b) tension higher than 0.1 MPa.

Relatively to compression, 3.86 MPa is the value for the maximum principal stress that appear in the higher points of the vault upperface, mainly in the vaults near the north

façade and in the areas closer to the columns representing a decompression in the connection between the vaults with the columns and walls (see Figure 5.48).

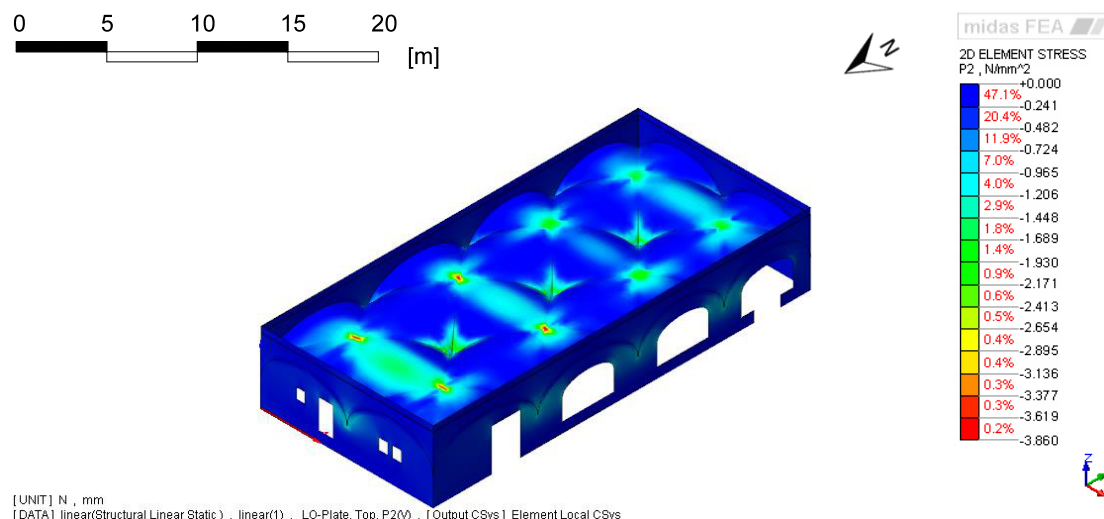


**Figure 5.48** - Maximum principal stresses for compression.

Contrary to what happened in the continuous model, in the present analysis the maximum displacements in the XX direction are situated in the simulated cracking position as expected, that is in longitudinally along the vaults with the maximum value of 1.9 mm (see Figure 5.49 a).

Regarding Figure 5.49 b), the displacements in YY direction, the higher values appear closer to the columns and to the vaults – masonry walls connection, more precisely in the north and south façade, occurring the maximum in the north façade, 1.9 mm, since this wall is less thicker than the south faced one.

The higher vertical displacements are distributed along the cracks, longitudinally. It should be noted that the maximum ZZ displacement is in the area near the front door and that displacement is around 10 mm as shown in Figure 5.49 c), a value that stands out relatively to the previous YY displacement.



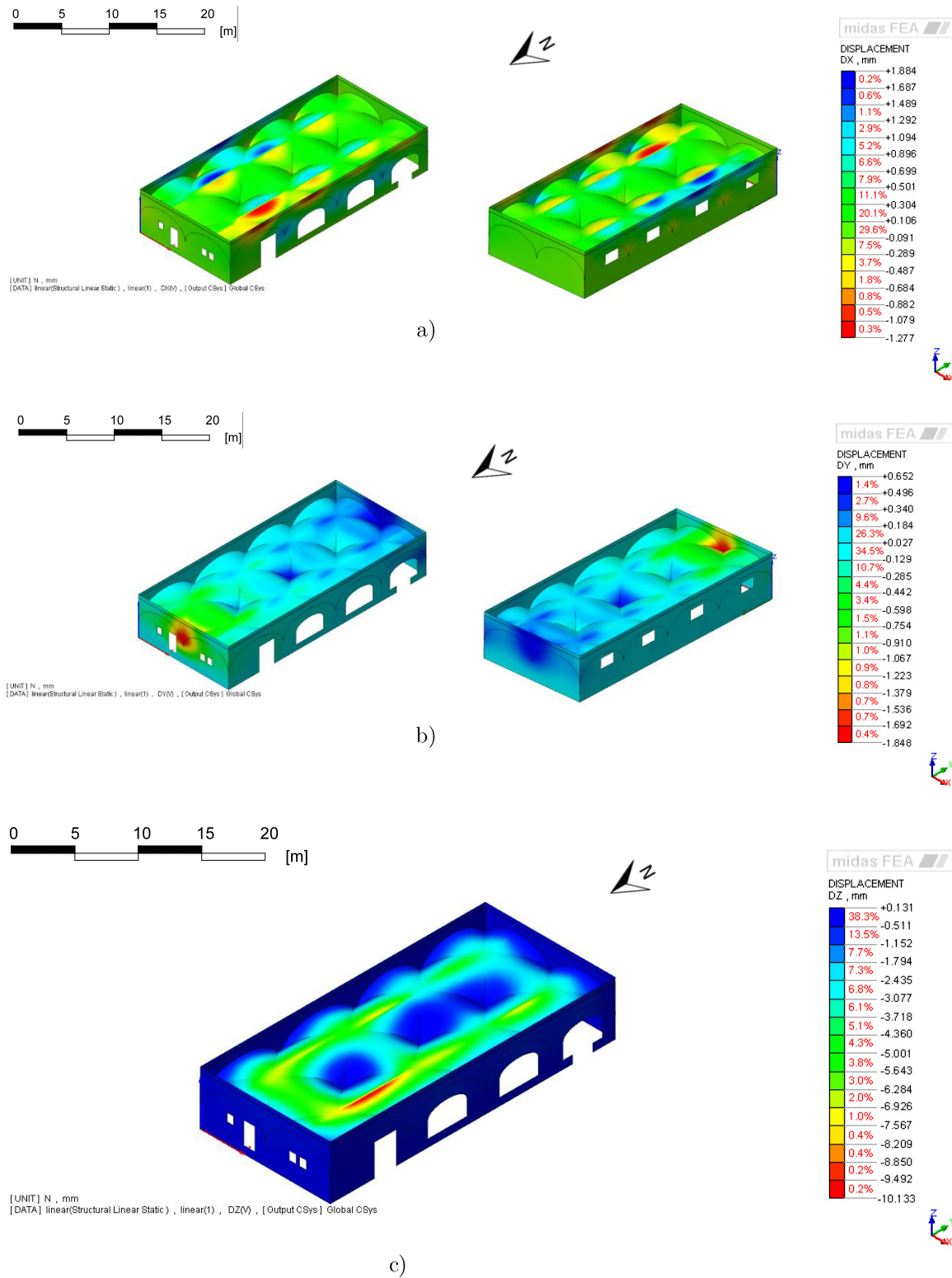


Figure 5.49 – Displacements in the direction a) XX; b) YY and c) ZZ.

### 5.6.3 Non-linear analysis with a continuous undamaged model

Regarding the non-linear analysis, it will be analysed again a continuous and damaged numerical model, and will be discussed the displacements either in the transversal and in the longitudinal direction, XX and YY direction, respectively. These displacements will be presented considering the load multiplier for the vertical load analysis (gravitational) and for the pushover analysis in the XX and YY direction. Taking into account the location, (Lisbon, Portugal) the ground type A (rock or other rock-like geological formation), the importance class III of the building (buildings whose seismic resistance is of importance in view of the consequences associated with a collapse, e.g. schools, assembly halls and cultural institutions, in this case) and the frequency, it is estimated, in Lisbon, an earthquake around 0.55g for the buildings first frequency according to the Eurocode 8 response spectrum, value that will be considered for comparison proposes in the analysis of the pushover results.

As mentioned in the introduction of the present sub-chapter, these analyses were performed through a total strain crack model type using functions and laws for the simulation of the non-linear behaviour of the materials used in previous research studies.

The vertical load analysis was achieved with 10 load steps with the maximum of 20 iterations per step, for the pushover analysis and it was increased the number of load steps to 100 with a maximum of 10 iteration per step. It is also important highlight that these iterations were performed resourcing to the Newton Raphson algorithm.

For the transversal displacements, XX direction, were analysed six distinct points of the structure: four in the corners and more two located in the middle (out-of-plane of the walls) and for the longitudinal displacements, YY direction, only the four points in the corners, as shown in Figure 5.50.



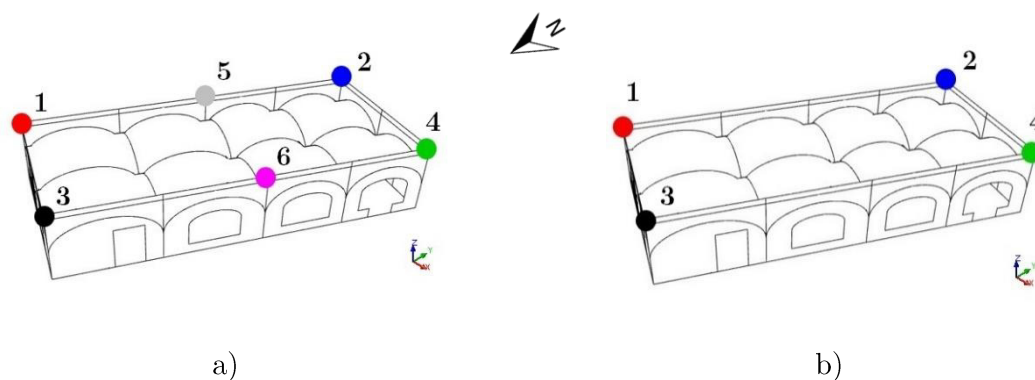


**Figure 5.50** – Position of the analysed points in the: a) transversal direction and b) longitudinal direction.

Regarding the vertical load analysis, the displacement in the XX direction that stands out, from Figure 5.51 occurs at the point number 6 with a value of around 6 mm, in the remaining points the higher displacement is 1mm. For the displacements in the YY direction (longitudinal displacements), the displacements are nearly zero being the maximum value slightly higher than 1 mm at the third point (Figure 5.52). It should be noted that any of these displacements are negligible comparing to the limit values.

The pushover analysis leads higher displacements, principally the displacements with the same direction of the analysis. Concerning the pushover analysis in the XX direction, the maximum transversal displacement, that is in the direction of the analysis, is around 130 mm at point number 6 (see Figure 5.53). This point exhibits this displacement due to the fact that it is positioned at half span of the more vulnerable/fragile wall since there are considerable openings and the other parallel longitudinal wall is semi buried. Still in the pushover analysis in the XX direction, the longitudinal displacements are unimportant when compared to the obtained for the transversal direction, being the higher value only 28 mm at the point number 4, as shown in Figure 5.54. Regarding the expected earthquake in Lisbon, the displacements

of the building are around 30 mm and 5 mm for the transversal and longitudinal displacements, respectively.

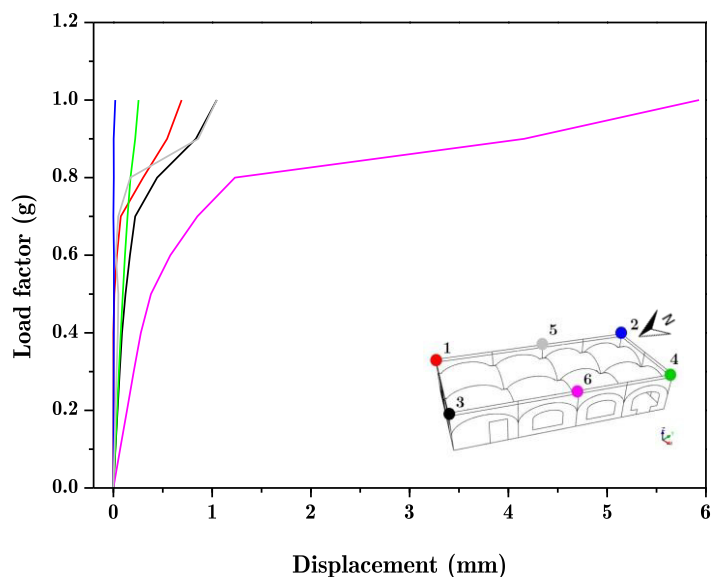


**Figure 5.51** – Transversal displacement vs load factor regarding the vertical load analysis with a continuous undamaged model.

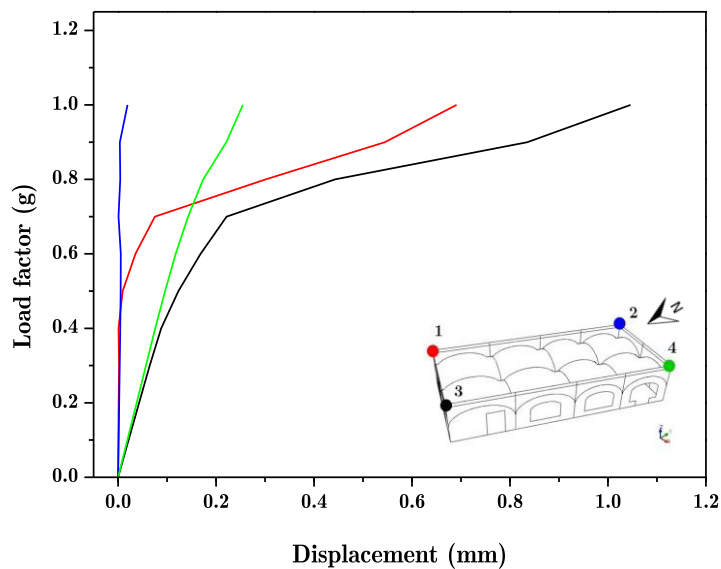


**Figure 5.52** – Longitudinal displacement vs load factor regarding the vertical load analysis with a continuous undamaged model.

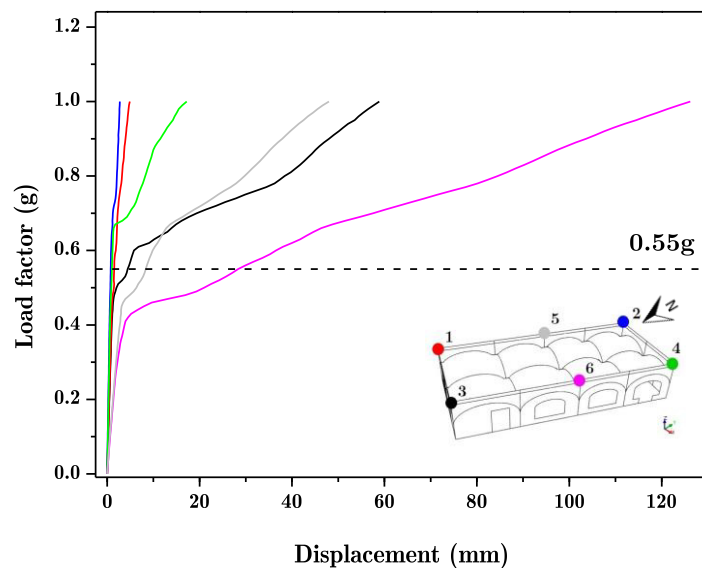


**Figure 5.53** – Transversal displacement vs load factor regarding the pushover analysis in the XX direction with a continuous undamaged model.

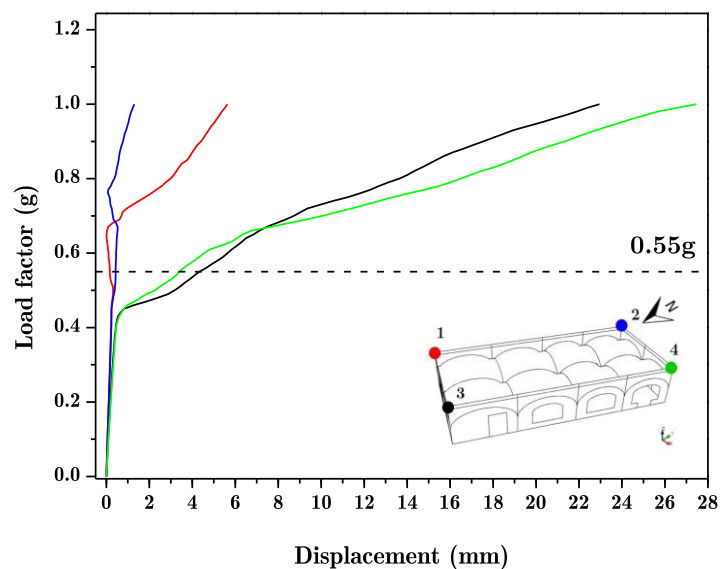


**Figure 5.54** – Longitudinal displacement vs load factor regarding the pushover analysis in the XX direction with a continuous undamaged model.

The displacements obtained through the pushover analysis in the YY direction are lower since the exposed area of the walls to this seismic load in this direction is inferior (north and south façade). The higher transversal displacement (XX direction) occur at point number 6, once more for the same reasons previously discussed, and is about 11 mm (see Figure 5.55). It is at the point number 4 that the maximum displacement in the direction of the analysis occurs and is around 40 mm, as shown in Figure 5.56. This maximum displacement arises at this point because it is closer to a considerable opening area.

The displacements for the 0.55g are practically inexistent, being the maximum displacement in the direction XX about 0.6 mm and 2 mm for the displacements in the YY direction.

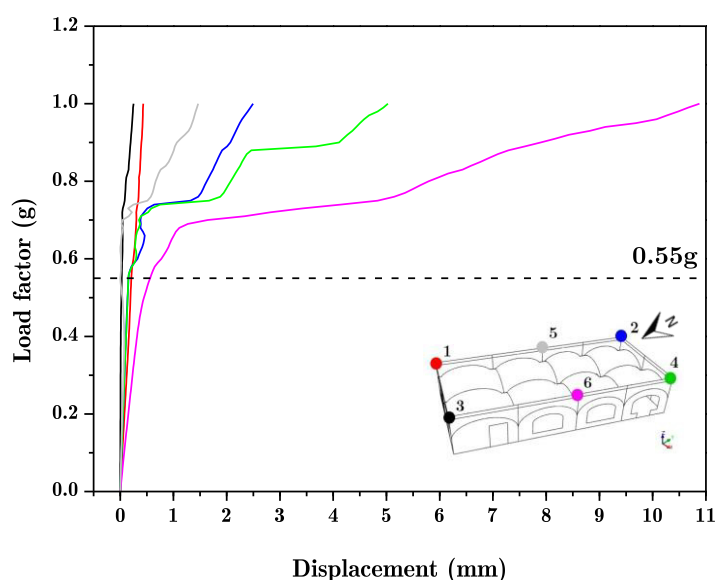


**Figure 5.55** – Transversal displacement vs load factor regarding the pushover analysis in the YY direction with a continuous undamaged model.

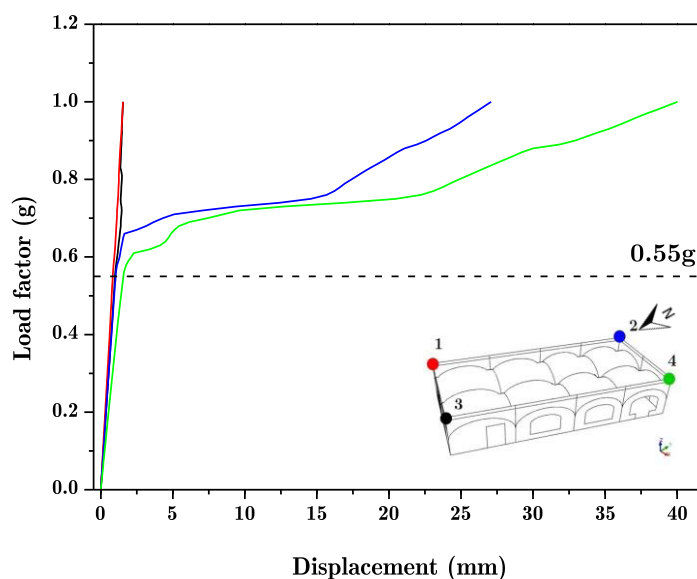


**Figure 5.56** – Longitudinal displacement vs load factor regarding the pushover analysis in the YY direction with a continuous undamaged model.

#### 5.6.4 Non-linear analysis with a damaged model

As referred above, in addition to the non-linear analysis with a continuous model, it was also performed a non-linear analysis on a damaged model in order to simulate the longitudinal crack in the masonry vaults in the structure before defining any retrofitting strategy.

As expected, all the displacements obtained with this model increased their value, being the most notorious the transversal displacement regarding the vertical load analysis, that increased up to 250 mm at point number 6 (see Figure 5.57), once more the point that lies half span of the most fragile wall. Regarding the YY displacements yet in the gravitational analysis, are highlighted the corner points in the north façade, as shown in Figure 5.58, with values around 18 and 20 mm.

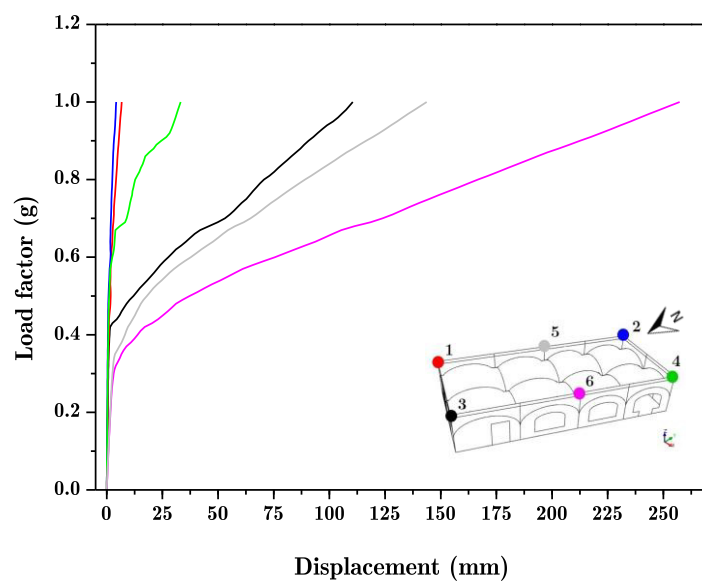


**Figure 5.57** – Transversal displacement vs load factor regarding the vertical load analysis with a damaged model.

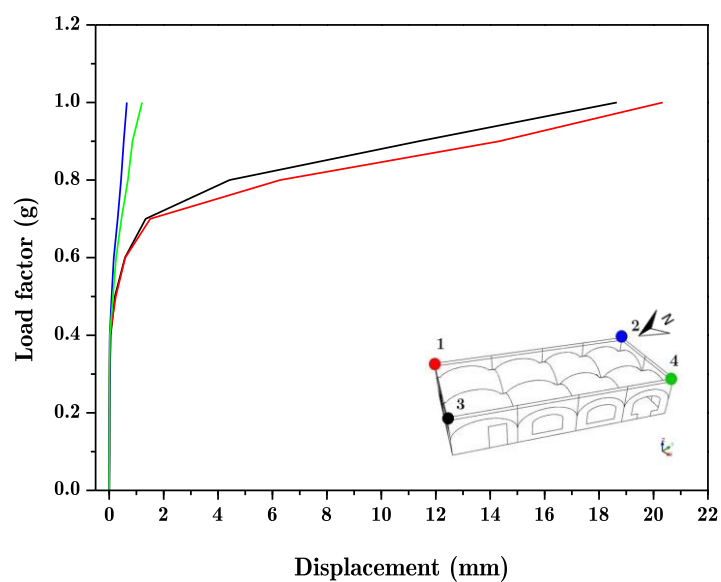


**Figure 5.58** – Longitudinal displacement vs load factor regarding the vertical load analysis with a damaged model.

When the building experienced a pushover analysis in the XX direction, the structure exhibited a very similar behaviour to the continuous model, however, as predictable, with higher values, occurring the maximum displacement at the point number 6 with a value of 250 mm, see Figure 5.59.

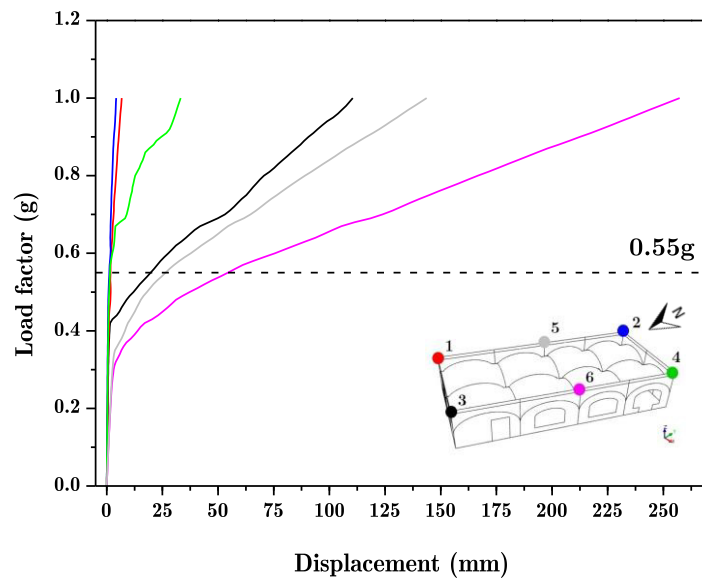


**Figure 5.59** – Transversal displacement vs load factor regarding the pushover analysis in the XX direction with a damaged model.

For the longitudinal displacements, as shown in Figure 5.60, the corner points of the west façade (entrance) feature displacements around 55 and 65 mm, once again higher values than the obtained for the continuous model. In relation to the pushover analysis in the YY direction, the highest transversal displacement attained is around 23 mm and appears at the half node of the most fragile wall, point number 6 (see Figure 5.61).

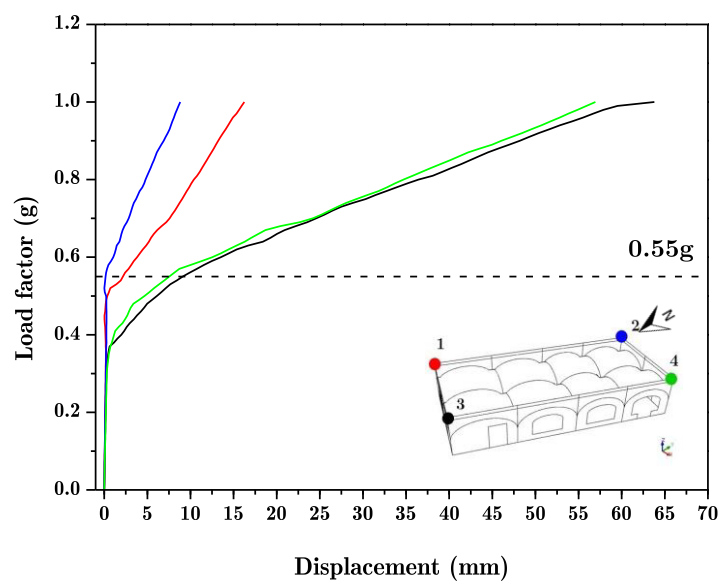


**Figure 5.60** – Longitudinal displacement vs load factor regarding the pushover analysis in the XX direction with a damaged model.

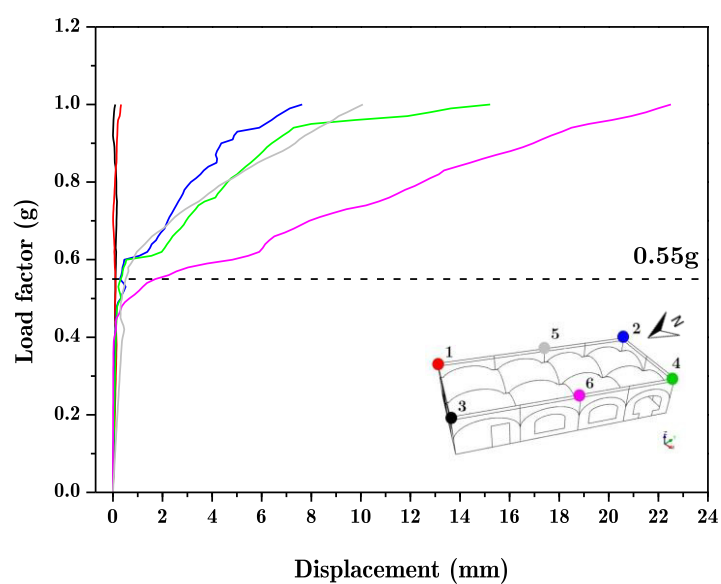


**Figure 5.61** – Transversal displacement vs load factor regarding the pushover analysis in the YY direction with a damaged model.



The displacements in the direction of the pushover analysis (longitudinal displacements) are more significant when compared with the transversal displacements, being the maximum 130 mm at point number 4, a corner point between the south and west façade, as shown in Figure 5.62.

For the expected earthquake, the maximum displacement for the pushover analysis in the XX direction (transversal direction) is around 60 mm.

Regarding the pushover in YY direction, the maximum displacement occurs in the direction of the pushover, as before, and is about 10 mm.

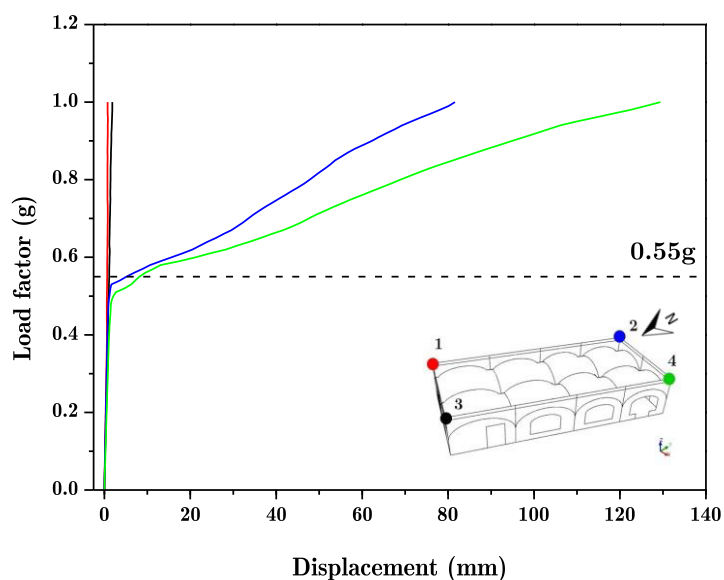


**Figure 5.62** – Longitudinal displacement vs load factor regarding the pushover analysis in the YY direction with a damaged model.

For better analysis of results of this sub-chapter, it is presented a comparison between the undamaged and damaged model for the pushover analysis in the XX (see Figure 5.63) and YY direction (see Figure 5.64).

Once again it was compared the displacements vs the load factor, but only for the obtained displacements in the direction of the pushover analysis since the perpendicular displacements are insignificant. It is possible to conclude that the presence of damage in the building increases the horizontal displacements to about the double in the case of the pushover analysis in the XX direction and to the triple for the YY direction pushover analysis, thus indicating the need of a retrofitting and strengthening action.

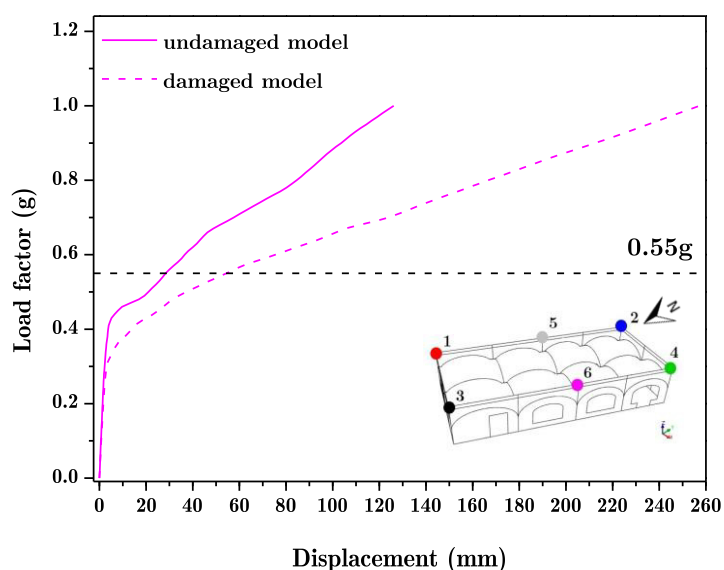


**Figure 5.63** – Transversal displacement vs load factor regarding the pushover analysis in the XX direction with an undamaged and a damaged model.

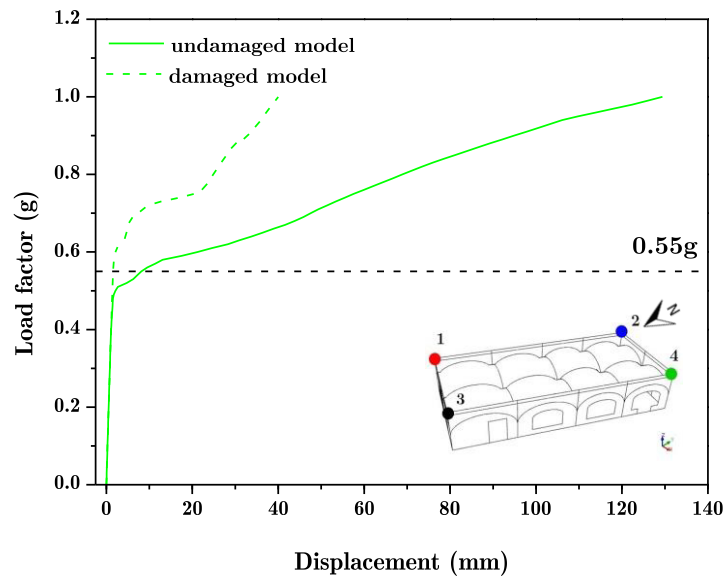


**Figure 5.64** – Longitudinal displacement vs load factor regarding the pushover analysis in the YY direction with an undamaged and a damaged model.

## 5.7 Retrofitting strategy proposals

Prior to any structural retrofitting strategies, it is important and necessary to perform structural consolidation works through inorganic grout injections in structural cracks on the interior XX of the masonry vaults in order to proceed to reclosing and consolidate the masonry.

This procedure begins with the removal of loose materials, joints opening and sanitation of these areas; joint grouting with lime and sand based mortar including the placement of PVC tubes for the grouts injection; provision, preparation and injection of the lime and sand based mortar through the appropriate equipment and finally the removal of the vent and injection pipes. After the cracks consolidation, the building is prepared for any retrofitting strategy implementation which will be described in this subchapter. The modelling of the retrofitting proposals will be based on non-linear analysis with a

continuous model since the cracks are considered already sealed. It should be noted that the retrofitting strategies were modelled taking into account not only the current use of the building but also the possibility to transform the terrace roof accessible for visiting and commercial purposes (esplanades for example), thus adding an overload of 4 kN/m<sup>2</sup>, according the RSA. For the evaluation of the structural capacity of the building with the reinforcement strategies also a seismic load analysis was assessed by a pushover analysis involving a gradual application (100 steps) of lateral equivalent static forces, in both directions x and y, individually, on the structure.

Given the extent of the results, for the implementation of the retrofitting strategies, only the actual condition of the building will be discussed in this sub-chapter, that is with no accessible terrace since this accessibility is only a future possibility and not a requirement. However, the results for the retrofitting strategy proposals with an accessible roof are presented in Appendix A.

### 5.7.1 Remove excess load

The first proposal for the building retrofitting goes through the removal of the excess load, thereby removing the first two layers, the red clay tiling and concrete screed layer. The load removal values and considering the load removal and making the terrace roof accessible over the masonry vaults is presented in Table 5.5.

**Table 5.5** – Terrace roof load over the vaults after the removal of the two first layers and considering an accessible roof.

---

	P <sub>sd</sub> central area (kN/m <sup>2</sup> )	P <sub>sd</sub> lateral area (kN/m <sup>2</sup> )
<b>Initial condition</b>	7.35	16.35
<b>Non-accessible roof (load removal)</b>	4.15	13.15
<b>Accessible roof (load removal)</b>	8.15	17.15

---

As referred above, it was stated that the results for the retrofitting proposals with the possibility of convert the terrace roof in an accessible area will be displayed in the Appendix A. However, for this first strategy it would make no sense, as shown in Table 5.5, to transform the terrace roof in an accessible area by removing the excess load and combating the aggravation of the live load, however possible. If required the accessibility of the terrace roof, deeper structural strengthening action is necessary.

Evaluating the vertical load analysis, removing the excess load reduces the maximum displacement in the XX direction in 83% and in YY direction 73%, as shown Figure 5.65 and Figure 5.66.

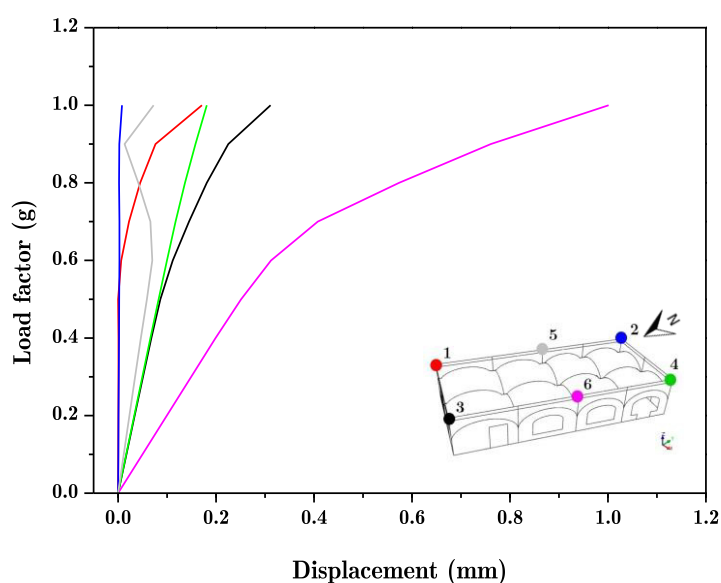


**Figure 5.65** – Transversal displacement vs load factor regarding the vertical load analysis.

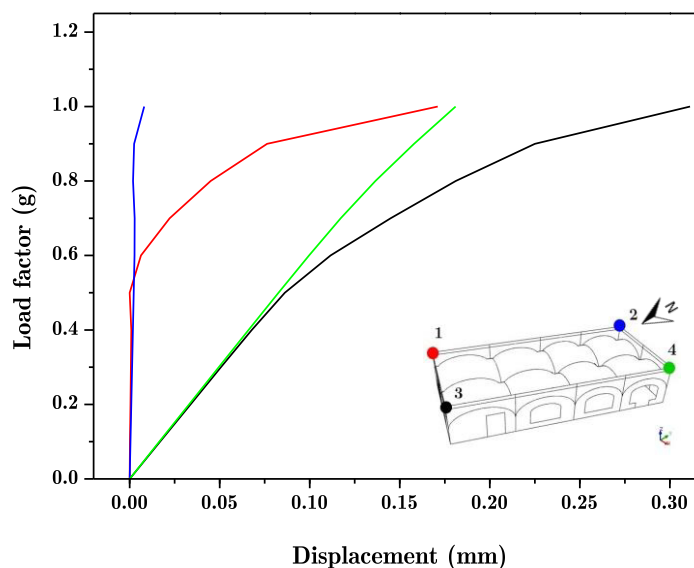


**Figure 5.66** – Longitudinal displacement vs load factor regarding the vertical load analysis.

Regarding the pushover analysis in the XX direction, this reduction is not so significant, being only 12% and 18% for the transversal and longitudinal displacements, respectively (see Figure 5.67 and Figure 5.68).

For the pushover analysis in the YY direction a reduction by half of the longitudinal displacements occurs (see Figure 5.69), although for the displacements in the direction of the analysis the reduction is very slight, being only 5% (see Figure 5.70).

Facing these results, it is possible to conclude that this retrofitting strategy is adequate considering the vertical load, exclusively, but incompatible with the pushover analyses, once the reduction of the displacements is not notorious.

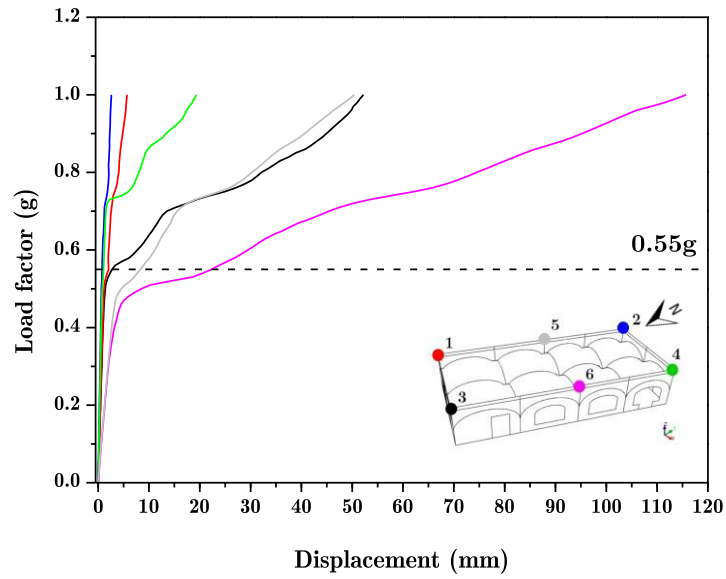


**Figure 5.67** – Transversal displacement vs load factor regarding the pushover analysis in the XX direction.

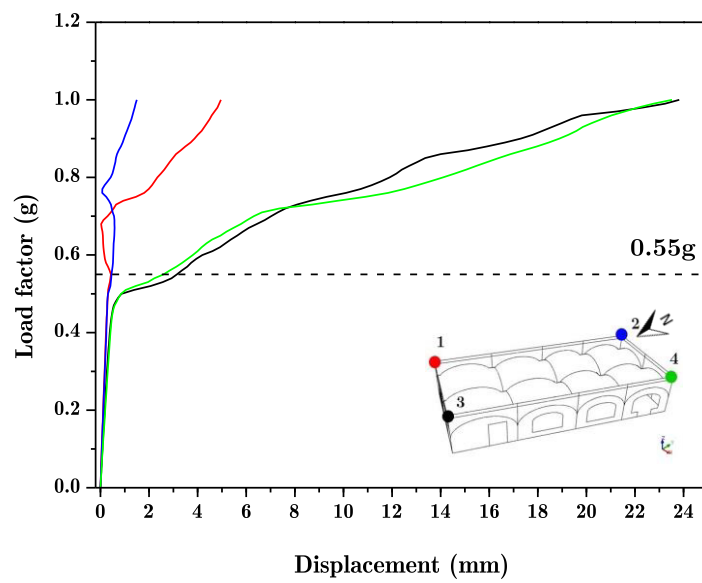


**Figure 5.68** – Longitudinal displacement vs load factor regarding the pushover analysis in the XX direction.

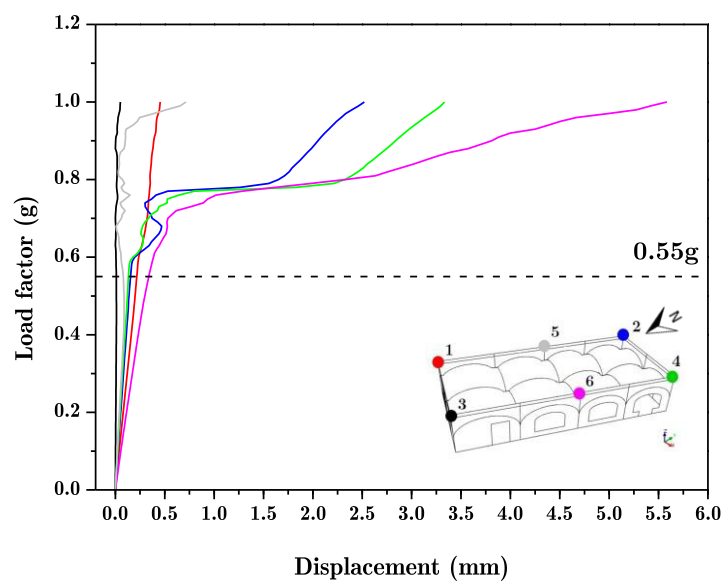


**Figure 5.69** – Transversal displacement vs load factor regarding the pushover analysis in the YY direction.

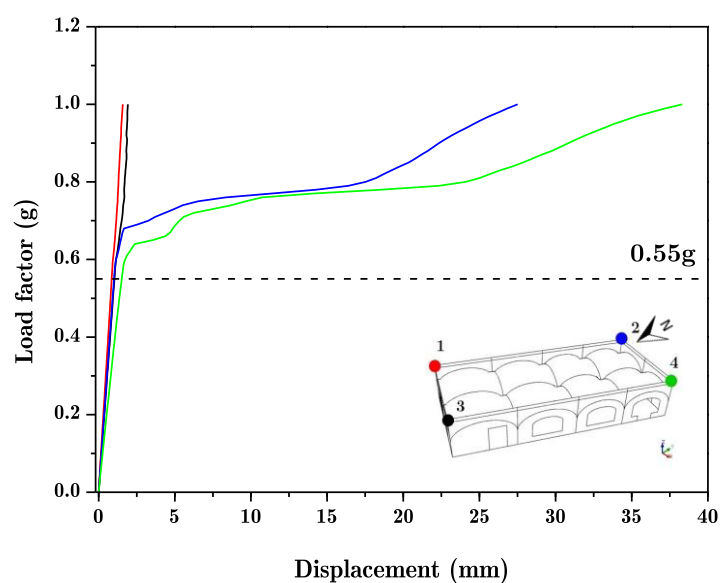


**Figure 5.70** – Longitudinal displacement vs load factor regarding the pushover analysis in the YY direction.



Regarding the distribution of tension stresses, for the pushover analysis in the XX direction (see Figure 5.71) it is visible that there is a reduction of the higher values of tension compared with the structure without any retrofitting strategy, increasing the percentage of the elements with tension stresses near to zero.

For the pushover analysis in the YY direction, as shown in **Figure 5.72**, the tension stresses are smaller than the obtained with the pushover in the other direction, inducing a more uniform distribution of stresses. With the removing of the excess load, the most stressed areas are relieved increased, mainly in the areas between the masonry vaults, in both directions (longitudinally and transversally).

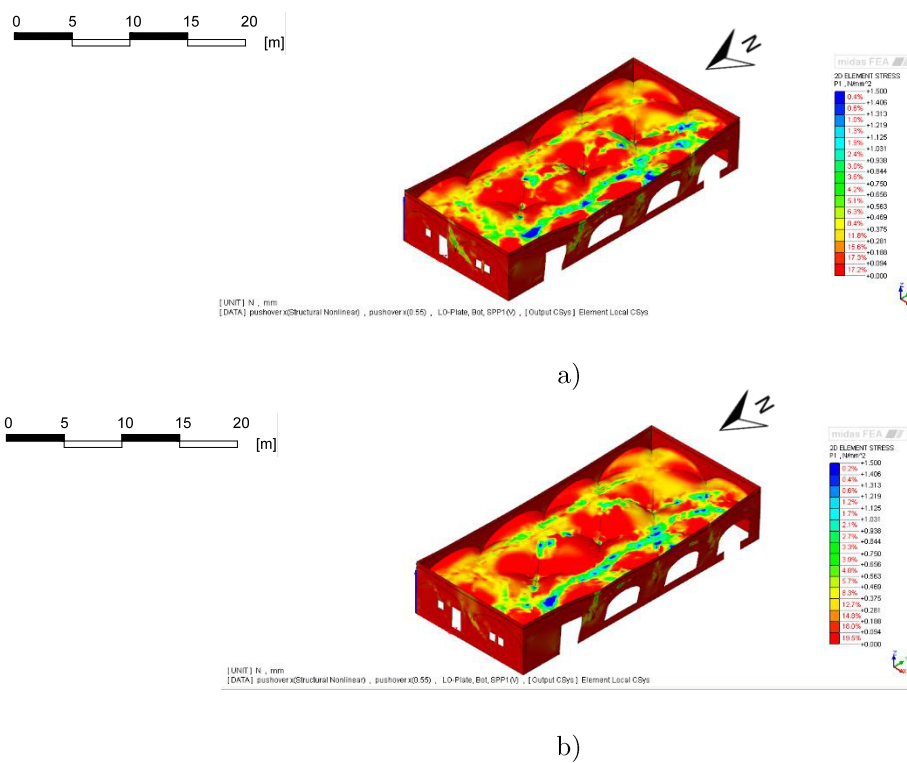


**Figure 5.71** – Tension stress distribution for the pushover analysis in XX direction: a) before and b) after the retrofitting strategy.

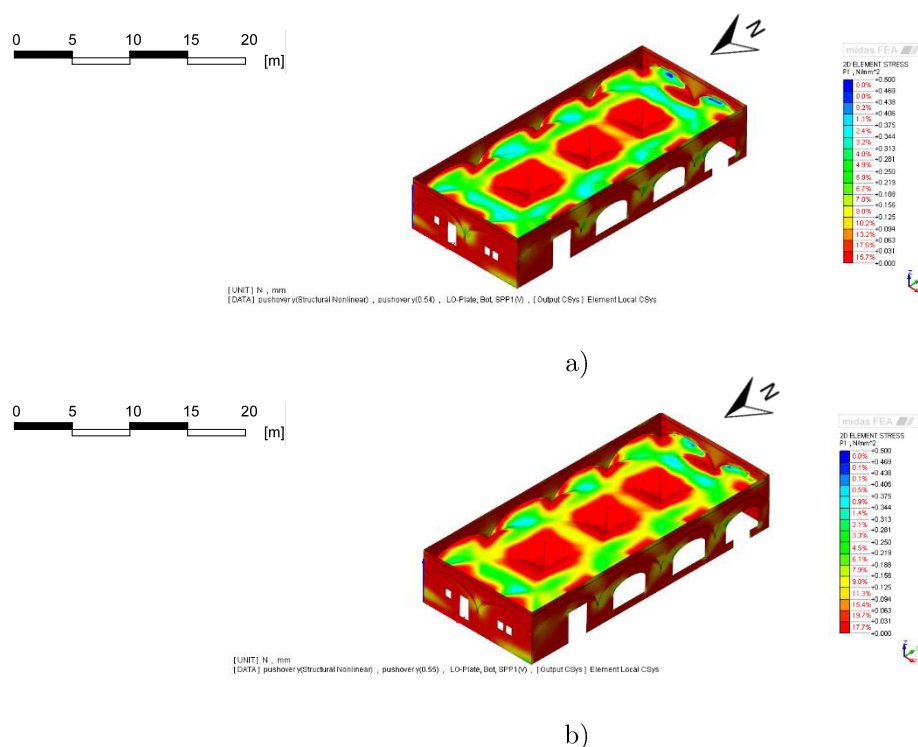


**Figure 5.72** – Tension stress distribution for the pushover analysis in YY direction: a) before and b) after the retrofitting strategy.

### 5.7.2 Steel tie-rods

Another retrofitting strategy proposal is the introduction of steel tie-rods to compensate the thrust induced by the vaults over the external masonry walls. These tie-rods should be fixed with a slight pre-stressing with the purpose of guarantying that they will always be under tension state (Asteris and Plevris 2015).

For this strategy, it was adopted two distinct solutions regarding the steel tie-rods location, intrados or extrados of the vaults, across the building (see Figure 5.73). When placed in the vaults intrados, three tie-rods are positioned in the lower area of the vaults, adjacent to the masonry columns, the opposite happens when the tie-rods are in the extrados, they will be positioned at an upper height, going through and above the vault structure, making a total of four tie-rods. It was used tie rods with a diameter

of 25 mm and steel A500 and those tie-rods were fixed with a pre-stressing of 2 kN to guarantee that they will always be under tension.

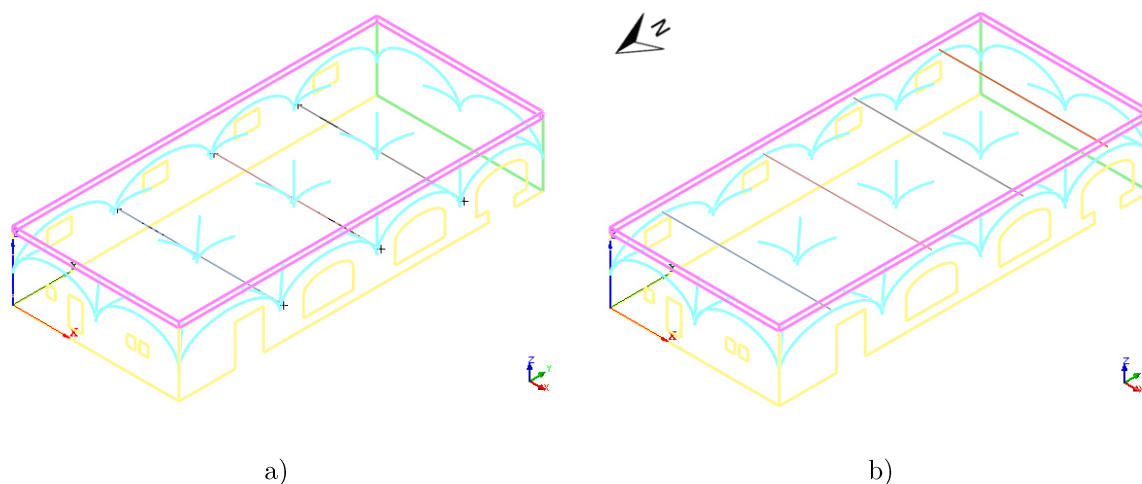


**Figure 5.73** – Steel tie-rods positioning: a) vaults intrados and b) vaults extrados.

#### 5.7.2.1 Intrados steel tie-rods

Regarding the vertical load analysis, with the present retrofitting proposal, it is possible to decrease the displacements in the XX direction and YY direction about 83% and 25%, respectively, being both of the maximum values no more than 1 mm, value in practical terms insignificant, as can be observed in Figure 5.74 and Figure 5.75.

For the pushover analysis, in the XX direction, either in the transversal (see Figure 5.76) and longitudinal displacements (see Figure 5.77) were reduced around 70% in respect to the maximum value. For the expected earthquake in Lisbon, using intrados tie rods decreased the displacement in the XX direction to 22 mm and in YY direction to 4 mm.

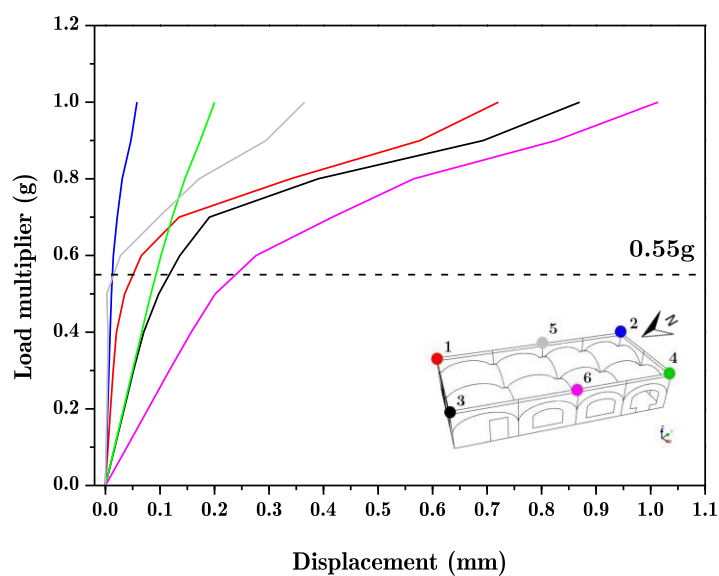


**Figure 5.74** – Transversal displacement vs load factor regarding the vertical load analysis.

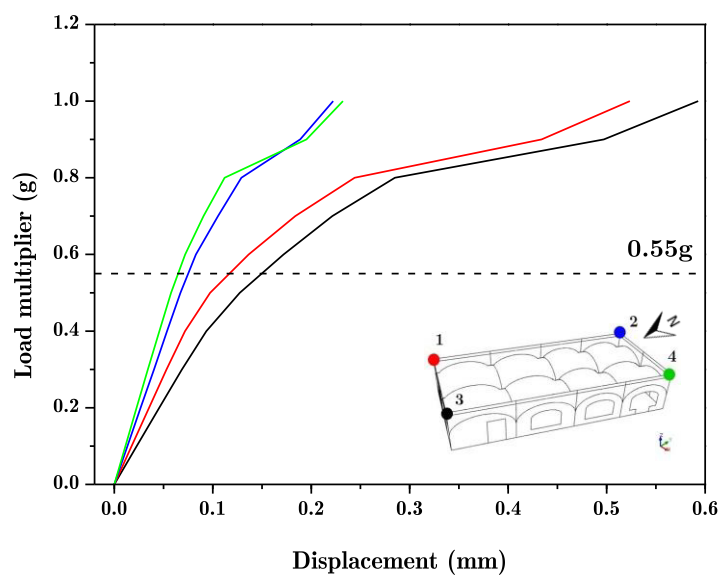


**Figure 5.75** – Longitudinal displacement vs load factor regarding the vertical load analysis.

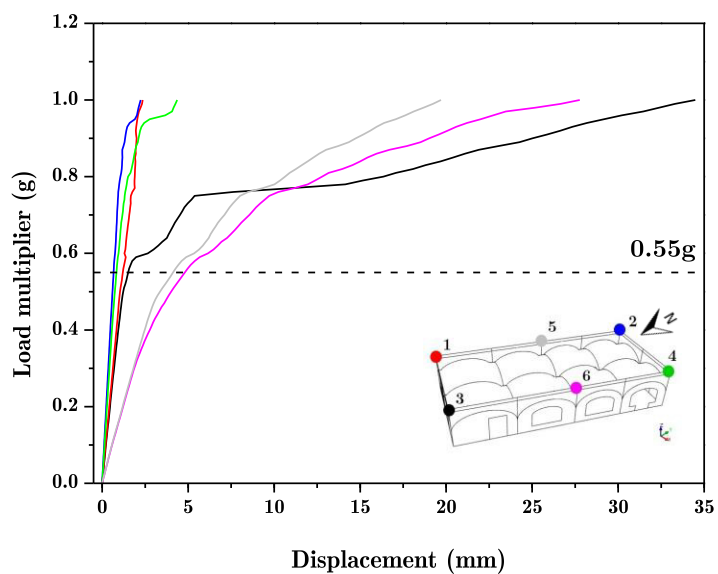


**Figure 5.76** – Transversal displacement vs load factor regarding the pushover analysis in the XX direction.

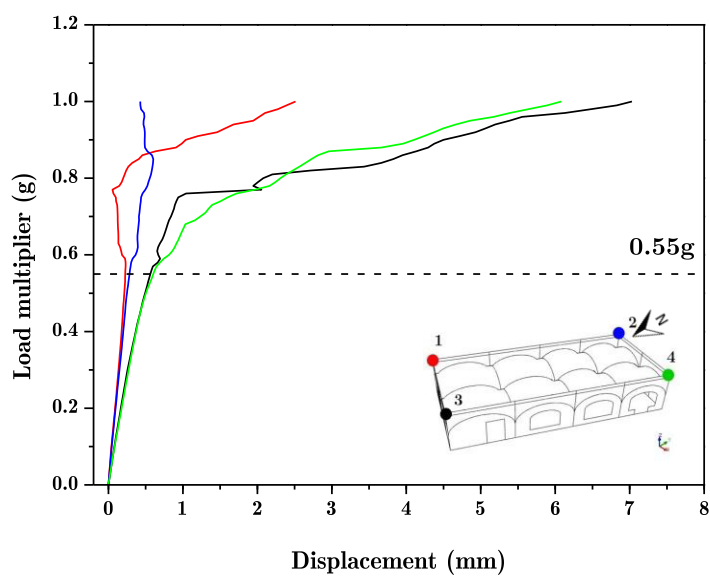


**Figure 5.77** – Longitudinal displacement vs load factor regarding the pushover analysis in the XX direction.

Regarding the pushover analysis (see Figure 5.78 and Figure 5.79) in the YY direction, the displacements reduction is around 62% in the XX displacements and a slightly increase of 3% in the displacements that occur in the direction of the analysis. This happens, possibly, due to the fact that the dimension of the walls in the direction YY is inferior, causing smaller displacements and consequently less observable effects of this proposal, since is not the significant direction in the global response of the structure.

It is important to highlight that the nodes where the higher displacements occur remain the same as before, of the non-retrofitted model.

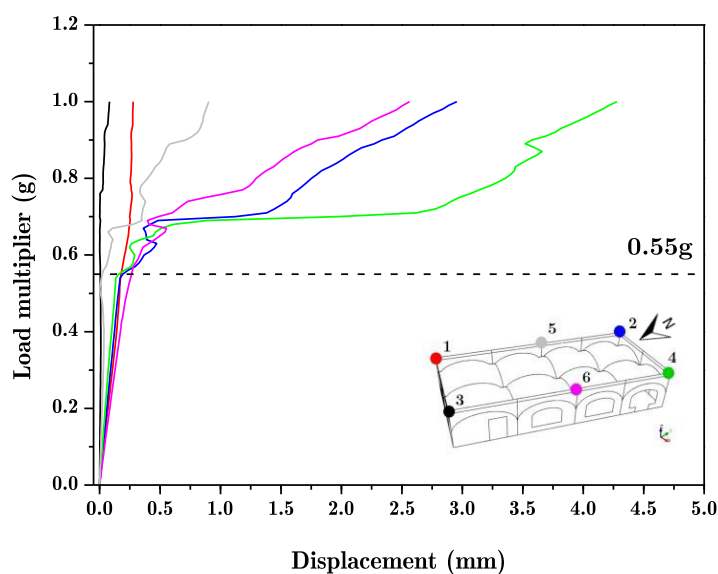


**Figure 5.78** – Transversal displacement vs load factor regarding the pushover analysis in the YY direction.

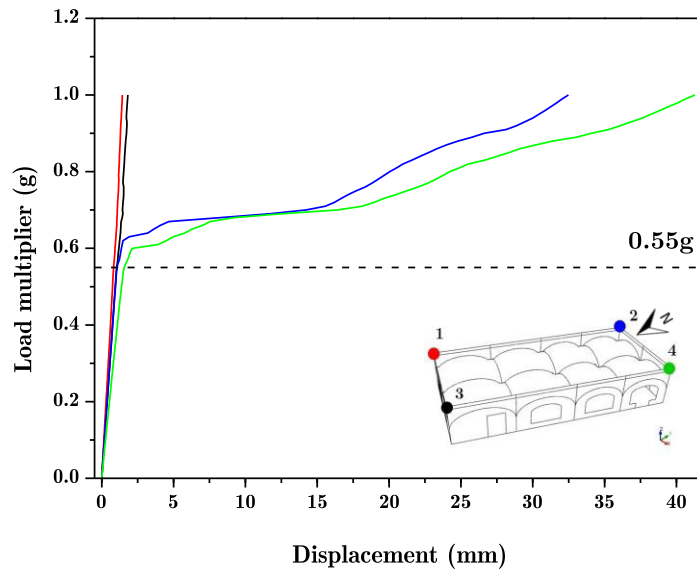
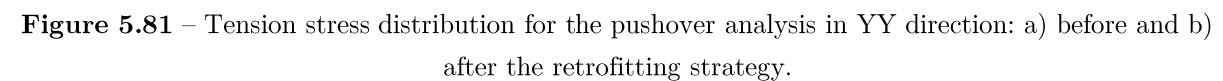
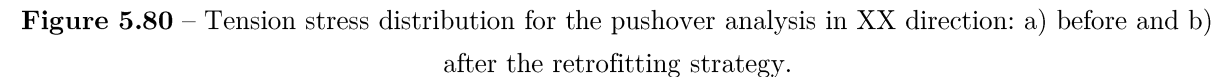


**Figure 5.79** – Longitudinal displacement vs load factor regarding the pushover analysis in the YY direction.

Analysing the tension stress distribution for the pushover analysis in the XX direction, as shown in Figure 5.80 a slight reduction of the higher values of tension percentage are reduced when compared with the structure without any retrofitting strategy, increasing the percentage of the elements with tension stresses.

Regarding the pushover analysis in the YY direction, through the observation of Figure 5.81 the reduction of the percentage of tension stress is not visible, however this happens because it was analysed the maximum values at certain points and not for the overall behaviour of the building.

The positioning of the steel tie-rods in the masonry vaults intrados allowed a stresses reduction mainly for the higher heights of the vaults and longitudinally along the masonry vaults where the cracks are located.





### 5.7.2.2 Extrados steel tie-rods

Examining the obtained results for this retrofitting proposal which positions now the tie-rods in the extrados of the masonry vaults, for the vertical load analysis there is a reduction of the displacements in XX direction of about 77% and in the YY direction around 14% (see Figure 5.82 and Figure 5.83).

For the pushover analysis in the XX direction, as shown in Figure 5.84, the extrados steel tie-rods allowed a reduction around 60% of the displacements that occur in the direction of the analysis, and 41% in the YY direction (see Figure 5.85). The maximum displacements for 0.55g are 12 mm and 3 mm for the transversal and longitudinal displacements, respectively.

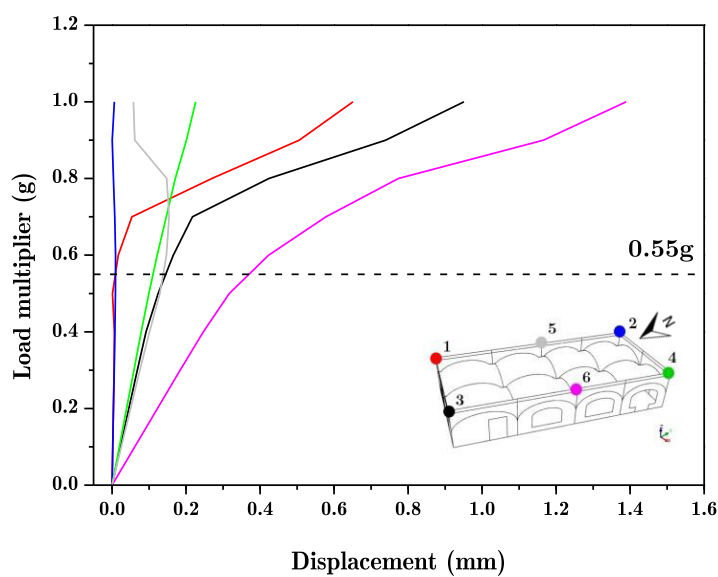


**Figure 5.82** – Transversal displacement vs load factor regarding the vertical load analysis.

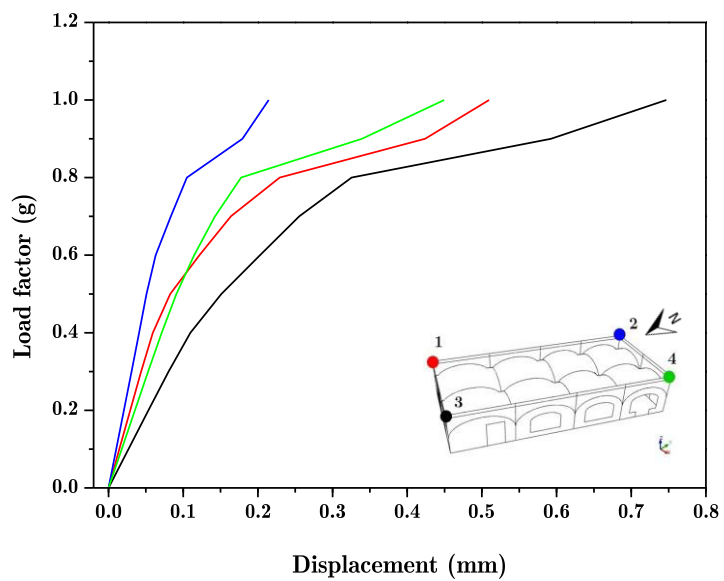


**Figure 5.83** – Longitudinal displacement vs load factor regarding the vertical load analysis.

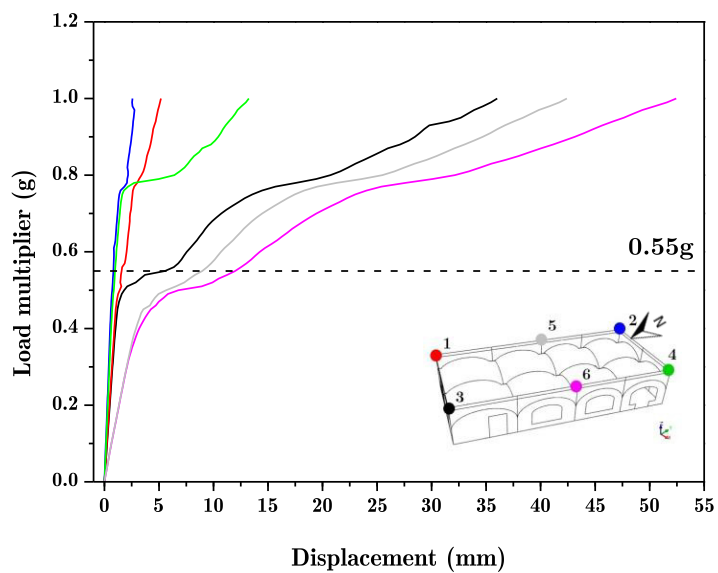


**Figure 5.84** – Transversal displacement vs load factor regarding the pushover analysis in the XX direction.

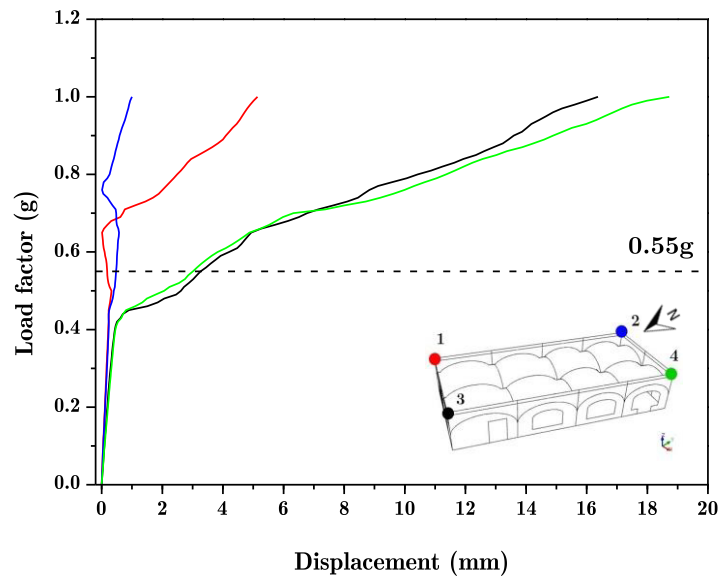


**Figure 5.85** – Longitudinal displacement vs load factor regarding the pushover analysis in the XX direction.

Regarding the seismic analysis, in the YY direction, the same occurs in the structure when used the tie-rods in the intrados of the vaults, there are a reduction of the transversal displacements about 6 mm (see Figure 5.86) and in the longitudinal displacements the effect is not perceptible (see Figure 5.87).

As in the other retrofitting strategy solution, the points where the higher displacements occur do not change.

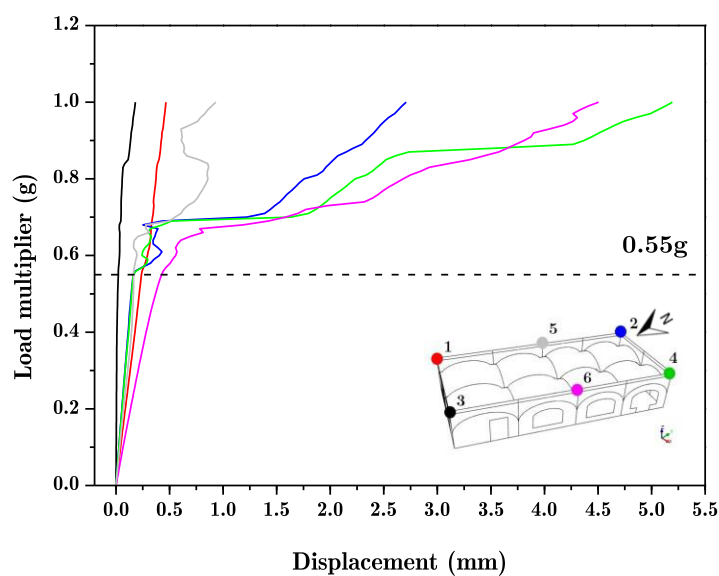


**Figure 5.86** – Transversal displacement vs load factor regarding the pushover analysis in the YY direction.

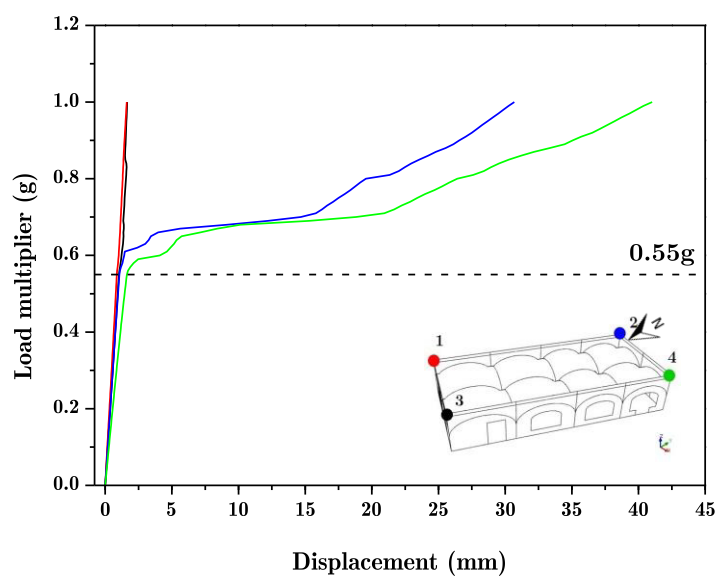


**Figure 5.87** – Longitudinal displacement vs load factor regarding the pushover analysis in the YY direction.

The positioning of extrados steel tie-rods leads to a reduction of the tension stresses when a pushover analysis in the XX direction is performed (see Figure 5.88), reducing the higher values of the stresses in the tension field and increasing the percentage of the areas with lower and near to zero tension stresses.

For the pushover analysis in the YY direction, compared to what was verified with the intrados steel tie-rods for the pushover in this direction, when the tie-rods are positioned in the extrados of the masonry vaults the tension stresses do not decrease, but the contrary was observed, as shown in Figure 5.89. This happens because the positioning of the tie-rods lead to a tension increase but only in specific areas and not on global level of the structure.

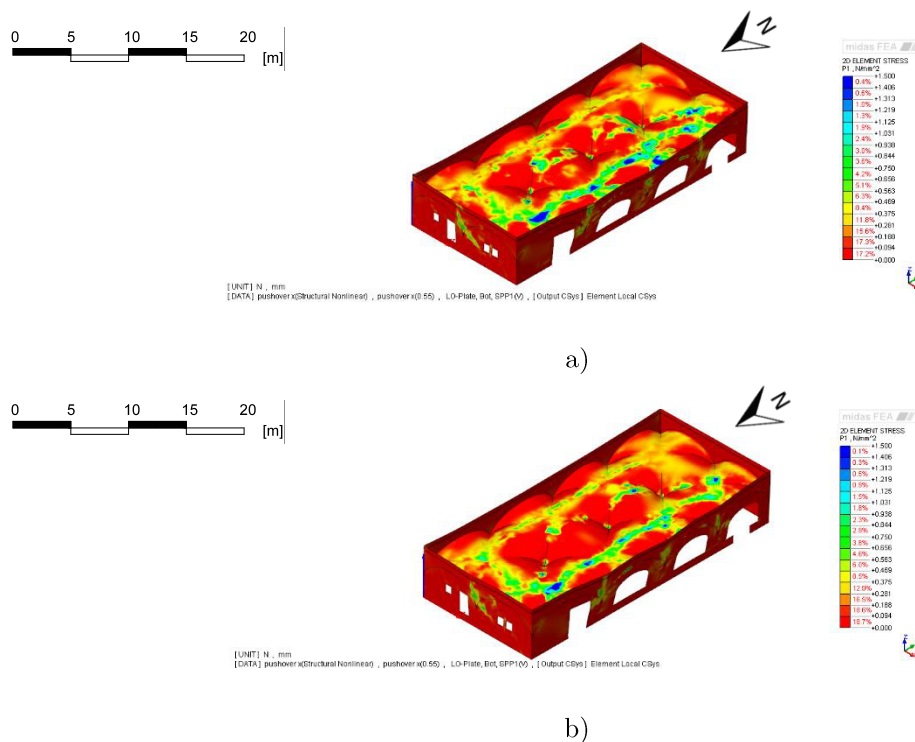


**Figure 5.88** – Tension stress distribution for the pushover analysis in XX direction: a) before and b) after the retrofitting strategy.

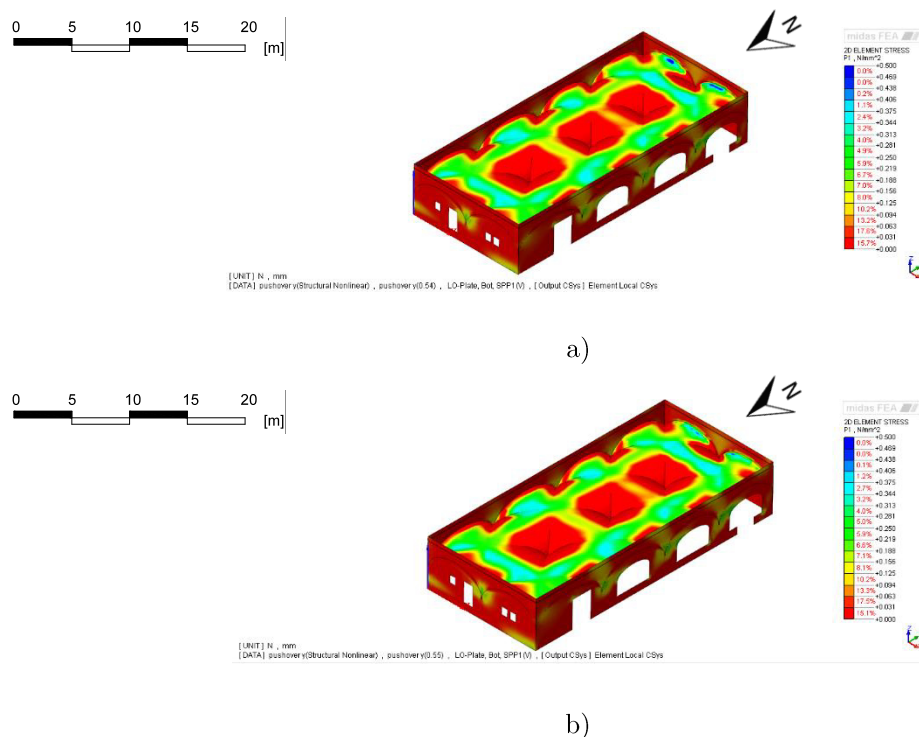


**Figure 5.89** – Tension stress distribution for the pushover analysis in YY direction: a) before and b) after the retrofitting strategy.

Comparing the proposed retrofitting strategies, it is possible to conclude through the analysis of Figure 5.90, for a pushover analysis in the XX direction, in respect to the obtained displacements in that direction (the most significant) are drastically reduced to more than a half, being the removal of the excess load the strategy with less impact and the positioning a steel tie-rods in the intrados of the masonry vaults the proposal with the better results. Analysing the point 6, the introduction of steel tie-rods in the vaults intrados provides better results, however analysing the overall behaviour of the structure relatively to the steel tie-rods in the vaults intrados the maximum displacement appears in the point number 3. For the pushover analysis in the YY direction, only the removal of the excess load proposal reduces the displacements (see Figure 5.91), once the introduction of the steel tie-rods in the building designed to reduce the vulnerability in the XX direction, will cause a slightly increase of the longitudinal displacements in case of an earthquake in YY direction. It should be noted,

however, that these displacements are much lower when compared with the obtained results for a pushover analysis in the XX direction.

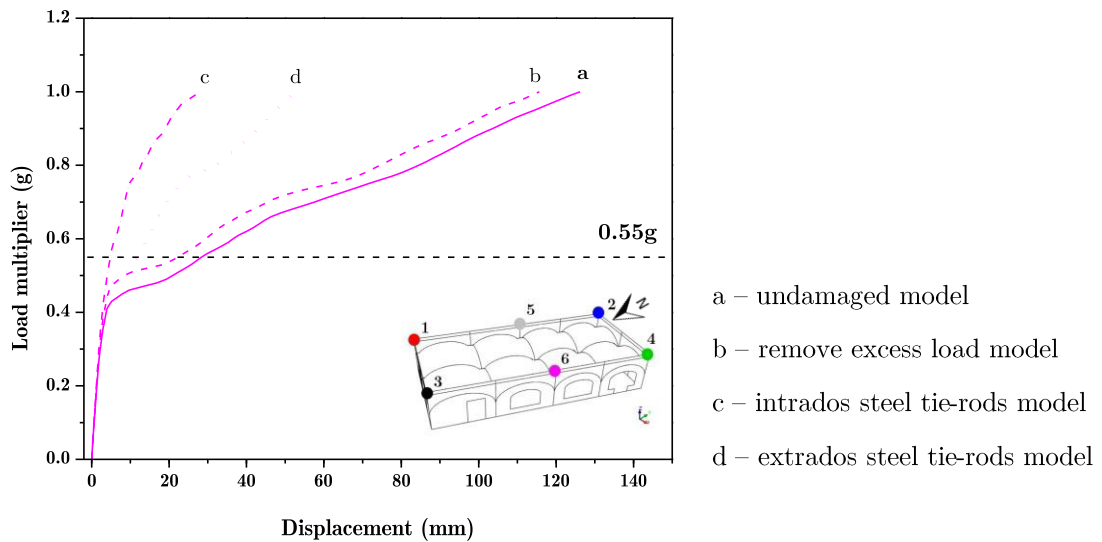


**Figure 5.90** – Transversal displacement vs load factor regarding the retrofitting strategy proposals through a pushover analysis in the XX direction.

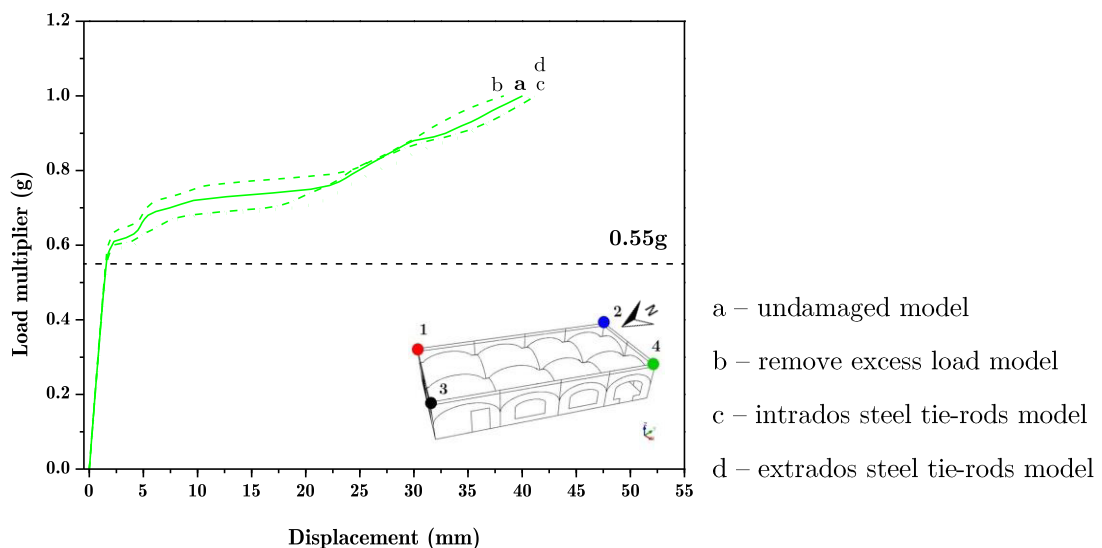


**Figure 5.91** – Longitudinal displacement vs load factor regarding the retrofitting strategy proposals through a pushover analysis in the YY direction.

### 5.7.3 Fibre Reinforced Polymer strips (FRP)

Generally, the collapse of the masonry elements is induced by the fractures opening due to the limited strength in tension. The existence of fibre reinforced polymers in the tensile areas of the masonry structure will prevent the fracture opening (Szołomicki, Berkowski et al. 2015). These polymers are based on materials that present favourable effects on the structural response and load capacity such as carbon fibre and glass fibre reinforced polymer, CFRP and GFRP, respectively.

The composites of fibre reinforced polymer bring a significant contribution of load bearing capacity by the lack compensation of the tensile capacity of brick masonry elements. The application of FRP strips (see Figure 5.92) in the inside and outside surfaces of the groined vaults can avoid the opening of the cracks and the formation of collapse mechanism of the structure (Szołomicki *et al.*, 2015).

Nevertheless, this type of retrofitting strategy is incapable of preventing masonry from cracking or yet repairing an existent crack but instead, transmitting the tension between the two edges of the crack causing an embroidery of the crack stitching the crack together.

The tension force goes over the existent crack and is transferred directly to the reinforcement which means that the reinforcing of the extrados or intrados of the vaults, successfully prevent the collapse mechanism triggering, compelling the structures to fail by another failure mode such as: crushing, sliding and FRP rupture (Corradi, Borri et al. 2015).





**Figure 5.92** - FRP retrofitting strategy in Via Roma San Pio, L'Aquila: a) placement of the FRP strips and b) final result (SismyGroup 2016).

Facing the numerical modelling difficulties that this technique presents and the extension of the present work, the retrofitting strategy proposal based on strips of fibre reinforced polymer will not be modelled. Using of FRP composite materials exhibit several benefits as high strength and stiffness in the fibre direction, simple execution and the offer of an extensive range of possible applications in distinct damage situations (Szołomicki, Berkowski et al. 2015). Besides the complexity of the modelling of the process of FRP strip, there are some drawbacks in the use of fibre reinforced polymer such as the intolerance to uneven bonding surfaces, the possibility of fragile failure modes, risk of fire and high material costs (Hollaway 2011). Hereupon, the economics of the fibre composites and other systems depend upon the circumstances requiring a comparison between the advantages and disadvantages in short and long term (Hollaway 2011).

Applying this retrofitting technique to this case of study, either carbon fibre or glass reinforced polymers can be considered for the FRP strips externally bonded on the existent masonry vaults. The numerical analysis of the FRP strips can be performed based on several literature data (Szołomicki, Berkowski et al. 2015), where it is indicated the location and the layout of the strengthening strips as shown in Figure 5.93.

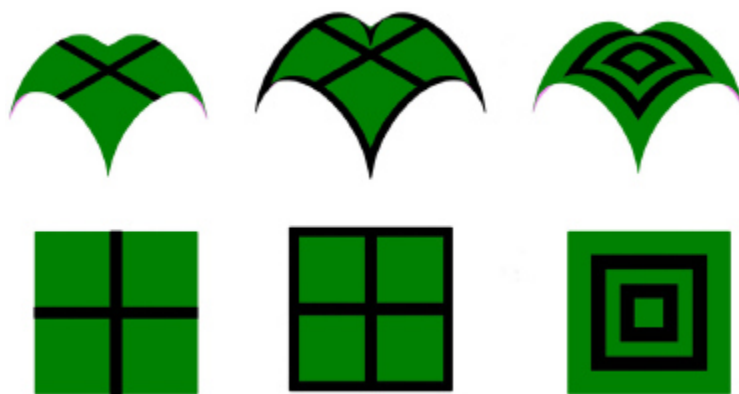


**Figure 5.93** – Possible layout of the FRP strips application for vault strengthening.

## 5.8 Final synthesis

In this chapter is presented the study case of an one-story building of the São Jorge Castle. A calibrated numerical model was defined and the results of the retrofitting strategies proposals presented.

The first main conclusion focuses in the differences between the linear and non-linear analysis being the non-linear analysis more adequate, mainly because it is studied a historical construction, becoming essential to understand the non-linearity of the materials, however with the linear analysis it was possible to detect where the most damage occurs and the development of damage mechanisms.

The fact that the building is semi-buried, leads to torsion, in other words, displacements in the other direction of the analysis, for example in the pushover analysis in the XX direction it is visible displacements in the YY displacements, although insignificant values. Still in the seismic vulnerability study, as expected, the displacements of the building in the XX direction are of higher amplitude than the obtained displacements through the pushover analysis in the YY direction, since the exposed area of the building in the direction XX is greater, causing more effects on the overall behaviour of the structure.

Analysing the retrofitting strategy proposal, it is possible to conclude that removing the excess load is a good strategy in respect to the vertical loads of the building but when a pushover analysis is performed, the strength increase of the building structure is not improved. For the possibility of a future earthquake (0.55g), the steel tie-rods present a better response of the structure facing horizontal loads. Comparing the position of the tie-rods, vaults intrados or extrados, the results are very similar, although the intrados vaults present slightly inferior displacements. It should be noted that the introduction of the steel tie-rods improves the global response of the building, however can imply local increase of the tension stresses but only in certain and specific points of the structure.



# CHAPTER 6

## FINAL CONSIDERATIONS

This dissertation focused mainly on the evaluation of the structural capacity of two historical constructions, the Palma de Mallorca Cathedral and the Paço Real II (a one-story masonry arched building of the São Jorge Castle). For both was performed numerical modelling resorting to different finite element software's, developing a parametric study to understand the influence of the material properties on the overall behaviour of the structure and as well as proposing and analysing retrofitting strategies.

Next is presented the main conclusions of the present work and identified suggestions for possible future research.

## 6.1 Conclusions

As previously referred, this thesis has the main aim of evaluating the structural capacity of historical constructions, Palma de Mallorca Cathedral and a building of the São Jorge Castle complex based on numerical modelling.

- As discussed in the Chapter 2, it is crucial, first of all, to recognise and understand the different macro-elements and possible damage mechanisms of historical construction (façade, nave, transept, triumphal arch, dome, amongst others), that can occur in the structure, thus allowing a more precise and accurate analysis and future retrofitting strategy proposals. It is possible to conclude that there are several damage mechanisms that are common considering the distinct macro-elements, as the out-of-plane movement and shear mechanisms that lead to cracking.
  
- A literature review of historical constructions structural analysis is presented in the third chapter, in which are introduced several methods of structural analysis as the method based on limit analysis, finite elements that can be based on macro or micro-modelling approaches and discrete elements. There is no better method to perform a structural analysis but a most suitable and adequate based on the analysis purpose, the adoption of an appropriate approach to carry out a structural analysis should bear in mind behind the objectives, also the cost, the need of an experienced user and the results use. An important subject also discussed in this chapter are the existence of difficulties and constraints in the modelling of historical constructions which are an obstacle that must be overcome with research, as well as the uncertainty that may be related to aspects as the geometry, material, actions, existent damage and possible alterations.

Because of these possible ambiguities, it is not so correct to propose a single method of analysis, but rather complement it with other methods to compare the results and also validate the models with analytical calculations.

### **6.1.1 Mallorca Cathedral**

In chapter 4 is introduced the case study of Palma de Mallorca Cathedral that allowed to understand the influence of the material properties variation over the behaviour of the structure, through a sensitivity analysis. This variation has more influence when performed a seismic analysis than a long-term deformation analysis, being more notorious the effects in the global response of the building the reduction of the material properties rather than its increase. For this case study, the variation of the properties had no influence in the damage mechanism, appearing the most damaged areas with higher stress concentration at the base of the window in the buttress, the base of the piers and the joining areas of the clerestory with the piers and buttresses.

### **6.1.2 São Jorge Castle – Paço Real II building**

In the more extensive chapter, Chapter 5, is presented the other study case, a building in the complex of the São Jorge Castle – Paço Real II. This chapter allowed to understand the influence of some important aspects that characterize the building and the development of a numerical model such as the fact the building be semi-buried influencing the boundary conditions, the existent cracks, the geometrical configuration and the importance of defining the material properties. These model difficulties were overcome with research, damage and deformation surveys, core samplings of the building and several tests such as the dynamic identification in situ, allowing the calibration and validation of the numerical model. The global response of the building is influenced by several aspects, such as the material properties, boundary conditions,

loading and the geometrical configuration, as shown for example in the obtained displacements regarding the direction of the pushover analysis, being higher in the XX direction since the exposed area of the building to this load is bigger causing more horizontal displacements in the structure.

#### **6.1.2.1 Retrofitting strategy proposals**

Regarding the retrofitting proposals, it was concluded that removing the excess load is an adequate proposal considering the vertical loads however when faced with seismic loads in the XX direction, the strength increase through this strategy is not notorious, proving the need to combine with other action such as the steel tie-rods application, improving the response when performed a pushover and also for the vertical load analysis. Comparing the position of the steel tie-rods, when positioned in the intrados of the masonry vaults, better results are obtained. For the pushover analysis in the YY direction only the removal of the excess load proposal reduces the displacements.

The choice of the most adequate retrofitting proposal should regard not only the results but also the costs, the level of intrusion into the building and limitation in terms of use and functionality, being therefore a rational and caution choice trying to maintain, as much as possible, the authenticity of the building since dealing with a historical construction, acknowledge on the national and international level.

### **6.2 Future developments**

Since this dissertation focuses on study cases there are several developments that can be made to better understand the actual structural state of the buildings and also to define strategies to safety strengthen and maintain the authenticity of the original structure.



### 6.2.1 Mallorca Cathedral

- Continue the existent dynamic monitoring of the building to build on the information obtained to improve and complement the numerical model;
- Perform the sensitivity analysis with a 3D model and with the simulation of the existent damage and deformations to compare with the obtained results for the 2D model;
- To better understand the structural capacity of the Cathedral it should be analysed several conditions, for which can be combined the dynamic effects of seismic and wind loads, construction process simulation, material creep and existent cracking allowing a rigorous evaluation of the global response of the building.

### 6.2.2 São Jorge Castle – Paço Real II building

- As for the previous case, it is important to continue the topographic monitoring of the building to obtain more data on building movements and model calibration and carry out more bore holes in masonry vaults and external walls;
- Develop a bigger and more complete numerical model, for example including the adjacent building connected with Paço Real II, through a small pedestrian bridge, and also simulate the ancient link to the Castelejo;
- Perform a geotechnical study to better comprehend the actual state of the building, trying to understand the influence of the surrounding tree roots on the existent cracking as well as study the slope stability;
- Carry out time history analysis for the building using real/artificial accelerograms;

- Add to the sensitivity study more retrofitting strategies mainly the simulation of the FRP strips, the effect of reinforced mortar renders and placement of buttresses, constituting again the connection between the existent buttresses with the entrance wall, for example.

## REFERENCES

### (A)

Acary, V. and M. Jean (1998). Numerical simulation of monuments by the contact dynamics method. Monument-98, Workshop on seismic performance of monuments, Lisbon, Portugal.

Asteris, P. G. and V. Plevris (2015). Handbook of Research on Seismic Assessment and Rehabilitation of Historic Structures, IGI Global.

### (B)

Brasão Farinha, J. S. and A. Correia dos Reis (1993). Tabelas Técnicas. Setúbal, Edições Técnicas.

Brincker, R., C. Ventura and P. Andersen (2001). Damping estimation by Frequency Domain Decomposition. IMAC-XXI: Conference & Exposition on Structural Dynamics - Innovative Measurement Technologies Kissimmee, Florida, USA.

### (C)

Caetano, E. (1992). Identificação experimental de parâmetros dinâmicos em sistemas estruturais. Master thesis, Universidade do Porto.

Cantieni, R. (2005). Experimental methods used in system identification of civil engineering structures. 1<sup>st</sup> International Operational Modal Analysis Conference (IOMAC). Copenhagen, Denmark: 249-260.

Casolo, S. (2004a). "Macroscopic modelling of structured materials: Relationship between orthotropic Cosserat continuum and rigid elements." International Journal of Solids and Structures **43**(3): 475-496.

Casolo, S. (2004b). "Modelling in-plane micro-structure of masonry walls by rigid elements." International Journal of Solids and Structures **41**(13).

CasteloSãojorge. (2016). "10 MOMENTOS Website:

<http://castelodesaojorge.pt/pt/historia/>."

Cervera, M., C. Saracibar and M. Chiumenti (2002). COMET - Coupled Mechanical and Thermal Data Input Manual version 5.0.

CIMNE. (2015). "CIMNE - International Center for Numerical Methods in Engineering Website: <http://www.cimne.com/>."

Clemente, R., P. Roca and M. Cervera (2006). Damage model with crack localization – application to historical buildings. Structural analysis of historical constructions: pp 1125-1133.

COMET. (2015). "COMET - Coupled Mechanical and Thermal Website:

<http://www.cimne.com/comet>."

Corporation, N. I. (2016). "The Fundamentals of FFT-Based Signal Analysis and Measurement in LabVIEW and LabWindows/CVI Website:

<http://www.ni.com/white-paper/4278/en/>."

Corradi, M., A. Borri, G. Castori and K. Conventry (2015). "Experimental Analysis of Dynamic Effects of FRP Reinforced Masonry Vaults." Materials **8**(12): 8059-8071.

Cruz, A. (2013). Reabilitação do património: Castelo de S. Jorge: do Estado Novo à atualidade. Master thesis, Universidade Lusófona de Humanidades e Tecnologia.

Cundall, P. A. (1971). A computer model for simulating progressive, large-scale movements in blocky rock systems. Proc. Symp. Int. Rock Mech.

## (D)

D10.4-NIKER (2012). Guidelines for Reliable Seismic Analysis and Knowledge Based Assessment of Buildings., Report, work package 10, NIKER project (2010-2012): New Integrated Knowledge-based approaches to the protection of cultural heritage from Earthquake-induced Risk. Funded by EC under the 7th Framework program, contract n. ENV2009-1-GA244123.

Das, A. (2008). Safety assessment of Mallorca cathedral Master thesis, Universitat politècnica de Catalunya.

## (F)

Faria, R., J. Oliver and M. Cervera (1998). "A strain-based plastic viscous-damage model for massive concrete structures." International Journal of Solids and Structures **35**(14): pp 1533-1558.

Ferreira, A. (2013). Identificação modal e actualização de modelos de elementos finitos. Master thesis, Universidade Nova.

Furtado, A., H. Rodrigues and A. Arêde (2015). "Modelling of masonry infill walls participation in the seismic behaviour of RC buildings using OpenSees." International Journal of Advanced Structural Engineering (IJASE) **7**(2): 117-127.

## (G)

GaussianWaves. (2016). "FFT and Spectral Leakage Website:

<http://www.gaussianwaves.com/2011/01/fft-and-spectral-leakage-2/>."

Gésero, M. (2011). Configuração da paisagem urbana pelos grupos imigrantes. Master thesis, Universidade Técnica de Lisboa.

GiD. (2015). "GiD - The personal pre and post processor Website:

<http://www.gidhome.com/>."

Guerreiro, L., J. Azevedo, J. Proença, R. Bento and M. Lopes (2000). Damage in ancient churches during the 9 of July 1998 Azores earthquake. 12<sup>o</sup> World Conference of Earthquake Engineering (WCEE).

## (H)

Heyman, J. (1966). "The stone skeleton, International Journal of Solid and Structures 2." 249-279.

Hollaway, L. (2011). Key issues in the use of fibre reinforced polymer (FRP) composites in the rehabilitation and retrofitting of concrete structures. United Kingdom.

## (J)

Jean, M. (1995). "Frictional contact in collections of rigid or deformable bodies: numerical simulation of geomterical motions." Mechanicals of Geomaterial Interfaces: 463-486.

## (L)

Lagomarsino, S. and S. Podestà (2004). "Seismic Vulnerability of Ancient Churches: I. Damage Assessment and Emergency Planning." Earthquake Spectra **20**(2): 377-394.

LineeGuida (2006). LineeGuida per la valutazione e riduzione del rischio sismico del patrimonio culturale.

Lopes, V. (2009). Identificação mecânica e avaliação do comportamento sísmico de chaminés de alvenaria. Master thesis, Universidade do Porto.

Lopes, V., J. Guedes, A. Arêde, J. Milheiro, E. Paupério and A. Costa (2010). Identificação dinâmica das estruturas: pp 1-21.

Lotfi, H. and P. Shing (1994). "Interface model applied to fracture of masonry structures." J Struct Eng ASCE **120**(1): 63-80.

Lourenço, P. (1996). Computational strategies for masonry structures. PhD Thesis, Delft University.

Lourenço, P. (2001). Analysis of historical constructions: from thrust lines to advanced simulations. 3<sup>rd</sup> Int. Seminar on Structural Analysis of Historical Constructions, Guimarães, Portugal.

Lourenço, P. (2002). "Computations on historic masonry structures." Progress in Structural Engineering and Materials **4**(3): 301-319.

Lourenço, P. (2008). Structural masonry analysis: recent developments and prospects 14th international brick & brick masonry conference, Sidney, Australia.

Lourenço, P. and J. Rots (1997). "A multi-surface interface model for the analysis of masonry structures." J Eng Mech ASCE **123**(7): 660-668.

(M)

Magalhães, F. and Á. Cunha (2011). "Explaining operational modal analysis with data from an arch bridge. ." Mechanical Systems and Signal Processing **25**(5): 1431-1450.

Mallardo, V., R. Malvezzi, E. Milani and G. Milani (2008). "Seismic vulnerability of historical masonry buildings: a case study in Ferrara." Engineering Structures **30**: 2223-2241.

ManualMidasUser. (2016). "Material: Isotropic Website:

[http://manual.midasuser.com/en\\_common/fea/296/FEA/06\\_Analysis/02\\_Material/Isotropic.htm](http://manual.midasuser.com/en_common/fea/296/FEA/06_Analysis/02_Material/Isotropic.htm)."

Mark, R. (1982). Experiments in Gothic structure. Cambridge, England, The Massachusetts Institute of Technology.

Martínez, G. (2007). Vulnerabilidad sísmica para edificios históricos de obra de fábrica de mediana y gran luz. PhD thesis, Technical University of Catalonia.

Maynou, J. (2001). Estudi estructural del pòrtic tipus de la catedral de Mallorca mitjançant l'estàtica gràfica. Graduation thesis, Universitat Politècnica de Catalunya.

Medart. (2015). "Glossary of Medieval Art and Architecture, website:

<http://www.pitt.edu/~medart/menuglossary/INDEX.HTM> ".

MIDAS. (2016). "MIDAS: Engineering software Website: <http://en.midasuser.com/>."

Milani, E., G. Milani and A. Tralli (2008). "Limit analysis of masonry vaults by means of curved shell finite elements and homogenization." International Journal of Solids and Structures **45**(20): 5258-5288.

Mohamed, A. (2015). Integrated monitoring and structural analysis strategies for the study of large historical construction. Application to Mallorca cathedral. PhD thesis, Universitat Politècnica de Catalunya.

Murcia-Delso, J., A. Das, P. Roca and M. Cervera (2009). Seismic safety analysis of historical masonry structures using a damage constitutive model. International Conference on Computational Methods in Structural Dynamics and Earthquake Engineering. Rhodes, Greece.

(N)



Neves, N., A. Costa and A. Arêde (2004). Identificação dinâmica e análise do comportamento sísmico de um quarteirão localizado na cidade da Horta - Ilha do Faial. 6º Congresso Nacional de Sismologia e Engenharia Sísmica. Guimarães, Portugal.

NTC (2008). Nuove Norme Tecniche per le Costruzioni, G.U. n. 29, 4 Febbraio 2008, S.O. n. 30. D.M del Ministero delle Infrastrutture e dei Trasporti 14 Gennaio 2008.

NYT. (2009). "The New York Times - Where Culture is Another Casualty Website: [http://www.nytimes.com/2009/04/11/arts/11abroad.html?\\_r=1](http://www.nytimes.com/2009/04/11/arts/11abroad.html?_r=1)."

### (O)

Orduña, A. and P. B. Lourenço (2001). Limit Analysis as a tool for the simplified assessment of ancient masonry structures. 3<sup>rd</sup> Int. Seminar on Structural Analysis of Historical Constructions. Guimarães, Portugal: 511-520.

### (P)

Pelà, L., A. Aprile and A. Benedetti (2009). "Seismic assessment of masonry arch bridges." Engineering Structures **31**: 1777-1788.

Pelà, L., J. Bourgeois, P. Roca, M. Cervera and M. Chiumenti (2014). "Analysis of the Effect of Provisional Ties on the Construction and Current Deformation of Mallorca Cathedral." International Journal of Architectural Heritage: Conservation, Analysis, and Restoration **10**(4).

Pelà, L., M. Cervera and P. Roca (2011). Continuum model for inelastic behaviour of masonry. Congresso dell'Associazione Italiana di Meccanica Teorica e Applicata. Bologna, Italy.

Pimentel, R. (2008). Caracterização do tráfego ferroviário e dos seus efeitos em pontes de pequeno vão. Master thesis, Universidade do Porto.

**(R)**

Roca, P., M. Cervera, G. Gariup and L. Pelà (2010). "Structural Analysis of Masonry Historical Constructions. Classical and Advanced Approaches." Archives of Computational Methods in Engineering **17**(3): 299-325.

Roca, P., M. Cervera, L. Pelà, R. Clemente and M. Chiumenti (2013). "Continuum FE models for the analysis of Mallorca Cathedral." Engineering Structures **Volume 46**: Pages 653–670.

Roca, P., M. Massanas, M. Cervera and G. Arun (2004). Structural analysis of Küçük Ayasofya Mosque in İstanbul. Structural analysis of historical constructions, Amsterdam.

Rodrigues, J. (2004). Identificação modal estocástica - Métodos de análise e aplicações em estruturas de engenharia civil. PhD thesis, Universidade de Porto.

Rubió, J. (1912). Lecture on the organic, mechanical and construction concepts of Mallorca Cathedral. Anuario de la Asociación de Arquitectos de Cataluña. Barcelona, Spain.

**(S)**

Salas, A. (2002). Structural study of the typical bays of Mallorca cathedral. Graduation thesis, Universitat Politècnica de Catalunya.

Silva, A. V. (1898). O Castelo de S. Jorge. Revista de Engenharia Militar.

Silva, A. V. (1948). A Cerca Fernandina de Lisboa. Lisbon, Portugal.

Silva, B. (2008). Aplicação de um Modelo de Dano Contínuo na Modelação de Estruturas de Alvenaria de Pedra. Igreja de Gondar - Um caso de estudo. MSc Thesis, Faculdade de Engenharia da Universidade do Porto.

Silva, B., J. M. Guedes and A. Costa (2010). Estratégias de Modelação Numérica no estudo de Estruturas Históricas. Experiência do NCREP (FEUP). Porto, Portugal, Faculdade de Engenharia da Universidade do Porto.

SIPA. (2016). "Castelo de São Jorge e cercas de Lisboa Website:

[http://www.monumentos.pt/Site/APP\\_PagesUser/SIPA.aspx?id=3128](http://www.monumentos.pt/Site/APP_PagesUser/SIPA.aspx?id=3128)."

SismyGroup. (2016). "Lavori eseguiti - Via Roma S.Pio L'Aquila (2013) Website:

<http://sismygroup.it/lavori/via-s-pio-laquila-2013/>."

Sutcliffe, D., H. Yu and A. Page (2001). "Lower bound limit analysis of unreinforced masonry shear walls." Computational Structures **79**(14): 1295-1312.

Szólomicki, J., P. Berkowski and J. Barański (2015). "Computer modelling of masonry cross vaults strengthened with fiber reinforced polymer strips." Archives of Civil and Mechanical Engineering **15**(3): 751–766.

Szolomocki, J. (2009). Structural behaviour of masonry vaults. 18th International Conference on the Application of Computer Science and Mathematics in Architecture and Civil Engineering. Weimar, Germany.

## (T)

Tavares, M. (2013). Identificação modal e monitorização dinâmica de uma ponte em arco. Master thesis, Universidade do Porto.

TheNationalGallery. (2016). "Glossary Website:

<https://www.nationalgallery.org.uk/paintings/glossary/groined-vault>."

## (V)

Vicente, R., S. Parodi, S. Lagomarsino, H. Varum and J. A. R. M. Silva (2011). "Seismic vulnerability and risk assessment: case study of the historic city centre of Coimbra, Portugal." Bulletin of Earthquake Engineering **9**(4): 1067-1096.

(W)

WaveletToolbox. (2016). "De-noising Website:

<http://www.ece.northwestern.edu/local->

[apps/matlabhelp/toolbox/wavelet/ch06\\_a44.html](http://www.ece.northwestern.edu/local-apps/matlabhelp/toolbox/wavelet/ch06_a44.html)."

WSJ. (2009). "The Wall Street Journal - Earthquake Damage in L'Aquila Website:

<http://www.wsj.com/articles/SB123938772876409087>."

## **APPENDIX A**

### **RETROFITTING STRATEGIES PROPOSALS**

In the present appendix are presented the results of non-linear analysis with the possibility of the accessible roof condition, for the three retrofitting strategies proposal.

## A.1 Remove excess load with accessible roof

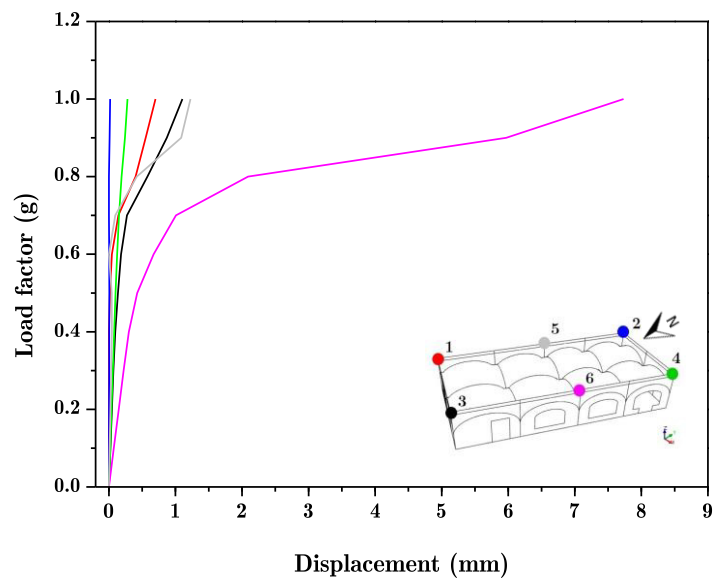


**Figure A.1** – Transversal displacement vs load factor regarding the vertical load analysis.

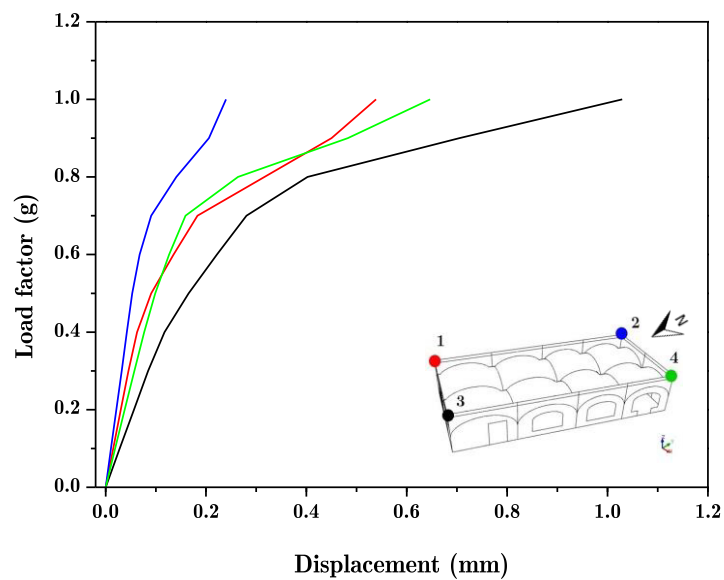


**Figure A.2** – Longitudinal displacement vs load factor regarding the vertical load analysis.

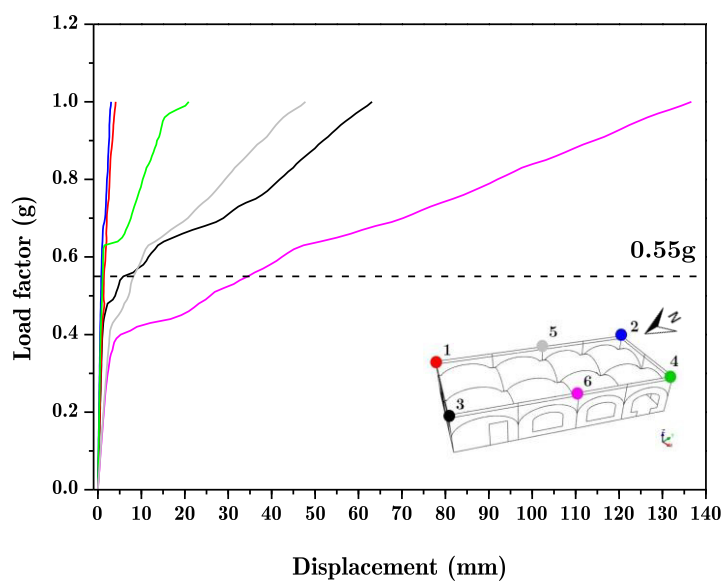


**Figure A.3** – Transversal displacement vs load factor regarding the pushover analysis in the XX direction.

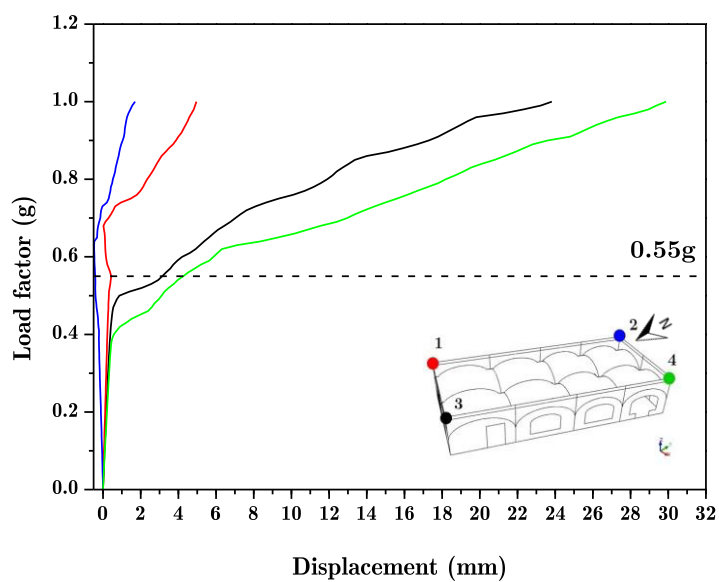


**Figure A.4** – Longitudinal displacement vs load factor regarding the pushover analysis in the XX direction.

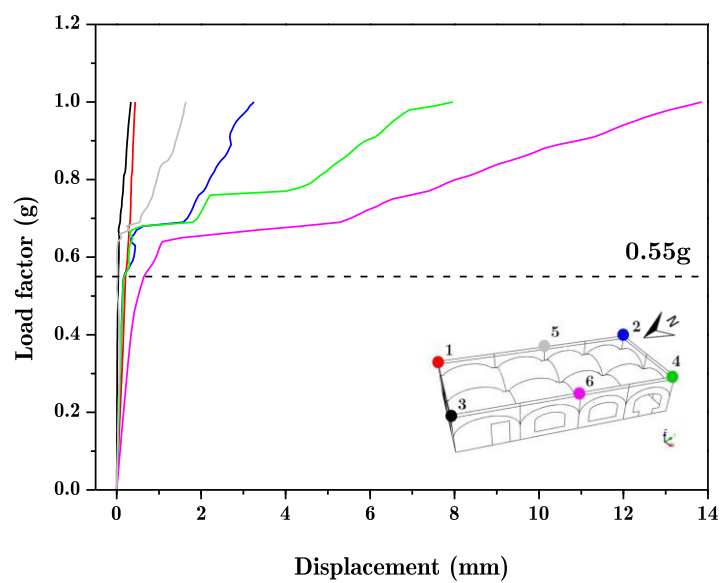


**Figure A.5** – Transversal displacement vs load factor regarding the pushover analysis in the YY direction.



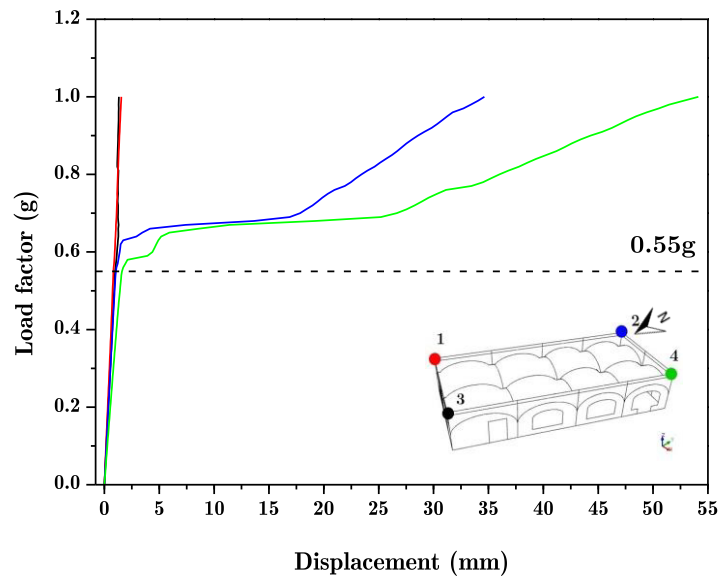


**Figure A.6** – Longitudinal displacement vs load factor regarding the pushover analysis in the YY direction.

## A.2 Steel tie-rods with accessible roof

### A.2.1 Intrados steel tie-rods

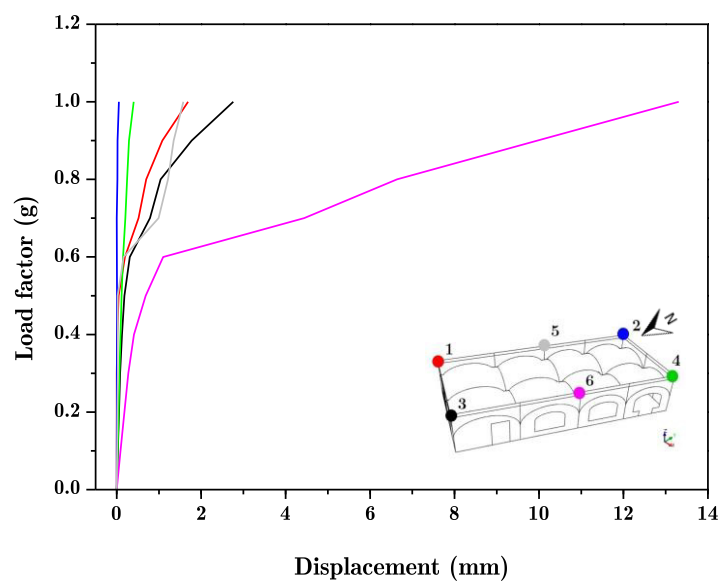


**Figure A.7** - Transversal displacement vs load factor regarding the vertical load analysis.

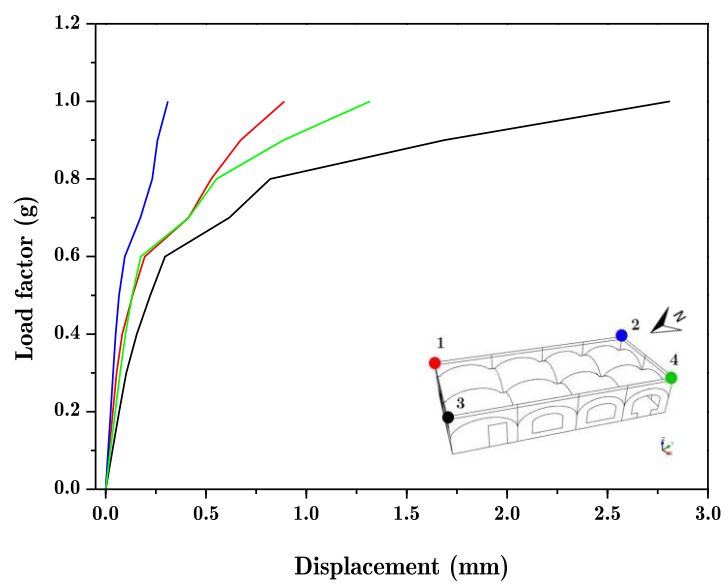


**Figure A.8** – Longitudinal displacement vs load factor regarding the vertical load analysis.

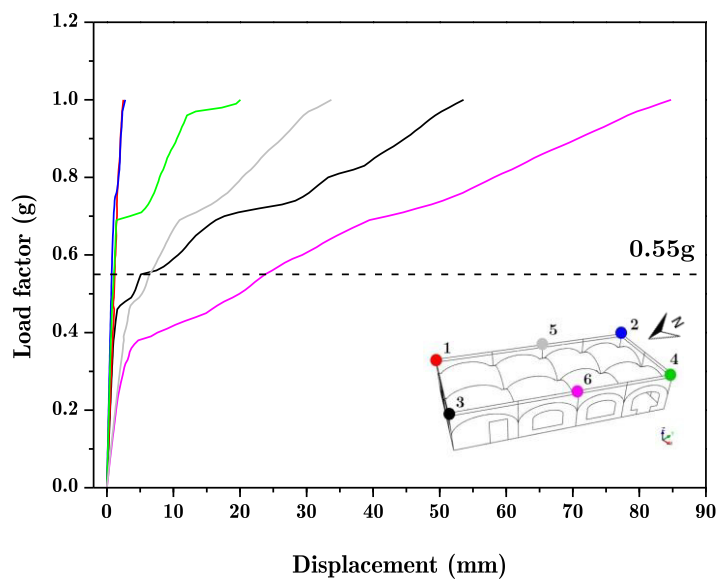


**Figure A.9** – Transversal displacement vs load factor regarding the pushover analysis in the XX direction.

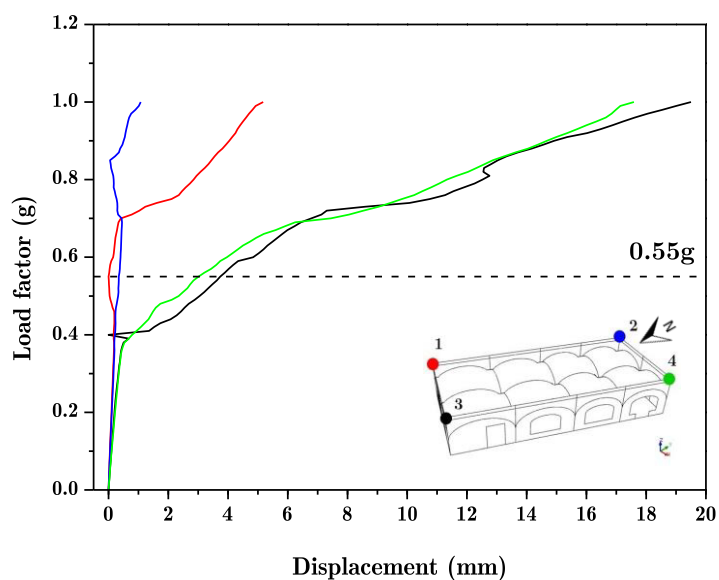


**Figure A.10** – Longitudinal displacement vs load factor regarding the pushover analysis in the XX direction.

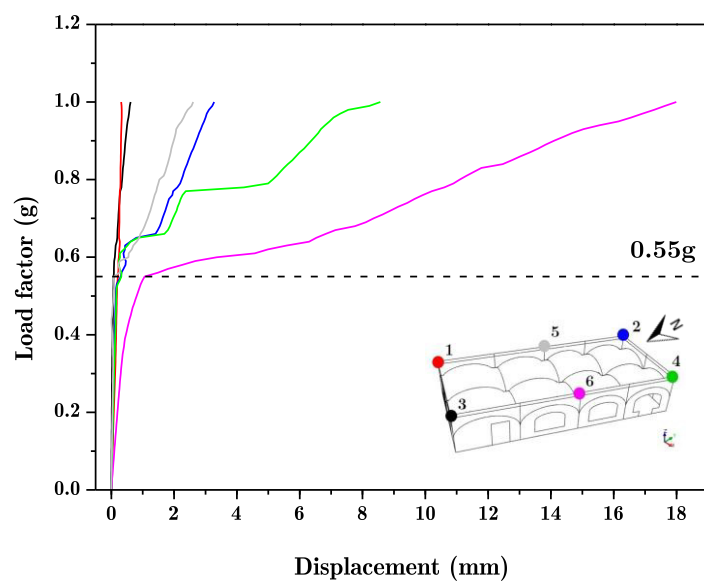


**Figure A.11** – Transversal displacement vs load factor regarding the pushover analysis in the YY direction.

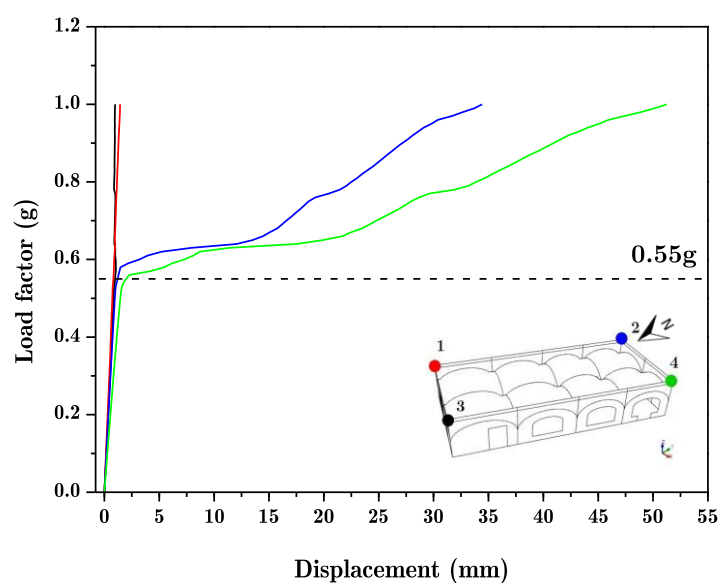


**Figure A.12** – Longitudinal displacement vs load factor regarding the pushover analysis in the YY direction.

### A.2.2 Extrados steel tie-rods

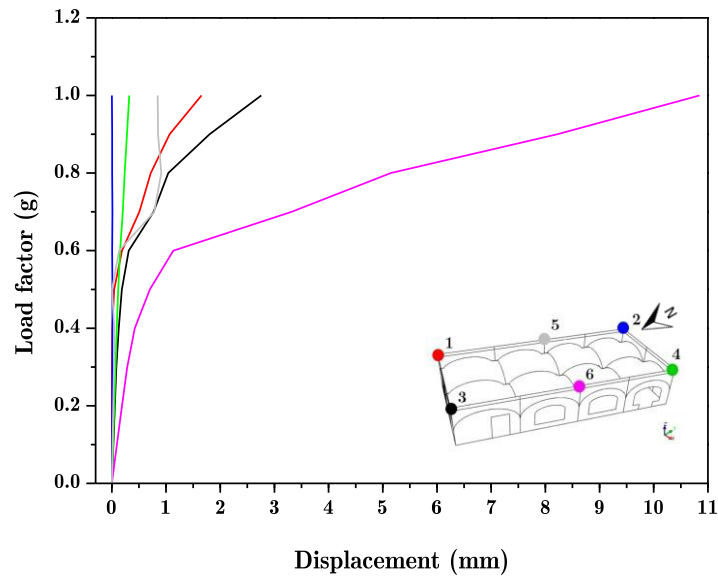


**Figure A.13** – Transversal displacement vs load factor regarding the vertical load analysis.

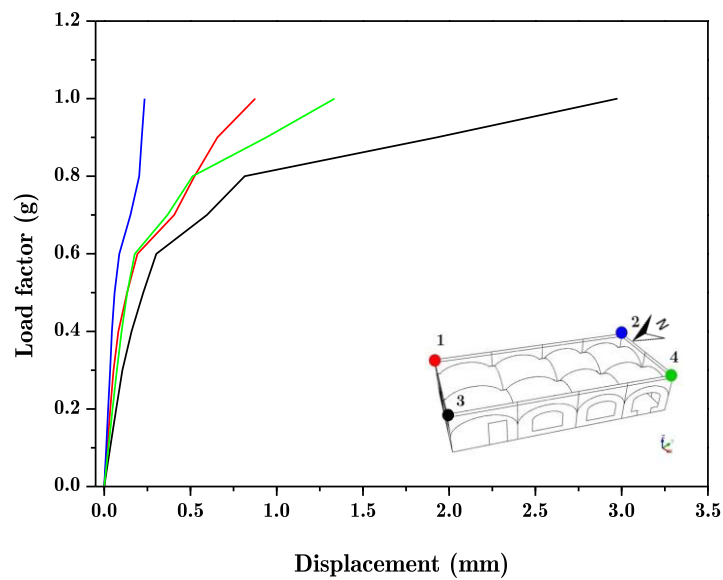


**Figure A.14** – Longitudinal displacement vs load factor regarding the vertical load analysis.

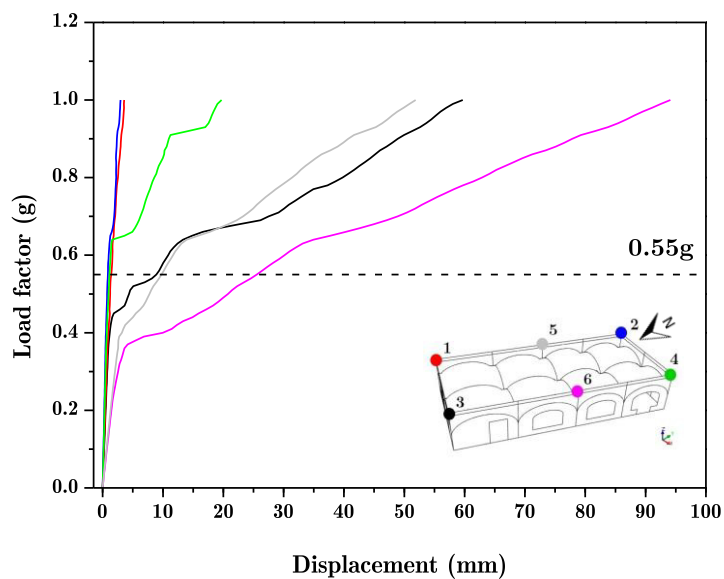


**Figure A.15** – Transversal displacement vs load factor regarding the pushover analysis in the XX direction.

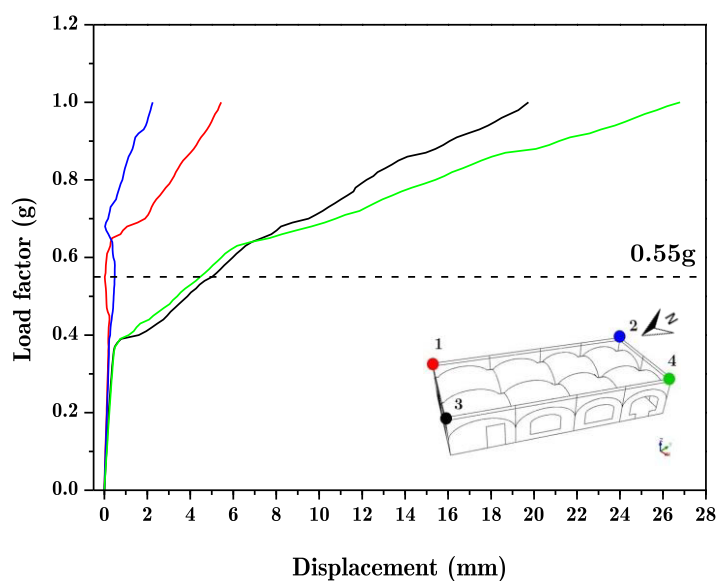


**Figure A.16** – Longitudinal displacement vs load factor regarding the pushover analysis in the XX direction.

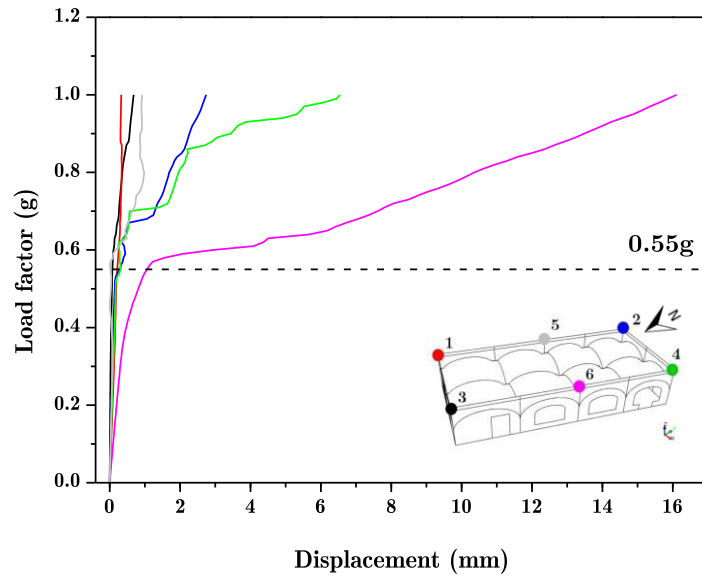


**Figure A.17** – Transversal displacement vs load factor regarding the pushover analysis in the YY direction.

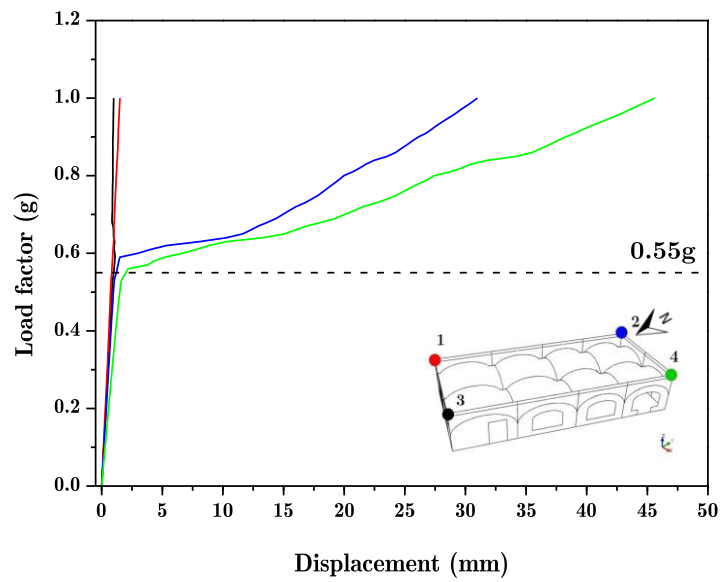


**Figure A.18** – Longitudinal displacement vs load factor regarding the pushover analysis in the YY direction.